The intertwining roles of mechanosensitive channels, cellular stress, and the proteasome in β cell function

By Mallory Brayer

B.S. in Biology and Chemistry, May 2019, The University of Scranton
M.S. in Biology, August 2021, Villanova University

A Dissertation submitted to:

The Faculty of
The Columbian College of Arts and Science
of The George Washington University
in partial fulfillment of the requirements
for the degree of Doctor of Philosophy

May 18, 2025

Dissertation directed by

Aleksandar Jeremic
Professor of Biology

The Columbian College of Arts of Sciences of The George Washington University certifies that Mallory Brayer has passed the Final Examination for the degree of Doctor of Philosophy as of March 25th, 2025. This is the final and approved form of the dissertation.

The intertwining roles of mechanosensitive channels, cellular stress, and the proteasome in β cell function

Mallory Brayer

Dissertation Research Committee

Aleksandar Jeremic, Professor of Biology, Dissertation Director

Vesna Zderic, Department Chair and Professor, Committee Member

Ioannis Eleftherianos, Professor of Biology, Committee Member

Leon Grayfer, Associate Professor of Biology, Committee Member

Abstract of Dissertation

The intertwining roles of mechanosensitive channels, cellular stress, and the proteasome in β cell function

The pancreas is a retroperitoneal organ comprised of heterogeneous exocrine and endocrine tissues that broadly function in digestion, appetite regulation, and blood glucose homeostasis. The endocrine pancreas is comprised of clusters of neuroendocrine cells that each have a highly specialized role in blood glucose homeostasis. Endocrine pancreatic beta cells secrete insulin and islet amyloid polypeptide (IAPP) in response to increases in blood glucose. Insulin promotes skeletal muscle and adipose tissue to take up excess blood glucose. IAPP binds to multiple tissues including skeletal muscle and the hindbrain to elicit various responses.

The most common disease caused by pancreatic dysfunction is type two diabetes. Although chronic hyperglycemia and insufficient insulin secretion are hallmarks of this disease, heterogenous processes drive its development. Metabolic stress contributes to beta cell failure as constant glucose inundation creates oxidative stress and impairs beta cell blood glucose sensing, lowering insulin secretion. Cells damaged by oxidative stress release danger-associated molecular patterns that recruit innate immune cells into the tissue. As insulitis progresses, interleukin 1-beta production increases, reducing insulin secretion and inducing apoptosis mediated by TXNIP interactions with various binding partners. Despite the major roles metabolic and proinflammatory stress play in the development of type two diabetes, the potential signaling cross talk between stressors

remains poorly understood. Here, we observed concurrent high glucose and proinflammatory cytokines is required for changes in gene expression. Immunoprecipitation studies refuted direct binding between TXNIP and NF-kB in this process, suggesting two pro-inflammatory pathways operate in parallel in stressed beta cells.

As type two diabetes progresses, there is a further loss of insulin secretion due to beta cell apoptosis and de-differentiation. Beta cell amyloidosis contributes heavily to apoptosis as IAPP oligomers are found in most individuals with type two diabetes. The exact cause of IAPP oligomerization is unknown but is linked to impaired proteasome function seen in type two diabetes. These IAPP aggregates cause protein stress leading to reactive oxygen species formation, reduced mitochondrial membrane potential, and decreased proteolytic functions. To assess additional effects of protein stress, we compared changes in gene expression in human islet under acutely induced proteasome inhibition and type two diabetes induced proteasome inhibition. We observed downregulation of beta cell identity marker genes and genes required for glucose sensing and glucose induced insulin secretion in proteasome-inhibited samples. We also found impaired pyruvate production and decreased mitochondrial membrane potential under proteasome inhibition suggesting proteasome function and/or associated protein stress reduces beta cell ATP production to reduce ATP-dependent peptide hormone secretion from these cells.

Despite improving treatments, approximately half of people with type two diabetes will fail to achieve glycemic control leading to complications like nephropathy. Current pharmacological treatments reduce blood glucose by reducing appetite and gastric glucose absorption; however, they carry side effects like gastric disturbances while also having high financial costs and supply shortages. Given the need for improved type two diabetes treatments, non-pharmacological treatments have been developed including therapeutic ultrasound-induced insulin secretion. The broader effects of ultrasound treatment on beta cell physiology remain unknown as well as how these cells detect ultrasound stimulation. Here, we identified expression of mechanosensitive channels in human and rodent pancreatic beta cells that are implicated in both ultrasound-mediated reactive oxygen species formation and downregulation of essential beta cell genes.

Table of Contents

Abstract of Dissertation.....iii-v

List of Figures.....viii-ix

Introduction Figures.....viii

Chapter 1 Figures.....viii

Chapter 2 Figures.....viii-ix

Chapter 3 Figures.....ix

Introduction.....5-26

Chapter 1: Mechanosensitive Channels Mediate Pancreatic β Cells.....27-55
Reactive Oxygen Species Formation and Downregulation of Essential Genes during Therapeutic Ultrasound Treatment
Abstract.....28-29

Introduction.....30-33

Materials and Methods.....33-40

Results.....40-45

Discussion.....45-48

Chapter 2: Hyperglycemia is required for cytokine-induced transcriptional.....56-74
changes in pancreatic beta cells
Abstract.....56

Introduction.....56-59

Materials and Methods.....59-61

Results.....61-72

Discussion.....72-74

Chapter 3: Proteasome activity is critical for beta cell identity and glucose sensing.....75-96
Abstract..... 75

Introduction..... 76-80

Materials and Methods.....80-87

Results.....87-96

Discussion.....96-99

References.....99-120

List of Figures

Introduction Figures

Figure 1 Organization and function of Pancreas.....7

Figure 2 Glucose-induced insulin secretion.....9

Figure 3 Beta cell insulin and IAPP production and signaling.....14

Figure 4 Uncoupled protein response in beta cells.....16

Figure 5 IAPP-induced cellular stress.....17

Figure 6 Potential crosstalk between metabolic and proinflammatory beta cell signaling.....20

Figure 7 Mechanisms of common classes of type two diabetes drugs.....21

Figure 8 General mechanisms of mechanosensitive channel activation.....23

Figure 9 Therapeutic Ultrasound and its Effects on Tissues.....25

Chapter 1 Figures

Figure 1 Verification of TUS parameters.....50

Figure 2 Ultrasound application to rats.....51

Figure 3 MSC expression in INS cell line and human pancreatic islets.....52

Figure 4 ROS Formation in INS Cells.....53

Figure 5 TUS-induced changes in INS gene expression.....54

Figure 6 Rat histological analysis of essential β cell genes.....55

Chapter 2 Figures

Figure 1 Expression of glucose responsive genes in INS cells.....64

Figure 2 Expression of proinflammatory genes in INS cells.....66

Figure 3 NF-κB expression is increased by cytokine treatments only under 68
hyperglycemic conditions in INS cells

Figure 4 Human pancreatic islet expression of glucose-responsive and 70
proinflammatory genes

Figure 5 Representative western blots following TXNIP pulldown.....71-72

Chapter 3 Figures

Figure 1 Decreased proteasome activity alters expression of protein-stress 89
response genes

Figure 2 Beta cell marker genes are downregulated by proteasome impairment.....91-92

Figure 3 Effects of proteasome inhibition on beta cell peptide hormone secretion...94-95

Figure 4 Proteasome inhibition impairs beta cell ATP production 96

List of Tables

Introduction Tables

Table 1 Genes downregulated by proteasome inhibition and type two diabetes in primary human pancreatic islets ...18-19

Chapter 1 Tables

Table 1 Rat qPCR primer sequences 49

Table 2 Human qPCR primer sequences 49

Chapter 2 Tables

Table 1 Rat qPCR primer sequences 60

Table 2 Human qPCR primer sequences 60-61

Chapter 3 Tables

Table 1 Rat qPCR primer sequences 82-83

Table 2 Human qPCR primer sequences 83

Table 3 JC-1 Species Detection Spectra 86

The Endocrine Pancreas

The pancreas is a retroperitoneal organ comprised of heterogeneous exocrine and endocrine tissues (Fig. 1A). It broadly functions in digestion, appetite regulation, and blood glucose homeostasis. The pancreas is highly innervated by both sympathetic and parasympathetic systems. The pancreatic plexus, celiac ganglia, and vagus nerve help modulate endocrine and exocrine secretory functions (Travagli & Browning, 2011). The exocrine tissue consists of acinar and duct cells that assist in digestion (Fig. 1B). Acinar cells produce digestive enzymes including amylase and proteases while duct cells secrete sodium bicarbonate. This alkaline mixture of enzymes are released into the pancreatic duct for transport into the duodenum where they digest chyme from the stomach (Chandra & Liddle, 2009).

The endocrine portion of the pancreas is comprised of clusters of neuroendocrine cells scattered throughout the tissue referred to as islets of Langerhans (Fig. 1C). These neuroendocrine cells share some similarities with cells of the central nervous system but also have endocrine functions. They express biomarkers associated with the central nervous system like chromogranin A, neuron specific enolase, and synaptophysin (Bajetta et al., 1999). Similar to neurons, neuroendocrine cells are also able to metabolize amines to produce polypeptide hormones. The hormones produced by neuroendocrine cells work through autocrine and paracrine signaling; however, unlike neurons, they also travel in the blood to reach distal targets as endocrine hormones (Alvarez Fallas et al., 2021; Andersson-Rolf et al., 2000; Dasgupta & McCollum, 2019).

The pancreas has a dual blood supply coming from the celiac and superior mesenteric arteries that create numerous blood vessels that allow for this endocrine signaling (Pandol, 2010).

Despite only comprising 1 to 2% of total pancreas volume, endocrine islets receive approximately 10 times more blood than the surrounding exocrine tissue due to extensive vessel fenestration, which allow cells within islets to respond to changes to blood glucose and secrete peptide hormones for systemic effects (Henderson & Moss, 1985).

Within pancreatic islets of Langerhans, each cell type has a highly specialized role in blood glucose homeostasis. Pancreatic islets contain endocrine alpha, beta, and delta cells that respectively secrete the peptide hormones glucagon, insulin, and somatostatin. These cells influence the activity of each other through endocrine, paracrine, cell-to-cell, and neural communications. Cells within islets synergistically work to regulate blood glucose. Between species, the abundance and spatial distribution of these cell types vary. Within rodent islets, beta cells comprise approximately three quarters of cells within in islets while alpha cells account for approximately 20% of cells and delta cells make up the remaining 5 to 10%. Rodent beta cells preferentially localize to the outer perimeter of the islet while alpha and delta cells remain in the islet core. In contrast, human islets have a lower proportion of beta cells and higher proportion of alpha cells. Beta cells in these islets comprise approximately half of islet cells with alpha cells comprising approximately one third. Additionally, cell type distribution in human islets follow a random pattern resulting in the majority of beta cells being in contact with non-beta cells (Cabrera et al., 2006).

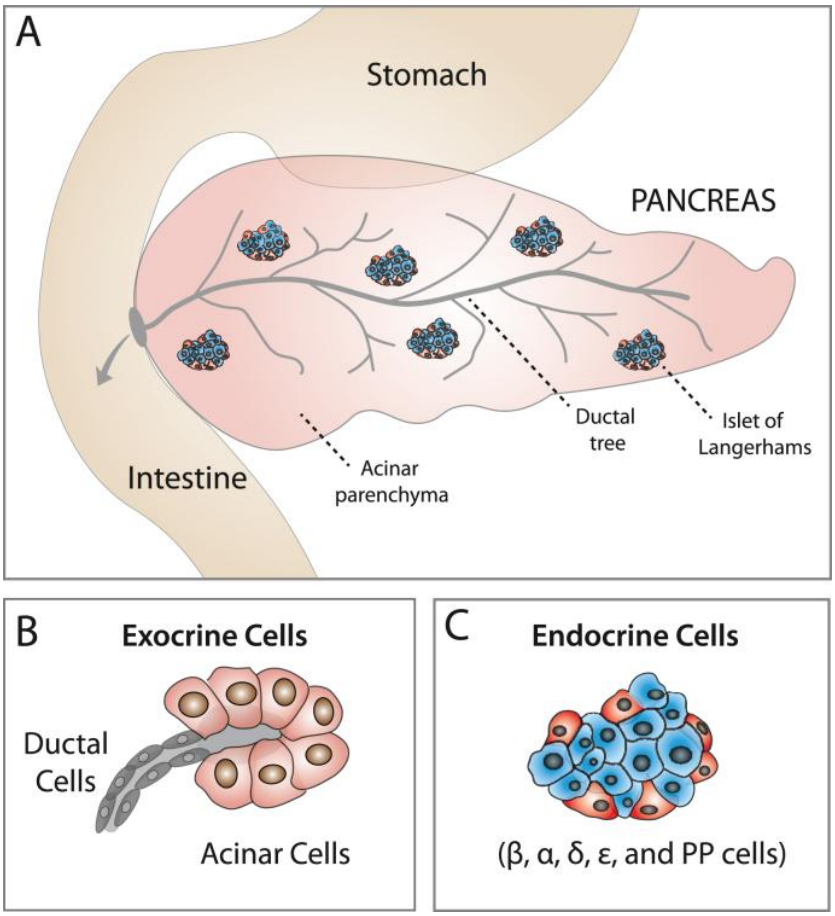

adapted from (Alvarez Fallas et al., 2021)

Figure 1. Organization and function of Pancreas: **A)** The pancreas is a retroperitoneal organ primarily comprised of exocrine tissue. Endocrine cells cluster together in islets of Langerhans that are scattered through the organ. Islets make up 1 -2% of total organ mass. **B)** Exocrine acinar cells produce digestive enzymes that are emptied into ducts created by ductal cells leading into the intestine. **C)** Endocrine islets of Langerhans contain multiple cell types. Beta, alpha, and delta cells make up the majority cells and regulate blood glucose.

Alpha cells secrete glucagon that travels to the liver to mobilize glucose through glycogenolysis and gluconeogenesis. Alpha cells undergo membrane depolarization in response to multiple stimuli including hypoglycemia and adrenaline that allow for calcium influx through L-type calcium channels. This calcium promotes exocytosis of glucagon granules (Gromada et al., 1997). Glucagon propagates its own secretion through both autocrine and paracrine positive feedback loops. Glucagon secretion is also regulated by neural inputs through stimulatory cholinergic signaling of muscarinic receptors (Berts et al., 1997). This process is negatively regulated by insulin and IAPP produced by neighboring beta cells.

Delta cells largely act as a paracrine regulator and suppresses secretory function of both alpha and beta cells. These cells specifically secrete somatostatin-14 while somatostatin-28 is domain in other tissues (Francis et al., 1990). Because delta cells regulate both alpha and beta cell secretory functions, they respond to a wide variety of stimuli. Somatostatin secretion is induced by glucose, glucagon, and GABA but inhibited by free fatty acids and adrenaline (Rorsman & Huising, 2018).

Beta cells secrete insulin and islet amyloid polypeptide (IAPP) in response to increases in blood glucose, using the lower glucose affinity GLUT-2 glucose transporter (Lan 1998) (Fig. 2). Because this transporter is constitutively expressed and has a low affinity but high capacity for glucose, it can bind glucose in a concentration dependent mechanism across physiological glucose concentrations (Leturque et al., 2005). Once glucose enters the beta cell, it is converted into ATP through glycolysis, the citric acid cycle, and oxidative phosphorylation. This ATP then binds to ATP-gated potassium channels inhibiting potassium influx and subsequently promoting plasma membrane depolarization. Depolarization activates voltage-gated calcium channels causing calcium influx (Light, 2010)(Fig. 2). Synaptotagmin on granules containing insulin and IAPP then binds to the influxed calcium to promote soluble N-ethylmaleimide-sensitive factor attachment protein receptor (SNARE)-mediated granule exocytosis. Once bound to calcium, synaptotagmin interacts with the accessory proteins Munc18 on the plasma membrane to bring the vesicle and plasma membrane in closer proximity to each other. Moving the vesicle membrane and plasma membrane is energetically unfavorable as they displace water from the hydrophilic heads of membrane phospholipids (Alberts, 2019). The SNARE proteins syntaxin 1a, vesicle-associated membrane proteins (VAMP), and synaptosomal-associated protein-25 help overcome this energy barrier. The VAMP expressed on the granule membrane forms an

energetically favorable helical bundle with synaptosomal-associated protein-25 and syntaxin on the plasma membrane to release large amounts of energy that drive membrane fusion and granule exocytosis (Wiederhold & Fasshauer, 2009) (Fig. 2). These cells secrete peptide hormones in response to additional nutritional stimuli including insulinotropic amino acids and acute fatty acid exposure.

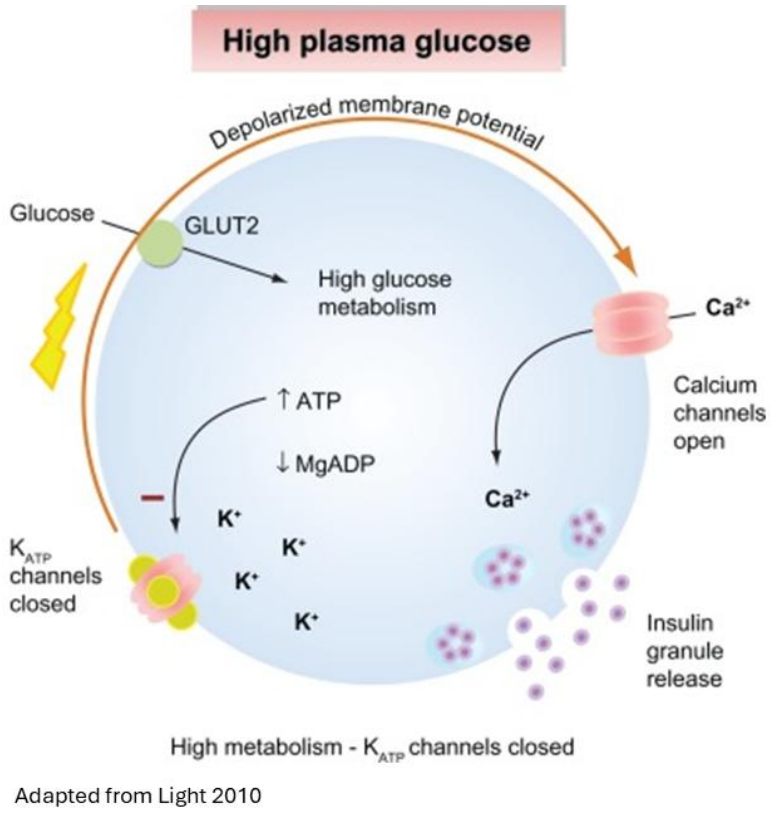

Figure 2: Glucose-induced insulin secretion Excess blood glucose is brought into beta cells by GLUT2. Through cellular respiration, this glucose is converted into ATP. ATP binds to ATP-potassium channels to inhibit potassium influx, causing plasma membrane depolarization. Depolarization causes voltage-gated calcium channels to open for calcium influx. Calcium then interacts with granules containing insulin and IAPP to promote their exocytosis.

In addition to classical, nutrient-induced insulin secretion, beta cells also secrete insulin in response to physical stimuli. This was first documented as beta cells undergo sustained volume increase under hyperglycemic conditions that is sufficient to cause insulin secretion (Miley et al., 1997). The SWELL1-LRRC8 channel has been shown to mediate this process by functioning as a chloride channel allowing for chloride to enter the cell (Kalwat & Thurmond, 2013). Anion

entry increases the osmolarity of the cell and promotes diffusion of water through aquaporin 7 channels to increase the cell volume (Best et al., 2010). Additionally, select mechanosensitive channels (MSC) can be activated by hypotonic stretch or heat to induce insulin secretion (Sawatani et al., 2019a; Skrzypski et al., 2013). Furthermore, our lab has demonstrated that low intensity, unfocused ultrasound evokes calcium oscillations and insulin secretion from pancreatic beta cells *in vivo* in rats, *ex vivo* in rabbit pancreas and human pancreatic islets, and *in vitro* with rodent glucose-responsive insulinoma cell lines (I. Suarez Castellanos, Jeremic, et al., 2017a; I. Suarez Castellanos, Singh, et al., 2017a; Suarez-Castellanos et al., 2021); however, the mechanism underlying this process remains poorly understood.

Beta Cell Peptide Hormone Production and Secretion

Insulin encoded by the *insulin* gene expressed exclusively by pancreatic beta cells (HGNC Database). Its expression is regulated at both a transcriptional and translational level and is largely dependent on nutrient status. The transcription factors MafA and PDX-1 work synergistically to regulate glucose-induced insulin transcription by binding to the metabolic responsive elements E1, A1, and A2/C1 to increase insulin transcription under acute hyperglycemic conditions (Zhao 2005) (Odagiri 1996). Additionally, glucose-induced insulin secretion also activates ICA512 to prevent STAT5 dephosphorylation and promote further insulin translation (Mziaut 2006). Furthermore, glucose can increase insulin mRNA stability by increasing binding of the polypyrimidine tract-binding protein to the 3'-UTR of insulin mRNA to limit its degradation (Tillmar 2002). In contrast, chronic excessive nutrient exposure can result in decreased insulin transcription. *In vitro* experiments have shown chronic hyperglycemia can reduce PDX-1 expression and subsequent DNA binding needed for insulin transcription (Olson 1995). MafA activity is additionally decreased by chronic hyperglycemia, however, its regulation

occurs at a post-transcriptional level likely through increased proteasome degradation (Harmon 2005).

IAPP is encoded by the *IAPP* gene the expression of which is regulated by nutritional status. Similar to *insulin, IAPP* is exclusively expressed by pancreatic beta cells, and its translation is partially regulated by PDX1. Under hyperglycemic conditions, PDX1 binds to the A-box elements in the *IAPP* promoter; however, PDX1 binds to the *insulin* in a calcium-independent manner but requires unidentified calcium response elements to bind to the *IAPP* promoter (Macfarlane et al., 2000b). Additional regulatory elements modulate *IAPP* expression and allow for different expression patterns from *insulin.* In response to both acute and chronic fatty acid exposure, *IAPP* expression is upregulated in a glucose-independent mechanism (Qi et al., 2010). The redox regulation protein and transcription factor TXNIP impacts *IAPP* but not *insulin* expression. TXNIP downregulates expression of microRNA miR-124a to indirectly upregulate *IAPP.* miR-124a inhibits expression of *FoxA2* which serves as another *IAPP* transcription factor. By releasing *FoxA2* from inhibition by this microRNA, this transcription factor can bind to its highly conserved proximal binding site within the *IAPP* promoter region (Jing et al., 2014). Despite their similar expression patterns and regulation, steady-state levels of *IAPP* mRNA make up to 10-fold less of the steady-state *insulin* mRNA levels (Mulder et al., 1996). Under hyperglycemic conditions, *insulin* transcription is minimally altered while *IAPP* mRNA levels increase by approximately 10-fold (Shalev et al., 2002).

Both insulin and IAPP are translated in a pre-pro hormone form that requires additional processing to reach an active form. mRNA encoding pre-pro insulin and pre-pro IAPP is translated directly into the lumen of the endoplasmic reticulum (ER) via synthesis of a signal peptide (Liu 2018). In the ER, the signal peptide is cleaved from pre-pro insulin to produce pro

insulin (Fu 2013). Pro insulin is then folded to create three highly conserved disulfide bonds (Tsuchiya et al., 2016). One occurs within the A-chain of the peptide while the other two occur between the A-chain and B-chain (Liu 2018). The folded pro insulin is then transported to the Golgi apparatus where it is sorted into granules (Kim 2012) (Fig. 3A). Concurrently, the signal peptide is cleaved from pre-pro IAPP to produce pro IAPP. Pro IAPP is then folded to create an intramolecular disulfide bond near its N terminal. Finally, IAPP undergoes a C terminus amidation essential for its function as a hormone (Akter et al., 2016) (Fig. 3B).

Insulin granules bud from the *trans* face of the Golgi apparatus. At this stage, granules contain proinsulin and proIAPP that requires further processing by the proteases carboxypeptidase and prohormone convertases PC1/3 and PC2 (Kiriyama & Nochi, 2018; Teitelman, 2019; Westermark et al., 2011) (Fig. 3 A and B). Under physiological conditions, approximately 1% of insulin granules are available for immediate secretion. This group is referred to as the readily releasable pool while the majority of insulin granules are held as a reserve pool (Fu 2013). This phenomenon is mediated by the maturation and organization of insulin granules. The adaptor protein AP-1 and ADP ribosylation factor 1 (Arf1) assist in sorting these proteins and forming a clathrin coat that promotes vesicle budding from the Golgi apparatus. They then travel along the cytoskeletal microtubule network via kinesin 1 towards the cell periphery. As the granules move towards the plasma membrane, the heat shock protein Hsc70 and adaptor protein auxilin remove the clathrin coat while proteases convert proinsulin into insulin (Omar-Hmeadi & Idevall-Hagren, 2021). Due to hydrophobic interactions, insulin first dimerizes and then interacts with zinc to form hexamers. This structure is less stable than the dimers and allows for dissociation once insulin is secreted from the beta cell (Fu et al., 2013). These insulin hexamers localize to

the center of the granule while IAPP localizes to the perimeter of the granules (Westermark et al., 1996).

Once secreted, insulin travels via the circulatory system to reach peripheral tissues. It binds to insulin receptors primarily expressed by skeletal muscles and adipocytes. Upon insulin binding, two insulin receptors undergo crosslinking and activation of receptor tyrosine kinase to phosphorylate the insulin receptor substrate (IRS). IRS then acts as a scaffold protein that allows for activation of multiple signal pathways. This can include Ras pathway activation leading to protein synthesis and cell growth (De Meyts, 2000). It also induces activation of phosphoinositide 3-kinase (P13K) that leads to SNARE protein-mediated GLUT4 translocation (Thurmond & Pessin, 2000). Specifically, the SNARE protein syntaxin 4 of the GLUT4 containing vesicle interacts with Munc18c on the plasma membrane to promote membrane fusion and translocation of GLUT4 to the extracellular face of the plasma membrane (Thurmond & Pessin, 2000). Here, GLUT4 will uptake glucose via facilitative diffusion (De Meyts 2016) (Fig. 3C).

Once secreted, IAPP can interact with its receptors both within islets and distal tissues. Its receptor is comprised of receptor activity modifying proteins that heterodimerize with a G protein coupled receptor. IAPP causes receptor activation resulting in increased cyclic AMP and intracellular calcium. Through paracrine signaling, IAPP modulates secretory functions of surrounding islet cells (Akter et al., 2016). Many other tissue types also express the IAPP receptor. IAPP receptors are highly concentrated within the central nervous system, especially in the hindbrain. Here, IAPP binding to receptors within the area postrema system result in reduced food uptake (Bortoletto & Parchem, 2023; Mietlicki-Baase & Hayes, 2014) (Fig. 3D). Similar to insulin, IAPP can also target skeletal muscle but creates nearly opposite effects. While insulin

promotes skeletal muscle glucose uptake, IAPP both increases glycogenolysis and decreases glycogen synthases in this tissue (Castle et al., 1998).

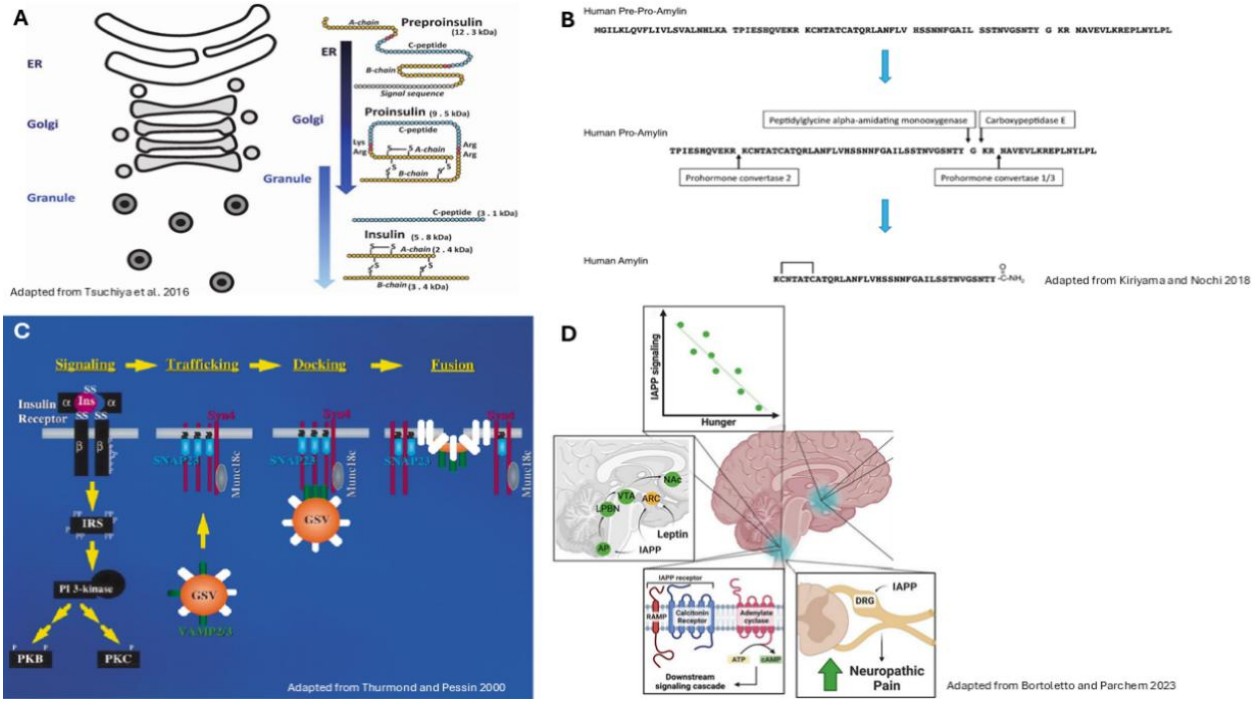

Figure 3: Beta cell insulin and IAPP production and signaling A) Insulin is synthesized as a preprohormone that undergoes cleavage and folding as it progresses from the ER to insulin granules. **B)** PreproIAPP follows a similar processing pattern as preproinsulin with cleavage by prohormone convertase 2 and 1/3 as well as C terminus amidation. **C)** Peripheral tissue insulin receptors dimerize upon insulin binding resulting in PI3-kinase activation. PI3-kinase promotes SNARE-mediated fusion of GLUT4-containing vesicles to the plasma membrane where these transporters can uptake excess blood glucose. **D)** IAPP binding to its G-protein coupled receptor results in cAMP production which creates different effects depending on the target tissue. Within the hindbrain, IAPP binding regulates blood glucose by modulating appetite and satiety.

Type Two Diabetes

Diabetes is the most common disease caused by pancreatic dysfunction. It is generally characterized by a loss of insulin secretion, leading to chronic hyperglycemia but has heterogenous causes. In type one diabetes, autoimmune-mediated elimination of beta cells and subsequent insulin production requires exogenous insulin supplementation. In type two diabetes, beta cells lose the ability to produce enough insulin to meet metabolic demands (Goyal et al., 2024a). This is partial due to insulin resistance in peripheral tissue where tissues express less insulin receptors and recycle them back to the plasma membrane slower to reduce their

sensitivity to insulin (Freeman et al., 2024). Additional defects in insulin secretion are required for disease development (Del Prato & Marchetti, 2004). In becoming "glucose blind", metabolic stress causes nuclear exclusion of the transcription factors hepatocyte nuclear factor-1α and forkhead box protein A2, leading to downregulation of *Mgtat4a,* which encodes the glycosyltransferase responsible for GLUT2 membrane localization. Without this enzyme, GLUT2 remains internalized. Furthermore, this nuclear exclusion also contributes to the downregulation of GLUT2 itself beta cells inundated with constant glucose lower their expression of GLUT2 and become less sensitive to glucose resulting in lower insulin secretion per beta cell (Thorens et al., 1990).

Chronic hyperglycemic and glucolipotoxicity lead to both oxidative stress and ER stress within beta cells leading to impaired insulin synthesis and secretion. Because beta cells have their low expression of the antioxidant enzymes catalase and glutathione, they are particularly vulnerable to oxidative stress caused by excessive buildup of metabolic byproducts from chronic hyperglycemia (Lei & Vatamaniuk, 2011a). The generated reactive oxygen species reduce *insulin* gene expression by preventing PDX1 from binding to the *insulin* gene promoter while also downregulating expression of PDX1 itself (Kaneto et al., 2010). The additional ER stress created initiates the unfolded protein response signaling pathways regulated by PERK, ATF6, and IRE1. These collectively work to restore ER homeostasis and prevent cell death through increased protein degradation, increased chaperon production, and decreased translation rates (Eizirik et al., 2008) (Fig. 4). While reduced translation protect the beta cell, it also reduces its function as insulin mRNA is rapidly decreased under ER stress (Pirot et al., 2007).

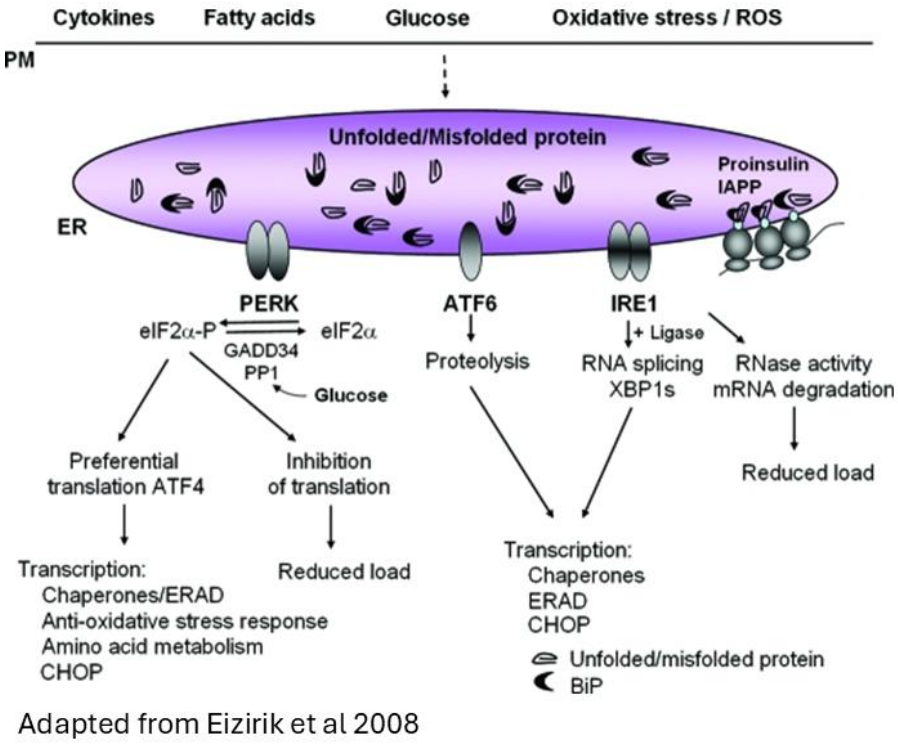

Figure 4: Uncoupled protein response in beta cells Chronic glucose, fatty acid, and/or oxidative stress contribute to ER stress that activates the unfolded protein response. Through PERK and IRE1, translation is inhibited, and RNase activity is increased. Through ATF6, proteolytic functions are increased. Through all three factors, transcription of chaperon proteins to limit and resolve protein misfolding are increased.

Despite improving treatments, approximately half of people with type two diabetes will fail to achieve glycemic control leading to microvascular and macrovascular complications like nephropathy and cardiovascular disease (Masaba & Mmusi-Phetoe, 2021)(Goyal et al., 2024a). As type two diabetes progresses, there is a loss of functional beta cell mass resulting in a further loss of insulin secretion due to a combination of beta cell apoptosis and de-differentiation (Prentki, 2006). Beta cell amyloidosis contributes heavily to apoptosis as amyloid fibrils are found in the majority of individuals with type two diabetes. These fibrils are comprised of IAPP oligomers. Interestingly, IAPP only oligomerizes in some species. While human IAPP is amyloidogenic, rodent IAPP will not oligomerize due to several proline substitutions that prevent beta-sheet formation (Betsholtz et al., 1989). The exact cause of IAPP oligomerization is

unknown but has been linked to impaired proteasome function. The 26S proteasome, comprised of a 20S proteolytic core and 19S regulatory component, degrade eukaryotic, non-lysosomal polyubiquitinated proteins including IAPP (Bhaumik & Malik, 2008). This process has been well described in age-related neurodegenerative diseases such as Alzheimer's Disease where protein plaques are a hallmark pathological feature (Stroo et al., 2017); however, the reason behind age-related proteasome impairment remains unknown. In type two diabetic islets, proteasome activity is similarly decreased. Without proteolytic activity, ubiquitinated proteins collect within the cell leading to protein stress that activates the unfolded protein response (Chatterjee Bhowmick & Jeremic, 2018a). Similar to ER stress, this response can protect beta cells acutely but leads to their dysfunction and apoptosis when chronic (Eizirik et al., 2008). Over time, IAPP oligomers cause protein stress leading to DNA damage, reactive oxygen species formation, ER dysfunction, reduced mitochondrial membrane potential, and decreased proteolytic functions through impaired autophagy and proteasome function (Stroo et al., 2017)(Fig. 5).

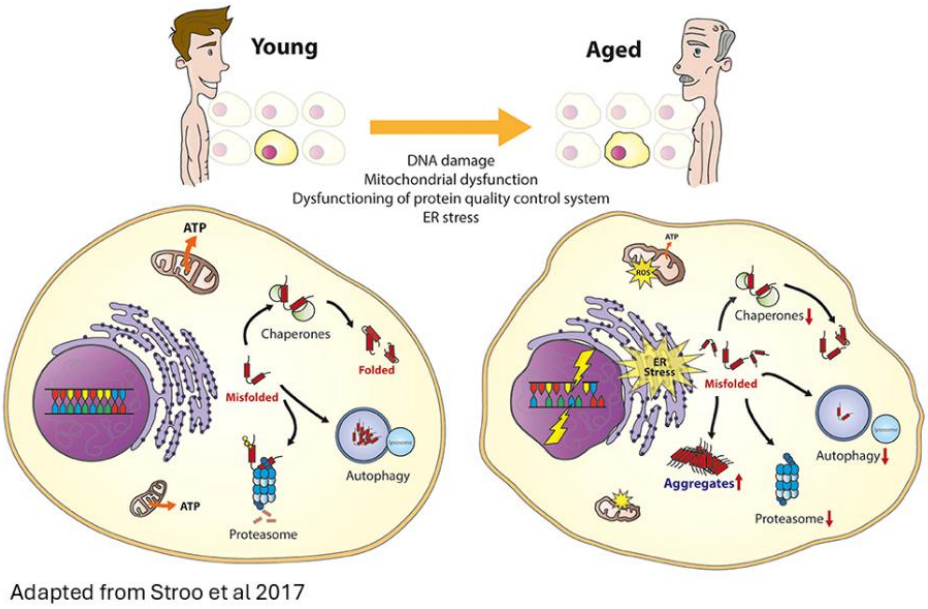

Figure 5: IAPP-induced cellular stress Age-related proteasome impairment allows for IAPP to misfold, form oligomers, and eventually form aggregated plaques. These oligomers and plaques create protein stress that disrupts essential cellular processes largely by overloading the protein quality control systems of the cell. This stress leads to DNA damage, mitochondrial impairment, ER stress, and decreased proteolytic function.

In both type two diabetic and proteasome-inhibited islets, both *IAPP* and *TXNIP* are downregulated (Chatterjee Bhowmick & Jeremic, 2018a). We have additionally identified several genes whose expression is downregulated in human pancreatic islets during both acute proteasome inhibition and type two diabetes (Table 1). Many of these genes are involved in either peptide hormone secretion, beta cell cellular respiration, or beta cell lineage commitment. Together, this data demonstrates the essential role of a functional proteasome in peptide hormone secretion as nearly every step of this process is affected including glucose uptake, ATP production, granule production, and peptide hormone transcription. Furthermore, the protective adaptation of beta cell dedifferentiation is seen within these proteasome impaired samples. Because human β cells replicate at low rates, dedifferentiation preserves β cell mass when cells are stressed by providing a protective alternative to apoptosis (Patel & Remedi, 2024a). By lowering expression of essential transcription factors, they lower the production of proteins needed to carry out their typical functions. This process preserves beta cells by lowering glucose uptake and cellular respiration, which lowers oxidative stress as well as decreasing IAPP production to limit oligomerization responsible for protein stress. We have found multiple genes responsible for beta cell lineage commitment such as *PDX1* and *NeuroD1* are downregulated during proteasome inhibition and type two diabetes suggesting that proteasome function may regulate beta cell dedifferentiation in type two diabetes (Table 1).

Table 1: Genes downregulated by proteasome inhibition and type two diabetes in primary human pancreatic islets

Gene Name	Encoded Protein	Protein Function
TXNIP	Thioredoxin interacting protein	Antioxidant protein; transcription factor
IAPP	Islet amyloid polypeptide	Peptide hormone
SLC30A8	Solute carrier 30 member 8	Granule secretion
SLC2A2	Glucose transporter 2	Beta cell glucose uptake
G6PC2	Glucose-6-phosphate catalytic subunit 2	Islet gluconeogenesis
PFKFB2	6-phosphofructo-2-kinase	Glycolysis
MAFA	MAF bZIP transcription factor	Insulin transcription factor
NeuroD1	NeuroD1	Insulin transcription factor

ISL1	Insulin gene enhancer-binding protein 1	Insulin and motor neuron transcription factor
NKX6.1	Homeobox protein Nkx6.1	Beta cell transcription factor
PAX4	Paired box 4	Beta cell transcription factor
PDX1	Pancreatic and duodenal homeobox 1	Pancreas transcription factor
FoxA2	Forkhead box protein A2	Liver and neuroendocrine transcription factor

In addition to metabolic and protein stress, proinflammatory conditions contribute to type two diabetes development. Resident macrophages within the pancreas maintain tissue homeostasis through remodeling and repair of tissue. As type two diabetes develops, more proinflammatory M1 macrophages accumulate within islets. Islet cellular stress produces danger-associated molecular patterns like fragmented DNA and amyloid plaque deposits recruit additional innate immune cells into the tissue (Meshkani & Vakili, 2016). As immune infiltration progresses, interleukin 1-beta (IL-1β) production increases, reducing insulin secretion and inducing apoptosis (Abdulreda & Berggren, 2013). Under chronic hyperglycemic conditions, pancreatic beta cells themselves also begin producing IL-1β. This process is mediated by hyperglycemia-induced O-GlcNAcylation of TXNIP (Filhoulaud et al., 2019). Across multiple cell types, TXNIP has also been implicated in the formation of the inflammasome (Filhoulaud et al., 2019). This post translational modification promotes TXNIP to interact with NOD-like receptor family pyrin domain containing 3 (NLRP3) required for beta cell inflammasome formation (Filhoulaud et al., 2019; Zhou et al., 2010). Interestingly, TXNIP utilizes other binding partners to form hyperglycemia-induced inflammasome formation in other tissues (Y. Liu et al., 2014; Zhou et al., 2010). Specifically, within cardiomyocytes binding between TXNIP and nuclear factor-κ B (NF-κ B) is required for NF- κ B nuclear import (Y. Liu et al., 2014). Additional work has shown the delirious effects of NF- κ B activation in pancreatic β cells as shown by NF- κ B-mediated upregulation of the proapoptotic Fas ligand by these cells (Maedler et al., 2002); however, little work has been done to confirm or refute TXNIP-NF-kB interactions within beta cells (Fig. 6).

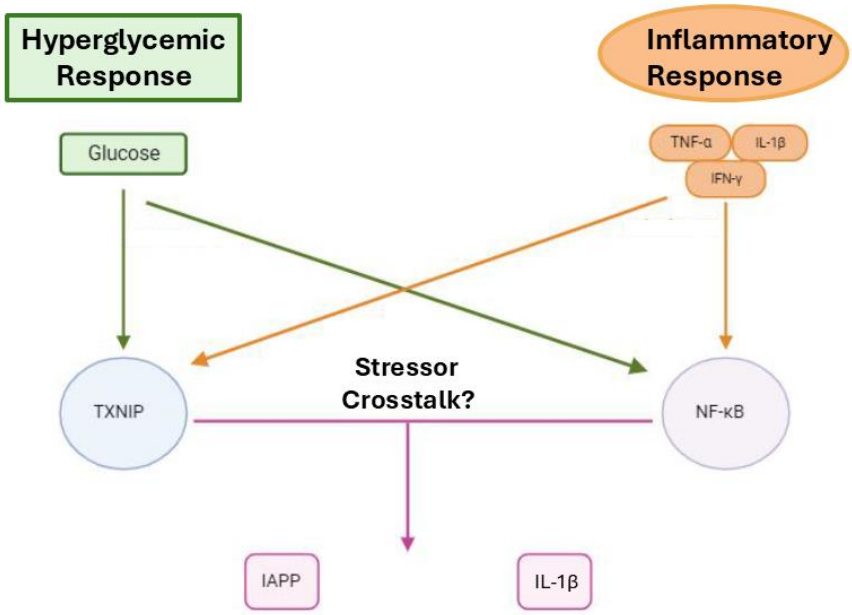

Figure 6: Potential crosstalk between metabolic and proinflammatory beta cell signaling Under hyperglycemic conditions, TXNIP is activated to increase IAPP production. Under proinflammatory conditions, NF-kB is activated to increase mature IL-1B production. Because TXNIP has been implicated in proinflammatory signaling with beta cells as well as other tissues, it may serve as a link between metabolic stress and initial stages of beta cell inflammatory signaling. This signaling may be through NF-kB as a binding partner as seen in cardiomyocytes.

Pharmacological Strategies to Target Diabetes Mellitus

At earlier stages of type two diabetes, treatments targeting beta cell insulin secretion have been used with success. Many of these treatments mimic physiological glucose-induced insulin secretion by promoting plasma membrane depolarization for calcium influx. Glucokinase activators increase glucokinase activity to increase the amount of glucose-6-phophate available for cellular respiration and subsequent ATP production for closure of potassium-ATP channels (Nakatsuma et al., 2016). Sulfonylureas promote plasma membrane depolarization by directly binding to and inhibition potassium-ATP channels (Ashcroft, 1996). GPR40, GPR119, and GLP-1 analogs all function by binding to their respective G-protein coupled receptors. GPR40 analog binding resulting in inositol triphosphate-mediated intracellular calcium mobilization from intracellular stores (Nakatsuma et al., 2016). Both GPR119 and GLP-1 analogs promote calcium

mobilization by through protein kinase A (Fig. 7). Despite their efficacy, these medications can cause gastrointestinal disturbances, nausea, and headaches. Others can exacerbate complications associated with type two diabetes as some sulfonylureas have been linked to further weight gain as well as cardiovascular events (Costello et al., 2024).

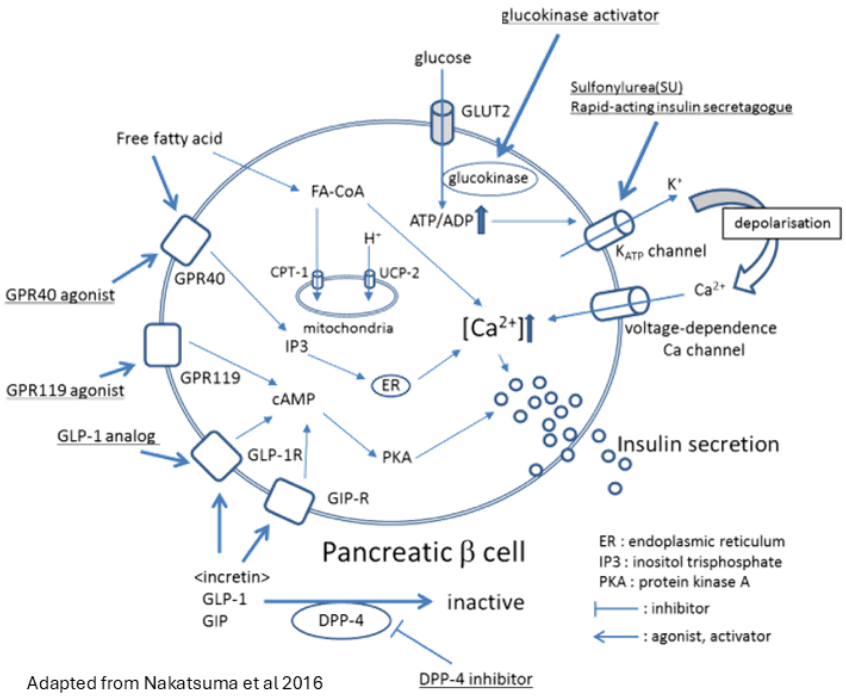

Figure 7: Mechanisms of common classes of type two diabetes drugs Many common type two diabetes drugs aim to increase free intracellular calcium within beta cells to promote insulin granule exocytosis. Both glucokinase activators and sulfonylureas inhibit potassium-ATP channels to cause plasma membrane depolarization resulting in calcium influx through voltage-gated calcium channels. Other pharmaceuticals target intracellular calcium stores to cause granule exocytosis through IP3 or cAMP signaling.

Nonpharmacological Strategies to Stimulate Hormone Release from Neuroendocrine Cells

Given the need for improved type two diabetes treatments, some groups have begun investigating mechanosensitive channels (MSC) as targets to promote insulin secretion from beta cells. MSC are broadly classified as membrane proteins that convert mechanical stimuli into an electrochemical response. Stimuli vary by specific channel but can include heat, cold, pressure, and stretch (Le Dain et al., 1998). Each specific MSC has its own unique stimuli; however, the

broad mechanisms of their regulation by stimuli type are similar. As MSC, this classification of membrane proteins is also sensitive to physical pressure, stretch, and deformations. All of these stimuli modulate MSC by causing physical deformations to the plasma membrane, which in turn causes deformation to the 3-dimensional structures MSC. By physically moving the membrane that the channel subunits are anchored to, the channel subunits themselves are moved into different conformations to modulate their gating properties (Fig. 8A). Additionally, many MSC function as intrinsic temperature-sensitive channels and respond to changes in temperature. Heating or cooling changes the free energy of a given system such as a cell. In MSC activated by heat, the additional free energy allows gating structures to change to a more disordered state. Conversely, MSC activated by the cold often function by stabilizing regions disordered at higher temperatures resulting in conformational changes to gating structures allowing ion influx (Fig. 8B). Similar to temperature, pH changes also modulate function of many MSC by altering protein stability. Specifically, pH changes alter protonation states of exposed channel regions. If the charge of a protein region changes, its current conformation may no longer be the most energetically favorable. This process would promote conformational changes that may alter channel structures to alter gating properties (Cesare et al., 1999). Like many other membrane proteins, MSC can be modulated by binding of specific ligands. Ligand binding causes structural changes influencing channel activity (Fig. 8C). Upon activation, MSC often function as nonselective cation channels that create an electrochemical response in cells by changing membrane potentials. Once inside the cell, these cations can also directly interact with their targets to promote protein conformation change and subsequent activity.

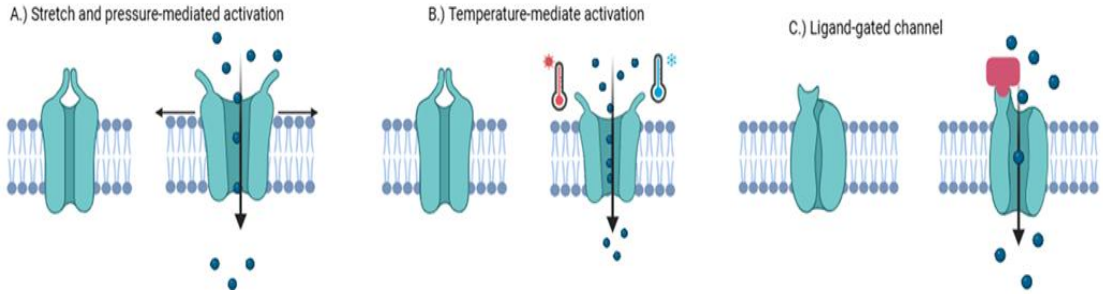

Figure 8 General mechanisms of mechanosensitive channel activation A) Stimuli that deform the membrane such as stretch and pressure activate MSC by inducing physical changes to the gating structures within the channels allowing for ion influx **B)** Thermal energy promotes changes in protein structure, including modulatory gating regions, that promote ion influx **C)** Ligand binding induces changes in channel structure resulting in ion influx.

Multiple groups have demonstrated the importance of mechanostimulation across various neuroendocrine cell types including chromaffin cells of the adrenal medulla, pulmonary neuroendocrine cells, and gastric X/A cells (Hu et al., 2009; Lembrechts et al., 2012; Y. Zhao et al., 2024). We have begun targeting these channels through therapeutic ultrasound (TUS) stimulation. Ultrasound energy travels as a wave with frequencies above the human hearing range at frequencies between 100 kilohertz and 18 megahertz (Fig. 9A) (Christensen, 1988). In clinical settings, ultrasound can be used in imaging or therapeutic modalities. In contrast to sonographic ultrasound used for diagnostic imaging, TUS is applied at higher intensities in order to evoke responses from treated tissues. This therapy has been used successfully in multiple applications including atrial ablation for the treatment of atrial fibrillation as well as promoting bone regeneration in fractures (Matthews & Stretanski, 2024). To elicit responses from tissues, several possible mechanisms exist. TUS is known to induce reactive oxygen species formation, likely due to shear stress associated with acoustic streaming or microstreaming of bubbles during treatment (Fig. 9B). Previous works have shown this effect occurs in a dose-dependent manner correlating with the degree of sample sonication (Jia et al., 2018). Regardless of the specific mechanism, TUS-induced activation of MSC channels results in cation influx (Fig. 9C). In neuroendocrine cells like beta cells, this calcium influx increases calcium-mediated hormone

secretion. Our electrophysiological studies demonstrated that TUS stimulates secretion in insulinoma cells via calcium influx (I. Suarez Castellanos, Singh, et al., 2017a). Although mechanism(s) behind this process remains to be fully elucidated, recent ultrasound studies demonstrated the important role of calcium in mechanostimulation-induced insulin release from pancreatic beta cells. Within the HIT-T15 pancreatic beta cell line, low intensity pulsed ultrasound has been shown to evoke both fast-irregular and slow periodic calcium oscillations in a purinergic receptor-dependent mechanism (Yoon et al., 2020). Given the integration of mechanical forces and cation influx, MSC are potential mediator of this mechanism. Specific channels like piezo1 have been directly linked to insulin secretion as application of the peizo1-specific agonist Yoda1 induces insulin secretion from both human and rodent pancreatic islets (Ye et al., 2022). Furthermore, mechanostimulation of thyroid neuroendocrine cells modulate gene expression. Physiological vibration similar to those created by the vocal cords decrease their expression of the hormone precursor thyroglobulin while pressure from hypergravity upregulates their expression of thyrotropin receptors (Meli et al., 1998; Wagner et al., 2016); however, the mechanism(s) through which mechanostimulation modulates gene expression through remains unknown. Thus, it is possible that TUS may activate mechano-sensitive channels like Piezo and/or transient receptor potential subtype vanilloid to induce gene expression and/or activate signaling pathways in beta-cells implicated in hormone secretion such as calcium and ROS mobilization (Fig. 9C), which was investigated in chapter 1 of this dissertation.

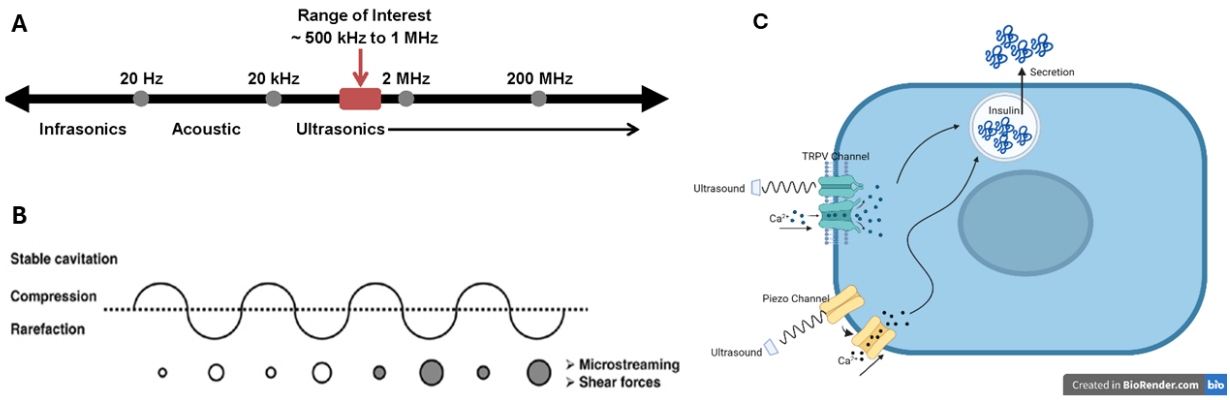

Figure 9: Therapeutic Ultrasound and its Effects on Tissues A) Ultrasound energy travels in longitudinal waves at frequencies higher than human hearing, ranging from 100 KHz to 18 MHz **B)** As ultrasound travels through a medium, it creates regions of high pressure known as compression and regions of low pressure referred to as rarefaction. These regions of varying pressures form microscopic voids characterized by small oscillations of bubbles through a phenomenon known as stable cavitation. The flow around these bubbles is referred to as microstreaming **C)** MSC like TRPV and Piezo may be activated by TUS to allow for calcium influx. In beta cells, this calcium influx results in insulin secretion.

Overview of Dissertation Structure

This dissertation investigates mechanisms driving type two diabetes development with an emphasis on the effects of proteasome dysfunction and inflammatory stress within pancreatic beta cells as well as elucidating possible mechanism(s) driving TUS-induced insulin secretion as a potential treatment for this disease. This work begins with an introduction, providing foundational knowledge required. It is followed by three chapters, driven by experimental data. Each addresses a distinct topic within the dissertation.

In Chapter 1, Mechanosensitive Channels Mediate Pancreatic β Cells Reactive Oxygen Species Formation and Downregulation of Essential Genes during Therapeutic Ultrasound Treatment, we investigate potential mechanism of TUS-induced insulin secretion by targeting MSC. We found expression of common MSC isoforms across our pancreatic beta cell model systems. Activation of these channels were then coupled to ROS formation and downregulation of essential beta cell genes including *insulin* and *IAPP.*

Chapter 2,

In Chapter 3, Proteasome activity is critical for beta cell identity and glucose sensing, we assess the effects of protein stress due to proteasome inhibition on pancreatic beta cells. Through RNA sequencing we found that both acute, pharmacological and chronic type two diabetic human pancreatic islets show downregulation of genes essential for beta cell phenotypic identity, glucose sensing, and peptide hormone secretion. Downregulation of select beta cell identity genes was confirmed through qPCR and western blot analysis. Functional studies demonstrated reduced pyruvate production and mitochondrial membrane potential, suggesting impaired glycolytic flux in proteasome inhibited beta cells.

Chapter 1: Mechanosensitive Channels Mediate Pancreatic β Cells Reactive Oxygen Species Formation and Downregulation of Essential Genes during Therapeutic Ultrasound Treatment

Abstract

Objective

Type two diabetes is partially caused by insufficient pancreatic β cell insulin secretion. Previous studies show therapeutic ultrasound (TUS) evokes insulin secretion from β cells; however, how β cells sense TUS and the broad effects of this treatment on cells remain unknown. Here, we identified mechanosensitive channels (MSC) expressed by β cells and TUS-mediated gene downregulation and reactive oxygen species (ROS) formation.

Methods

For all experiments, 1 W/cm^2 intensity and 800 kHz frequency TUS was continuously applied for 5 minutes. To determine MSC expression, RNA and protein were isolated from human pancreatic islets and the rat insulinoma cell line INS 832/13 and analyzed via rt-qPCR or western blot, respectively. INS cells treated with MSC agonists and/or antagonists during TUS were visualized via florescent microscopy to track ROS formation. Using the same treatments, rt-qPCR analysis of INS *insulin* and *IAPP* was performed. TUS treatments were replicated in rats that pancreatic sections were collected for immunohistochemistry analysis.

Results

We found expression of TRPV2, TRPV5, and piezo1 in human islets and INS cells. TUS increased ROS formation in INS cell compared to sham-treated controls ($p<0.0001$); however, modulation of MSC mitigated this effect ($p<0.001$). TUS decreased expression of the *insulin* and *IAPP* genes in INS cells compared to sham-treated controls ($p<0.001$ and $p<0.01$, respectively); however, complete MSC inhibition reversed this effect ($p<0.01$ and $p<0.05$, respectively). In our rat model, PDX1 expression was decreased by TUS compared to sham-treated controls (*$p<0.05$); however, TUS did not decrease insulin or IAPP levels ($p>0.05$).

Conclusion

We report expression of TRPV2, TRPV5, and piezo1 in human and rodent pancreatic β cells that are implicated in both TUS-mediated ROS formation and downregulation of essential β cell genes.

Introduction

Glucose homeostasis is largely regulated by endocrine pancreatic islets of Langerhans. Within these islets, β cells secrete insulin in response to increases in blood glucose. This insulin then travels to peripheral tissues like adipose and muscle tissue where it promotes translocation of glucose transporters for uptake of excess blood glucose. Inside peripheral tissues, this glucose can be metabolized to generate ATP for cellular energy or stored for future utilization as glycogen (Röder et al., 2016).

Type two diabetes mellitus (T2D) is a multifactorial disease where genetic and environmental factors in combination with lifestyle choices lead to chronic hyperglycemia. Endocrine pancreatic islet β cells lose the ability to produce enough insulin to meet metabolic demands. Peripheral tissues decrease their plasma membrane expression of insulin receptors and have defective insulin receptor cascades contributing to impaired responses; however, the exact mechanism varies by tissue type. Both of these mechanisms are seen in skeletal muscle insulin resistance where chronic hyperinsulinemia downregulates both the glucose transporter GLUT4 and the insulin receptor kinase required for intracellular signaling (Petersen & Shulman, 2018). Peripheral insulin resistance alone is insufficient to cause disease, and there must therefore be an additional defect in insulin secretion for T2D to develop (Del Prato & Marchetti, 2004). Beta cells under constant glucose stimulation must increase oxidative phosphorylation to metabolize the glucose into ATP; however, this process results in increased mitochondrial membrane potential and production of reactive oxygen species (ROS). Transient ROS play an important regulatory role in stress and function of islet b cells such as modulation of insulin release (Leloup et al., 2009a). Specifically, studies revealed that mitochondrial ROS species are indispensable for glucose-evoked, calcium-mediated insulin release from pancreatic b cells (Leloup et al.,

2009b). When too much ROS are produced, β cells activate uncoupling protein 2 that lowers mitochondrial membrane potential by promoting membrane proton leak as a protective adaptation. While protecting the cell, this process decouples mitochondrial function and ATP production resulting in lower ATP production and subsequent insulin secretion (Prentki, 2006). As disease further develops, β cells become "glucose blind" in which cells inundated with constant glucose lower their glucose transporter (GLUT) expression and become less sensitive to glucose. Under metabolic stress, nuclear exclusion of the transcription factors hepatocyte nuclear factor-1α and forkhead box protein A2 lead to downregulation of *Mgtat4a* which encodes the glycosyltransferase responsible for GLUT2 membrane localization. Without this enzyme, GLUT2 remains internalized. Furthermore, this nuclear exclusion also contributes to the downregulation of GLUT2 itself (Ohtsubo et al., 2011). This adaption protects cells from metabolic stress that, unchecked, leads to damage and cell death (Ohtsubo et al., 2011). Despite this adaptation, these β cells begin undergoing dedifferentiation and apoptosis that reduces functional β cells mass, resulting in a further decrease in insulin secretion as T2D progresses (Prentki, 2006).

Current treatments for T2D are focused on lifestyle changes and pharmaceutical interventions, but lifestyle modification can be ineffective due to high rates of patient noncompliance (Galaviz et al., 2018). Pharmaceutical interventions often target gastric glucose absorption or pancreatic β cell insulin secretion. Although effective in some cases, these drugs carry side effects that can exacerbate complications from T2D including weight gain and cardiovascular events. Treatments targeting insulin secretion lose efficacy over time as functional β cell mass decreases with disease duration(Marín-Peñalver et al., 2016). Furthermore, individuals with T2D are still at risk for other disorders like hypercholesterolemia and hypertension. More complicated

polypharmaceutic medication regimens contribute to higher rates of noncompliance and increased health care costs. Given that approximately 10% of the population of United States has T2D as of 2022, the lack of sustainable effective treatment creates a massive public health burden and lowers the quality of life for approximately 37 million people (Center for Disease Control and Prevention, 2024). Approximately half of people with T2D will fail to achieve glycemic control, leading to both microvascular complications like retinopathy and nephropathy as well as macrovascular comorbidities like cardiovascular disease (Goyal et al., 2024a; Masaba & Mmusi-Phetoe, 2021).

Additional works have found expression of select mechanosensitive channels (MSC) within both human and rodent pancreatic islets (Bulut Arikan, 2020; Matos et al., 2022; Philippaert & Vennekens, 2017; Sawatani et al., 2019b). These plasma membrane channels act as receptors to detect mechanical stimuli like temperature or pressure and convert these stimuli into electrochemical responses (Le Dain et al., 1998). To transduce these signals, these receptors function as cation channels so that their activation results in membrane depolarization required for hormone release (Skrzypski et al., 2013). Pharmacological activation of the MSC Piezo1 has been shown to induce insulin secretion from pancreatic β cell lines and mouse islets (Deivasikamani et al., 2019a). These findings have allowed mechanostimulation to become a potential therapeutic target for endocrine pancreatic diseases like T2D. Unfocused, low intensity ultrasound may provide an alternative non-pharmacological, non-invasive treatment for this disease. In contrast to sonographic ultrasound used for diagnostic imaging, therapeutic ultrasound (TUS) is applied at higher intensities in order to evoke responses from treated tissues. This therapy has been used successfully in multiple applications including atrial ablation for the treatment of atrial fibrillation as well as promoting bone regeneration in fractures (Matthews &

Stretanski, 2024). Our lab previously determined ultrasound parameters that promote pancreas insulin secretion without significant decreases in cell viability (I. Suarez Castellanos, Jeremic, et al., 2017b). We and other groups have also shown focused ultrasound modulate intracellular calcium as a major mediator of insulin vesicle exocytosis (I. Suarez Castellanos, Singh, et al., 2017a; Yoon et al., 2020), however, the broader effects of ultrasound on these cells such as redox homeostasis and gene regulation remains unknown. Currently, it is also unknown how pancreatic β cells sense ultrasound. Here, we examined the hypothetical impact and mechanism of TUS on redox state and b cell differentiation in human and rat pancreatic islets and the INS 832/13 cell line by analyzing changes in ROS levels and expression of essential β cell genes including *PDX1*, *islet amyloid polypeptide* (*IAPP)* and *insulin,* respectively. The expression of MSC and their possible mediatory role in provides a possible TUS detection mechanism within these cells. TUS-mediated ROS formation and expression of endocrine gene markers in rat β cells were concurrently analyzed. Data suggest that TUS stimulation of these cells mobilize ROS and induce loss of select β cell genes *in vitro* and *in vivo*. MSC inhibitors only partially reversed this modulatory effect of TUS in INS cells, suggesting additional mechanisms and mediators of TUS action in these cells.

Materials and Methods

Cell Cultures

Rat insulinoma INS 832/13 cells (a generous gift from Christopher Newgard, Duke University) were cultured in RPMI 1640 media (ThermoFisher Scientific catalog number 11875093) supplemented with 1% penicillin/ streptomycin (ATCC catalog number 30-2300), 10mM HEPES (Gibco catalog number 15630-080), 2mM L-glutamate (Sigma Aldrich G8415), 1 mM sodium pyruvate (Sigma Aldrich S8636), 0.05 mM 2-mercaptoethanol (Sigma M3148) , and 10% (v/v)

fetal bovine serum (ThermoFisher Scientific catalog number 26140079). Insulinoma cells were stored at 37°C in a humidified incubator with 5% CO_2 and passaged every 3 to 4 days. Prior to treatments, cells were plated in a 6 well plate (Grainger catalog number 38C786).

In addition to INS cell lines, human pancreatic islets from non-diabetic cadavers with >90% viability and purity were obtained through the Integrated Islet Distribution Program (IIDP) for Human Islet Research. These islets are from an approved cadaveric organ, therefore the tissue is exempt from human studies approval per IIDP guidelines. Privacy and personal identity information of all participants was protected. Studies using human islets were approved by The George Washington University Institutional Review Board (IBC#IBC-20-092). Upon arrival, intact islets were plated on a non-adherent 48 well plate in CMRL media (ThermoFisher Scientific catalog number 11530037) supplemented with 1% (V/V) fetal bovine serum (ThermoFisher Scientific catalog number 26140079) and 1% penicillin/streptomycin (ATCC catalog number 30-2300). Islets were cultured in a humidified incubator at 37°C with 5% CO_2 and given 48 hours to equilibrate before treatments.

For all experiments and treatments, cells were equilibrated in 5mM glucose media for 24 hours prior to treatments. To treat cells, media was supplemented with stimulatory 20 mM glucose (Sigma Aldrich catalog number G8270), the ROS donor 100 μM hydrogen peroxide (Fisher Scientific catalog number BP2633500), the Piezo1 agonist 10 μM Yoda-1 (Tocris Bioscience), the Piezo1 antagonist 10 μM Doku-1 (Tocris Bioscience), and/or the broad MSC inhibitor 1 μM ruthenium red (Sigma Aldrich).

Ultrasound Application to Cell Cultures and Islets

Previously, TUS at 800 kHz frequency and 1W/cm^2 applied continuously for 5-minute intervals was shown to induce insulin secretion from pancreatic insulinoma cells and mouse pancreas

without any toxic effects, and hence we adopted these parameters for our current studies (Singh et al., 2020a; I. Suarez Castellanos, Jeremic, et al., 2017a; I. M. Suarez Castellanos et al., 2016). A circular planar ultrasound transducer with an active diameter of 1.5 cm and center frequency of 800 KHz (Sonic Concepts, Inc., Bothell, WA, USA) was used to deliver ultrasound. Ultrasound waves were generated by an Agilent arbitrary waveform generator model 33220A (Agilent Technologies, Santa Cruz, CA, USA) and amplified with a 50 dB gain using an Ar RF/Microwave Instrumentation amplifier model 150A100D (Amplifier Research, Souderton, PA, USA) (Fig. 1 A). Prior to cell treatments, verification of ultrasound signal and intensity was performed by reflective radiation force balance measurements (Ultrasound power meter, Ohmic Instruments, Easton, MD, USA) to ensure that 1 W/cm^2 ultrasound intensity was consistently delivered to plated cells. During experiments, plated cells (Grainger catalog number 38C786) were positioned with a Thorlabs XYZ translation stage (Thorlabs) in a water bath. An Omega thermometer (model HH911T) was used to ensure there was minimal changes to media temperature because MSC can be activated by temperature stimuli as well as ultrasound. As shown by the 13°C increase in temperature, TUS significantly heated wells when no heat sink was present. When the system was placed into a water bath, only a 3°C increase was observed preventing convoluting effects from heating. (Fig. 1 B). Hence, all TUS treatments to plated cells were performed in a water bath to prevent heat impact, which assured that mechanical rather than thermal stimulation of our cells were achieved in our experiments. The face of the ultrasound transducer was placed 2.5 cm under the bottom of the well being treated which corresponds to its near-field to far-field distances (Christensen, 1988).

Real Time – Quantitative PCR

Twenty-four hours after treatment, total RNA was isolated from cells via Qiagen RNeasy mini kit per manufacturer instructions (Qiagen catalog number 74134). RNA concentrations were determined via Nanodrop. From each sample, 400 ng of RNA was converted into cDNA using a multiScribe reverse transcription kit with random primers following manufacture instruction (Applied Biosystems catalog number 4368814). qPCR was then performed with resulting cDNA via iTaq Universal SYBR Green supermix (BioRad catalog number 1725122) and primers listed in Tables 1 and 2. Bio Rad CFX 96 real-time system and C1000 Touch thermal cycler were used for amplification and gene detection. Expression levels of all genes were normalized to β -actin expression. Fold change in expression of these genes was calculated using the 2-delta CT method.

Western Blot

Twenty-four hours after treatments, whole cell extracts were collected in RIPA buffer (EMD Millipore, catalog number 20-188). Extracted protein concentrations were determined using the Pierce BCA Protein Assay Kit (Thermo Scientific reference number 23227). Four micrograms of protein were used for each well. Proteins were separated by SDS-PAGE on a 4-15% stacking gel (BioRad, catalog number 4561086). Resolved proteins were electrophoretically transferred to nitrocellulose membranes (BioRad catalog number 1704270) using the BioRad Trans-Blot Turbo System. Membranes were blocked with 5% nonfat dry milk. Membranes were probed with primary antibodies targeting MSC identified by rt-qPCR results for one hour at room temperature with shaking. The following proteins were targeted by primary antibodies: β-actin (Santa Cruz catalog number sc-47778 HRP, 1:500), TRPV2 (ThermoFisher catalog number OSRPOO19OW, 1:500), TRPV5 (Abcam catalog number 137028, 1:1000), and piezo1 (Proteintech catalog number 28511-1-AP, 1:1000). Then, corresponding horseradish peroxidase-

conjugated secondary antibodies were added at 1:2000 and incubated at room temperature for one hour. Resulting blots were developed using pico – (ThermoFisher Scientific no. 34580) or femto – (ThermoFisher Scientific no. 34095) ECL substrate kits and visualized with the ChemiDOC touch gel imaging system (BioRad). Intensity of the resulting bands was quantified using BioRad Image-Lab software where β-actin was used as a loading control.

Confocal Microscopy of Mechanosensitive Channels

INS cells were plated on poly-D-lysine coated 96-well glass bottom black microplates. Cells were incubated with 1μg/mL Cholera toxin subunit B (ThermoFisher Scientific catalog number C34776) at 4°C for 10 minutes. Cells were then fixed by 1 hour incubation with 4% paraformaldehyde (Sigma Aldrich catalog number 158127) and blocked in PBS supplemented with 1% BSA and 0.1% 100x-Triton. Next, primary antibodies listed in the previous section were incubated with cells at 4°C overnight. Corresponding secondary antibody was then added at 1:400 and incubated at room temperature for 1 hour. Cells were then incubated with DAPI (Cell Signaling catalog number 4083) in PBS for 20 minutes prior to imaging. Images were taken using a Zeiss LSCM-800 confocal microscope (Carl Zeiss, Thornwood, NY) at 40x magnification.

Reactive Oxygen Species Quantification

INS 832/13 cells were plated on poly-D-lysine coated 96-well glass bottom black microplates in 5 mM media. To treat cells, media was supplemented with 500 nM ATP (Sigma Aldrich catalog number 11140965001), 100 μM hydrogen peroxide (Fisher Scientific catalog number BP2633500), 10 μM Yoda-1 (Tocris Bioscience catalog number 5586), 10 μM Doku-1 (Tocris Bioscience catalog number 6568), or 1 μM ruthenium red (Sigma Aldrich catalog number 12790-48-6). Therapeutic ultrasound treatments are described above and illustrated in Fig. 1.

Cells were fixed to the plate with 4% paraformaldehyde 24 hours after treatments (Sigma Aldrich catalog number 158127). Five micromolar CellROX Deep Red Reagent for oxidative stress detection (ThermoFisher Scientific catalog number C10422) was used to visualize reactive oxygen species formation in cells. DAPI (Cell Signaling catalog number 4083) was used to counterstain nuclei. Two dimensional fluorescent optical sections were acquired across 6 randomly selected fields of view of each treatment. Quantitative analysis of images began with background subtraction of signal and determining the relative fluorescent intensity (RFUs) at the 647 nm wavelength using Zeiss section ROI analysis tools. Data was derived from three images from two sets of independent experiments.

Animal Experiments

All animal experiments were performed in accordance with the Institutional Animal Care and Use Committee (IACUC)-approved guidelines at The George Washington University Medical Center (protocol #A2023-035) and conform to NIH guidelines and federal law. Zucker Diabetic Fatty (ZDF) rats (obese fa/fa) and Zucker rat strain (lean) were purchased from Charles River Laboratories (Wilmington, MA). Rats were maintained on a 12hr/12hr light/dark cycle with free access to water and chow. Lean animals were provided standard chow while fatty animals were provided high fat chow (Purina 5008). Prior to treatment group assignments, all rats had blood glucose testing to confirm (fatty) or refute (lean) hyperglycemia indicating diabetic phenotype development. Blood samples for blood glucose testing were collected via tail nick.

Zucker Diabetic Fatty (ZDF) rats and matched lean Zucker rats were equally divided into two groups with 3 lean and 3 fatty animals in each group: ultrasound-treated and sham groups. Both groups were anesthetized via isoflurane inhalation delivered by an EX-SA800 Single Animal System to ensure animals remained still so the ultrasound transducer remained in place during

treatments. Fur was removed from the stomach via Nair. Ultrasound waves were generated by an Agilent arbitrary waveform generator model 33220A (Agilent Technologies, Santa Cruz, CA, USA) and amplified with a 50 dB gain using an Ar RF/Microwave Instrumentation amplifier model 150A100D (Amplifier Research, Souderton, PA, USA). Utilizing parameters determined in previous *in vitro* studies, rats were treated continuously with 800 KHz ultrasound for an intensity of 1 W/cm^2 for 5 minutes. An Omega thermometer (model HH911T) was used to ensure the ultrasound transducer did not heat enough to cause burns (Fig. 2 A). Temperatures rose from an initial average of 25°C to a final average of 41°C during animal treatment (Fig 2 B).

Immunohistochemistry

Following CO_2 asphyxiation euthanasia, whole pancreases were removed from rats, immediately fixed in 4% paraformaldehyde, and stored at 4°C. Fixed pancreases were sent to Histoserv (Germantown, MD) to prepare paraffin-embedded 4uM thick pancreatic sections. Sections were deparaffinized with xylene followed by ethanol washes. A Tris-EDTA buffer comprised of 10 mM Tris (VWR M151), 1 mM EDTA (Sigma Aldrich ED4SS), 0.05% Tween 20 (VWR M147), pH 9.0 was used for heat-mediated antigen retrieval. Sections were then blocked overnight in a blocking buffer comprised of 2% normal goat serum (Gibco PCN5000) and 0.2% Triton X-100 in PBS at 4°C. Primary antibodies against insulin conjugated to AlexaFluor 546 (Santa Cruz catalog number sc-8033), IAPP (AbboMax catalog number 500-3404), or PDX1 (Abcam catalog number 47267) were diluted 1:100 in blocking buffer and incubated on sections for 2 hours at room temperature. Sections were then washed three times in PBS with 0.01% Tween 20. Sections stained for PDX1 or IAPP were then incubated with donkey anti-rabbit IgG conjugated to AlexaFluor 488 secondary antibody (Life Technologies catalog number A11034) for one hour at room temperature. All sections were then mounted with SlowFade Diamond Antifade

Mountant (Invitrogen S36963) and imaged using a Zeiss LSM 800 confocal microscope (Carl Zeiss, Thornwood, NY). Histological data was collected from at least three random islet-containing fields per experimental group. Expression of the transcription factor PDX1 as well as the peptide hormones insulin and IAPP was assessed in these sections via immunohistochemistry.

Statistical Analysis

For all experiments, statistical analysis and graph plotting was performed using GraphPad Prism 10. Datasets were tested for Gaussian distribution and equal variance prior to analysis. If both tests were passed, data was analyzed via one-way ANOVA followed by a Tukey post hoc test with significance established at $p<0.05$. For datasets without normal distribution, a Kruskal-Wallis test was used followed by a Dunn's multiple comparison test with significance established at $p<0.05$. Microscopy analysis was performed using ≥ 3 images from 2 independent experiments for cell lines or 2 separate animals. Histograms depict the average of all collected data points +/- SEM.

Results

INS Cells and Human Islets Express Mechanosensitive Channels

First, we used rt-qPCR and western blot/microscopy approaches (Fig. 3) to screen for possible expression and location of multiple MSC in glucose-responsive, insulin-secreting rodent INS cells. In addition to insulinoma cells, we also used human islets for comparative analysis of MSC channel expression in different b cell backgrounds. Peizo1 was the only piezo mechanosensitive family member expressed by INS cells at transcriptional level (Fig. 3A). Two members of TRPV mechanosensitive channel family, TRPV2 and TRPV5, were also expressed (Fig. 3A). Similar to rat insulinoma cells, human islets expressed piezo1 as well as several TRPV isoforms including

TRPV2 and TRPV5 (Fig. 3B). Thus, across both b-cell model systems, these three mechanosensitive channels were expressed. Next, we tested if TUS modulates MSC expression or membrane localization, which are important for their mechanosensitive transduction and functions in cells. In addition to mechanical stimulation through TUS application, we tested effect of metabolic stimulus (20 mM high glucose) on MSC expression and trafficking, as both stimuli trigger calcium-mediated insulin release from these cells (Castellanos et al., 2016; I. Suarez Castellanos, Singh, et al., 2017b; Yoon et al., 2020). Interestingly, in the β cell model cell line INS 832/13, mRNA expression of both TRPV isoforms but not Piezo-1could be modulated by treatments. Specifically, high glucose significantly ($p<0.05$, $n=3$) decreased expression of both TRPV isoforms, while only TRPV2 gene expression was also decreased by TUS (Fig. 3A). Human islets did not share this trend as neither high glucose nor TUS significantly changed expression of the three tested mechanosensitive channels (Fig. 3B), highlighting some differences between the b-cell insulinoma cell line and human primary tissues in TUS-mediated MSC gene expression.

The expression of these channels was subsequently verified at protein levels. To this end, protein extracts were collected from INS cells and human islets for western blot analysis of MSC expression. Comparable MSC protein levels of TRPV2, TRPV5, and piezo1 were detected under control and stimulated (HG, TUS) conditions ($p>0.05$, $n=3$) in both rat INS cells (Fig. 3C) and human islets (Fig. 3D). Only TRPV2 and TRPV5 subunit monomers were detected as illustrated by the singular band western blot pattern (Fig. 3 E-H). In contrast, both piezo subunit monomers and homomeric complexes were detected as shown by the variances in molecular weights (Fig. 3 E and G). This result supports the general trend seen in islets where MSC mRNA levels are unaffected by chemical and TUS stimulation.

To verify western blot findings and to assess subcellular localization of channels, fixed INS cells were first stained with CTX-B to show the plasma membrane and counterstained with DAPI to show the nucleus. MSC were then localized using isoform specific primary antibodies followed by fluorescently labeled secondary antibodies staining. LSCM revealed that all three MSC proteins were expressed by INS cells but with different staining patterns: TRPV2 and Piezo1 had more diffuse staining, while TRPV5 showed more punctuated staining at the plasma membrane (Fig. 3 I-K). LSCM uncovered many MSC channels sequestered in the reserved, vesicular pool near the plasma membrane (Fig. 3 I-K, insets).

TUS promotes ROS Formation through MSC

We previously demonstrated that TUS stimulates secretory responses and insulin release from insulinoma cells via calcium-dependent process (I. Suarez Castellanos, Singh, et al., 2017a). Mitochondrial ROS are essential for calcium oscillations required for insulin secretion (Leloup et al., 2009b); however the effect of TUS on ROS mobilization and dynamics in pancreatic b-cells remain unclear. Hence, to determine the specific effect of TUS on ROS formation in pancreatic β cells, ROS formation was assessed INS 832/13 through ROS-sensitive florescent probes and microscopy.

INS cells were treated with continuous, unfocused ultrasound at an intensity of 1W/cm^2 for 5 minutes and compared to the controls 5 mM glucose, 100 μM H_2O_2, or 500 nM ATP. As expected, extracellular H_2O_2 increased ROS formation with a mean of 12721 ± 5342 in comparison to 5 mM glucose mean of 6875 ±3626 (****$p<0.0001$). In contrast, the stimulatory molecule and calcium mobilizing agent ATP did not evoke significant changes to cellular ROS content shown by a mean RFU of 8139 ± 5405 (Blachier & Malaisse, 1988). Data also demonstrated a significant increase in ROS formation in TUS-treated INS cells relative to

untreated 5 mM glucose treated cells with a mean of 9228 ± 4276 (Fig. 4 A, ****p<0.0001). To determine if MSC expressed by β cells were involved in this TUS-induced ROS formation, INS cells were treated with the broad mechanosensitive channel inhibitor ruthenium red, the Piezo1-specific agonist Yoda-1, and/or the Piezo1-specific antagonist Doku-1. Application of these compound alone did not alter ROS accumulation in cells relative to 5mM glucose control treatments (Fig. 4 B). When cells were pretreated with compounds prior to TUS treatments, all agonists and antagonists caused significant decreases in ROS production. In comparison to the TUS treated cell mean RFU of 9228 ± 4276, TUS treatments in the presence of Yoda-1, Doku-1, both Yoda-1 and Doku-1, or ruthenium red yielded average means of 7581 ± 4522(***p<0.001), 5603 ± 2274 (****p<0.0001), 5295 ± 2204 (****p<0.0001), and 5132 ± 2310 (****p<0.0001), respectively. Overall, data suggest a role for MSC in TUS-induced ROS formation as any modulation of channel during TUS significantly alters ROS formation.

TUS Decreases Expression of β *Cell Identity Genes in the INS Cell Line*

To further examine the biological impact of TUS-evoked ROS formation in pancreatic β cells, expression of essential β cell genes and hormones, insulin and islet amyloid polypeptide (IAPP), was examined through rt-qPCR analysis. Like for ROS studies (Fig. 5), INS 823/13 cells were mechanostimulated with TUS in the presence or absence of selective MSC agonists and/or antagonists. TUS treatment decreased expression of both of these genes, whereas H_2O_2 treatment did not alter the expression of either gene relative to untreated controls, suggesting a TUS-induced H_2O_2-independent mechanism of gene downregulation (Fig. 5 A and C, n≥3, **p<0.01 and ***p<0.001). Without TUS treatment, no tested MSC agonist or antagonist significantly effected expression of *insulin* or *IAPP* relative untreated control samples (Fig. 5 A and C, n≥3, p>0.05). When additionally treated with TUS, neither the piezo1-specific agonist Yoda-1 or

antagonist Doku-1 effected *insulin* or *IAPP* expression in comparison to TUS samples suggesting a pizeo1 independent mechanism of TUS-induced gene downregulation (Fig. 5 B and D, $n \geq 3$, $p > 0.05$). In contrast, application of the general MSC antagonist, ruthenium red, during TUS treatment caused an increase in both *insulin* and *IAPP* expression relative to TUS treated samples suggesting that other MSC like TRPV isoforms may be implicated in TUS-induced gene downregulation ($n \geq 3$, $^{*}p < 0.05$ and $^{**}p < 0.01$). These data demonstrate a TUS-induced decrease in both *insulin* and *IAPP* expression that is prevented by complete MSC inhibition.

PDX1 but not Insulin nor IAPP Expression is Reduced in TUS-Treated Rat Pancreases

To determine if our transcriptomics findings in insulinoma cells could be replicated *in vivo,* the impacts of TUS on expression of the pancreatic β cell-specific genes *PDX1*, *insulin*, and *IAPP* were analyzed in lean and fatty Zucker Diabetic (ZDF) rats. Animals were divided into two groups where lean rats were fed standard chow while fatty animals were maintained on a high fat chow. Once hyperglycemia was established in fatty animals, both groups were further subdivided into TUS and sham treatment groups. TUS probe and the gel were placed on shaved animal's abdomen facing the pancreatic side and exposed to 800kHz TUS stimulation for 5 min used in previous cell line experiments (Fig. 2 A) and previously used in *in vivo* mouse studies (Singh et al., 2020b). Temperature sensitive probe showed no significant heating of the TUS stimulated abdomen areas. After 4 weeks of treatments, pancreatic sections were prepared from all animal groups. Sections were stained for insulin to show total islet area and morphology. Lean animals retained normal islet morphology while fatty animal islets showed fragmentation and irregular borders regardless of TUS or sham treatments (Fig. 6 B and D). Only fatty animals treated with TUS showed a significant reduction in insulin staining in comparison to lean, sham-treated control rats (Fig. 6 F, $n \geq 8$, $^{*}p < 0.05$). Sections were also stained to quantify IAPP expression. As

expected in diabetic animals, IAPP staining was decreased in both fatty animal treatment groups relative to lean, sham-treated rats (Fig. 6 K $n \geq 5$, $p < 0.05$). TUS alone did not alter IAPP staining (Fig 6 K $n \geq 5$, $p > 0.05$). Sections were additionally stained quantify PDX1 because it functions as a transcription factor of both *insulin* and *IAPP* that were decreased by TUS in our *in vitro* model (Fig. 6 A and C) (Macfarlane et al., 2000a). Regardless of treatment, fatty animals had decreased PDX1 expression as expected in a diabetic model. In both lean and fatty animals, TUS-treated animals had decreased PDX1 expression in comparison to sham-treated animals. This effect was more pronounced in lean animals (Fig. 6 A). Additionally, PDX1 expression localizes to the outer perimeter of the islets in lean animals as expected in rodent islets (Cabrera et al., 2006). *In vivo* results demonstrate minimal changes to islet function. Despite reduction to the transcription factor PDX1, islets continue to express both the constitutively expressed peptide hormone insulin as well as the inducible peptide hormone IAPP.

Discussion

Multiple groups have previously shown expression of various MSC in pancreatic β cells (Deivasikamani et al., 2019a; Philippaert & Vennekens, 2017; Sawatani et al., 2019b). Additional previous work has demonstrated that pancreatic β cells secrete insulin in response to TUS (Singh et al., 2020b; I. Suarez Castellanos, Jeremic, et al., 2017a, 2017b). So far only Piezo1 has been linked to TUS-induced insulin secretion and little other work has been done to assess the broader effects of TUS on MSC activation and expression in endocrine cells (Yoon et al., 2020). Here, we identified three mechanosensitive channels whose expression is shared between the common insulin secretion system, the INS cell line, and primary human pancreatic islets. We choose to focus on only on MSC shared between human and rodent model system to allow for optimization within an easily accessible cell line that can be readily translated to human models. We also

demonstrated TUS-induced ROS formation within INS cells that was prevented by broad and specific MSC antagonists, suggesting an MSC-mediated mechanism for TUS-induced ROS formation.

Furthermore, we found TUS induced a transcriptional downregulation of the essential pancreatic b-cell genes *insulin* and *IAPP* within INS cells through MSC-dependent mechanism. In rodent ZDF rat model, TUS treatments downregulated *PDX1 protein levels* within the rat islets*,* an essential pancreatic βcell identity transcription factor that plays a pivotal role in pancreatic cells differentiation; however, TUS did not affect rat expression of insulin or IAPP in lean or fatty animals likely due to different cytoarchitecture and/or cellular background of the two b-cell model systems. Although PDX1 contributes to the expression of both *insulin* and *IAPP* in rodent and human b-cells and its expression was downregulated by repetitive TUS treatments, β cell peptide hormone intracellular levels remained steady and comparable in control and TUS-treated rats.

Our work corroborates with previous reports of MSC expression in pancreatic β cells. Piezo1 is known to be expressed in the INS cell line, mouse pancreatic islets, and human pancreatic islets (Deivasikamani et al., 2019b; Ye et al., 2022). In these cells, the Piezo1-specific agonist Yoda1 induces ionic currents, calcium influx, and insulin secretion (Deivasikamani et al., 2019b). While we did similarly detect Peizo1 expression in INS cells and primary human islets, we were not able to replicate the exact effects of TUS through Yoda1 application. However, blocking this channel significantly reduced ROS formation when treated in combination with TUS. These findings suggest that Piezo1 is necessary for TUS-mediated ROS formation.

Although Peizo1 expression has been well characterized in both human and rodent models, expression of TRPV family members has been less characterized. Human genomic studies have

shown expression of TRPV2 (Matos et al., 2022). Further genomic work identified human TRPV2 polymorphisms that increase or decrease the risk of developing type two diabetes as well as other endocrine disorders (Bulut Arikan, 2020). In mouse islets and the mouse insulinoma cell line MIN6, TRPV2 expression has been confirmed at a gene, protein, and functional level where this channel mediates hypotonicity-induced insulin secretion (Sawatani et al., 2019b). In comparison, TRPV2 has only been identified in rat β cells and the INS cell line through unpublished results (Philippaert & Vennekens, 2017). We were able to confirm these findings in INS cells through rt-qPCR, western blot, and immunofluorescent microscopy analysis while also demonstrating TRPV2 expression in human pancreatic islets. TRPV5 expression has also been identified in rat pancreatic islets, although little else is known about this channel within the endocrine pancreas (Janssen et al., 2002). Our results indicate expression of this MSC in both the rat INS cell line as well as primary human islets at both a gene and protein level with constitutive expression of peizo1 in both cell types. Both TRPV2 and TRPV5 showed constitutive expression in human islet but inducible expression in the INS cell line.

Therapeutic ultrasound is known to induce ROS formation likely due to shear stress associated with acoustic streaming or microstreaming of bubbles during treatment (Jia et al., 2018). Previous works have shown this effect occurs in a dose-dependent manner correlating with the degree of sample sonication (Jia et al., 2018). Some groups have used this effect to create sonodynamic anti-cancer therapies in which targeted administration of sonosensitizers like porphyrin to enhance TUS-induced ROS formation in solid tumors (Giuntini et al., 2018). Similar to these results, we observed increased ROS formation in TUS-treated cells. Reactive oxygen species are known to contribute to both physiological insulin secretion and pathophysiological β cell failure as chronic hyperglycemia in type two diabetes allow metabolic

byproduct formation in these cells due to their low expression of the antioxidant enzymes catalase and glutathione (Lei & Vatamaniuk, 2011a). As disease develops, excessive ROS reduce *insulin* gene expression by preventing PDX1 from binding to the *insulin* gene promoter while also downregulating expression of PDX1 itself (Kaneto et al., 2010). In accordance with this data, we observed a decrease in *insulin* and *IAPP* expression within the INS cell line and decrease in PDX1 protein staining in our rat model. In contrast, we saw no significant change in insulin or IAPP protein expression in rat pancreas. This contrasting and selective action of TUS on genes expression can be at least in part attributed to differences in redox states between two model systems with different cellular backgrounds. Additionally, because insulin is one of the most abundantly expressed protein in β cells, comprising minimally 10% of all protein in these cells, the effects of acute decreased transcription may not translate *in vivo* to significantly influence the steady-state pool of insulin in these cells (Xin et al., 2018). It is also possible that the *in vivo* model allow for greater preservation of cell functions as normal regenerative processes can still occur such as β cell division and progenitor cell differentiation that have been observed in rat models in response to increased insulin demand (Zhong & Jiang, 2019). Because human β cells replicate at low rates, dedifferentiation preserves β cell mass when cell are stressed by providing a protective alternative to apoptosis (Patel & Remedi, 2024a). It is important to note that β cell dedifferentiation has been shown to be a reversible process. Diabetic models demonstrate a redifferentiation of β cells as metabolic stress is decreased, suggesting a similar process may occur post-TUS treatments (Patel & Remedi, 2024a). Although gene expression of pancreatic peptide hormones was decreased in cell lines, redifferentiation and regenerative processes present *in vivo* may mitigate any potential negative consequences of TUS in the pancreas.

In conclusion, we identified three MSC in rat pancreatic β cells that mediates TUS-stimulated ROS mobilization, which may contribute to previously reported TUS-evoke insulin release from these cells. Although TUS induced MSC-dependent downregulation of important b cell genes in insulinoma cells such as *insulin* and *IAPP*, it did not negatively impact expressions and function of these two vital b cell hormones in rat pancreas, demonstrating its potential safety in clinical applications.

Table 1: Rat qPCR primer sequences

Gene	Forward Primer Sequence	Reverse Primer Sequence
Beta-actin	5’-GCTACAGCTTCACCACCACA-3’	5’-ATCGTACTCCTGCTTGCTGA-3’
Insulin	5’-TGGCTTCTTCTACACACCCAAG-3’	5’-ACA ATG CCACGCTTCTGCC-3’
IAPP	5’-AGCTGTTCTCCTCATCCTCT-3’	5’-CTGTGTTGCACTTCCGTTTG-3’
TXNIP	5’-CGAGTCAAAGCCGTCAGGAT-3’	5’-TTCATAGCGCAAGTAGTCCAAGGT-3’
Piezo 1	5′-TTCTTCGGGGTGGAGAGGTA-3′	5′-TGTCACCATGTGGTTAAGGATG-3′
TRPV2	5’-TGCATACACAGAAGGCTCCA-3’	5’-CGGAATCCTTGTCAATCTG-3’
TRPV5	5’-TGGTGGGTCAGAGAACAAGA-3’	5’-ATGTGTACGGTTGGCATCAC-3’

Table 2: Human qPCR primer sequences

Gene	Forward Primer Sequence	Reverse Primer Sequence
Beta-actin	5’-CACATTCTGGAGAGCGAGAAG-3’	5’-CCAGCTTCTCGTATTTCTCCTT-3’
Piezo 1	5’-CATCTTGGTCTCCTCTGTCT-3’	5’-CTGGCATCCACATCCCTCTCATC-3’
TRPV2	5’-CTCTGGTGGCTAGCCTGTCCTGAC-3’	5’-TGCGATCCCGGAGCTTCTCA-3’
TRPV5	5’-GGGGACCGCTGCTTCCTGCGG-3’	5’-TCAAAAATGGTAGACCTCCTCTCC-3’

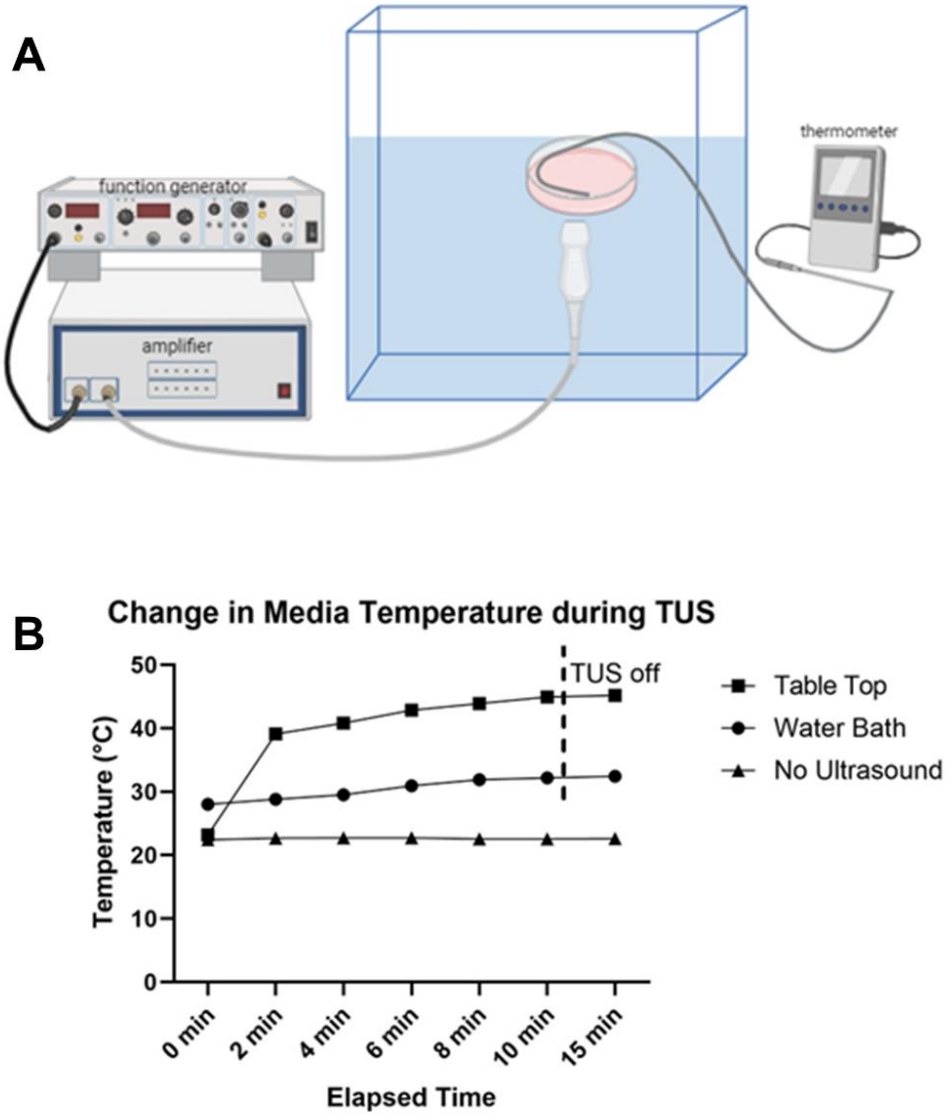

Fig 1: Verification of TUS parameters **A)** Ultrasound is generated by the function generator, and the signal is intensified by the amplifier. The ultrasound signal then travels to the ultrasound transducer. The transducer is placed 2.5 cm below the cell culture plate within a water bath. A temperature probe is placed within the media of the culture dish to monitor media temperatures changes during ultrasound application. **B)** Average media temperature increased by less than 3°C in the untreated and water bath samples while media temperature rose by 13°C during TUS without a heat sink averaged over three independent experiments

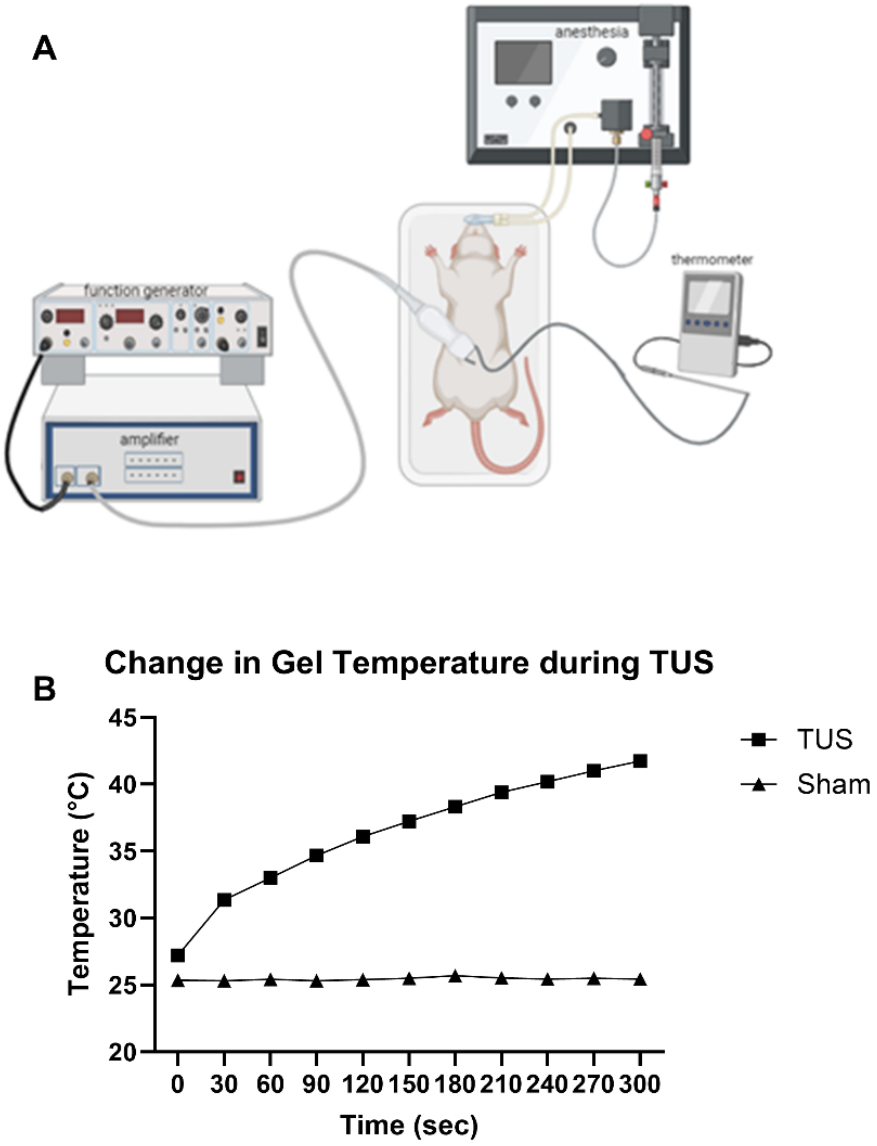

Fig 2: Ultrasound application to rats **A)** The anesthetized rat is laid supine on a heated bed and kept sedated through isoflurane inhalation via nose cone. The ultrasound transducer is coupled to the rat via ultrasound gel. A temperature probe is placed into the ultrasound gel to monitor temperature during ultrasound applications. **B)** Average gel temperature increased by 16°C during TUS averaged over six independent experiments

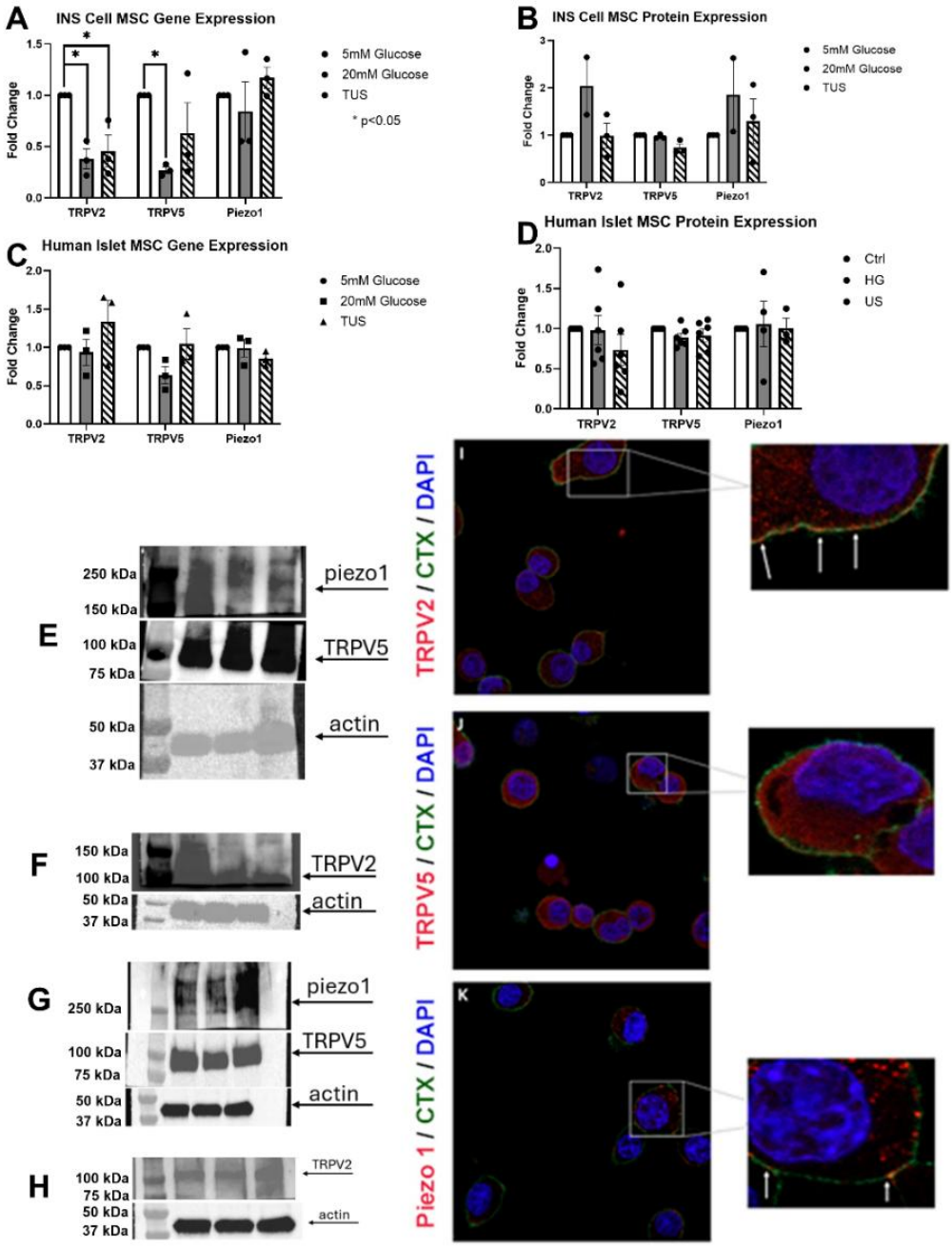

Fig 3: MSC expression in INS cell line and human pancreatic islets **A)** rt-qPCR analysis of INS cell line extracts showed constitutive expression of peizo1 and inducible expression of TRPV2 and TRPV5 (n=3, *p<0.05) **B)** Western blot analysis confirmed expression of TRPV2, TRPV5, and piezo1 in INS cells (n=3) **C)** rt-qPCR analysis of human pancreatic islet extracts showed constitutive expression of TRPV2, TRPV5, and piezo1 (n=3) **D)** Western blot analysis confirmed constitutive expression of TRPV2, TRPV5, and piezo1 in human pancreatic islets (n≥2) **E-H)** Representative western blots showing MSC expression in INS cells **(E,F)** and human islets **(G,H) I-K)** Microscopy images of INS cells show cell membrane (green), nucleus (blue), and the MSC (red) **I)** TRPV2, **J)** TRVP5, or **K)** Piezo1

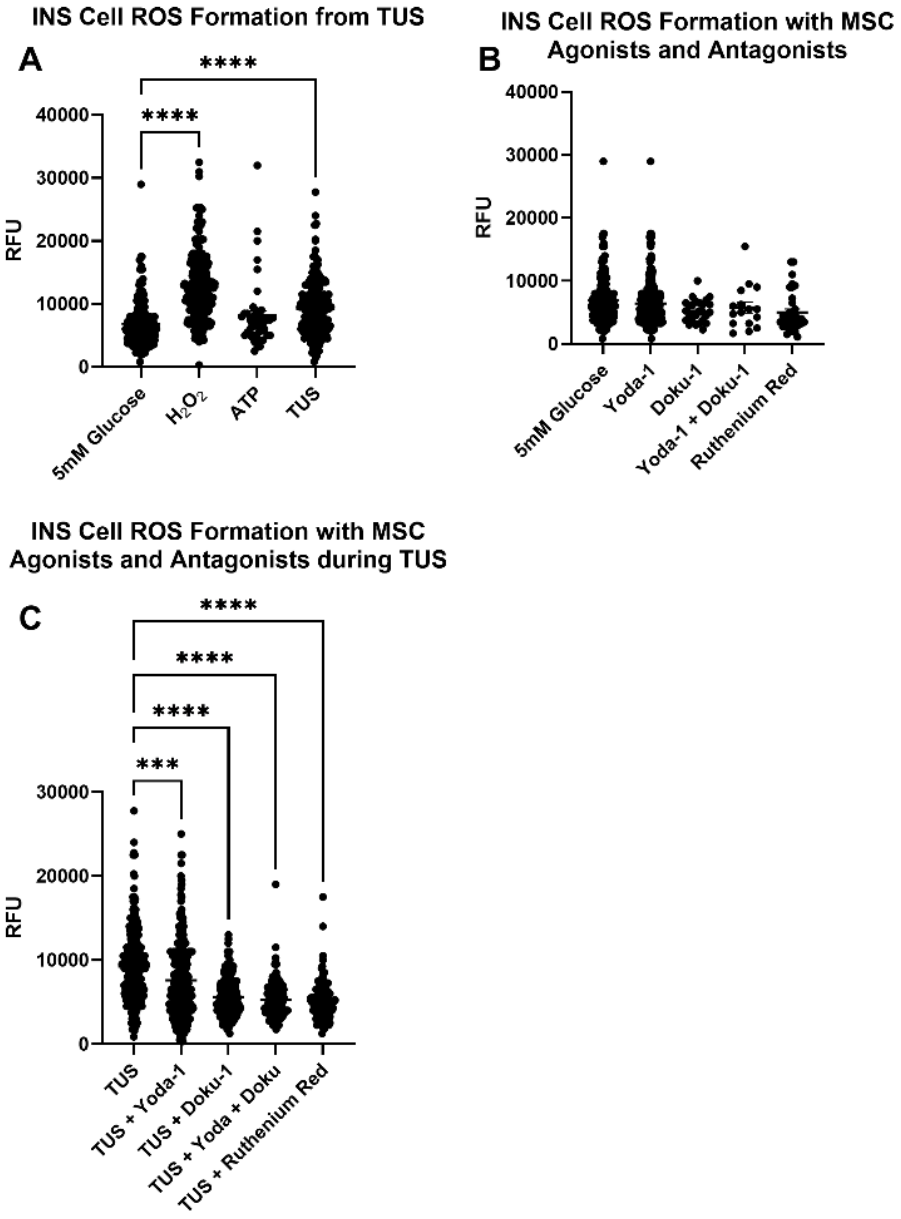

Fig 4: ROS Formation in INS Cells INS cells treated with TUS with or without MSC modulators were stained to show ROS accumulation in cells. Quantification of ROS staining showed **A)** Equally significant increases in ROS production in TUS treated and H_2O_2 treated cells relative to untreated cells (n=6, ****p<0.0001) **B)** MSC agonists and antagonists alone do not alter ROS formation relative to untreated cells (n=6) **C)** All MSC agonists and antagonist applied with TUS treatment significantly decrease ROS formation relative to only TUS treated cells (n=6, ***p<0.001, ****p<0.0001)

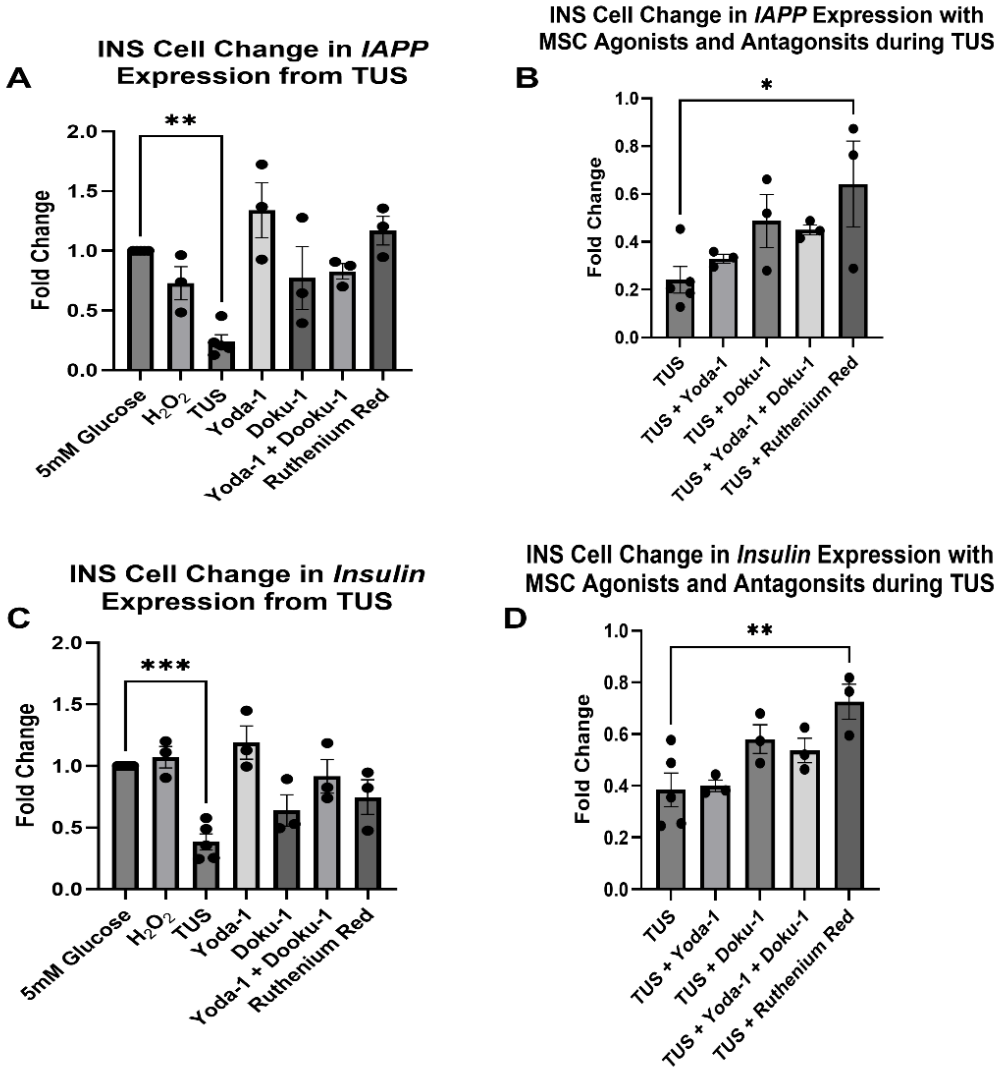

Fig 5: TUS-induced changes in INS gene expression Changes in gene expression were evaluated in INS cells treated with TUS or sham treated in the presence or absence of MSC modulators relative to untreated control samples **A)** *IAPP* expression was significantly decreased by TUS but unchanged by H_2O_2 and MSC treatments relative to control 5 mM glucose treated samples (n≥3, **p<0.001) **B)** *IAPP* expression was significantly increased by ruthenium red application during TUS treatment while no other MSC agonists or antagonists significantly altered expression of this gene relative to samples treated with TUS only (n≥3, *p<0.05) **C)** *Insulin* expression was significantly decreased by TUS but unchanged by H_2O_2 and MSC treatments relative to control 5 mM glucose treated samples (n≥3, ***p<0.001) **D)** *Insulin* expression was significantly increased by ruthenium red application during TUS treatment while no other MSC agonists or antagonists significantly altered expression of this gene relative to samples treated with TUS only (n≥3, **p<0.01)

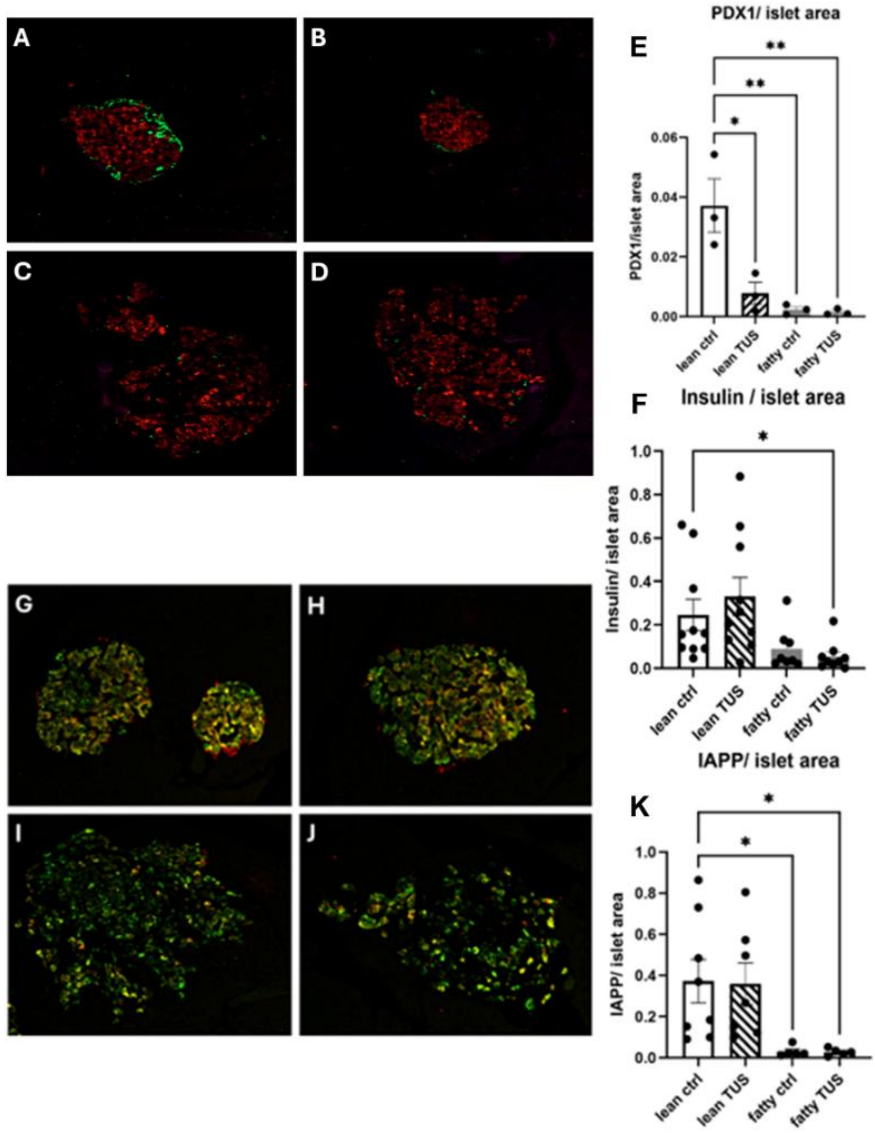

Fig 6: Rat histological analysis of essential β *cell genes* **A-D)** Rat pancreatic sections were stained to visualize PDX1 (green) and insulin (red) in **A)** lean, sham-treated **B)** lean, TUS-treated **C)** fatty, sham-treated **D)** fatty, TUS-treated rats **E)** PDX1 staining was quantified and normalized to total islet area showing a significant decrease in PDX1 in fatty animal relative to lean, sham-treated control animals (n=3, *p<0.05, **p<0.01) **F)** Insulin staining was quantified and normalized to total islet area showing a significant decrease in insulin content in fatty, TUS-treated animals relative to sham-treated, lean controls (n≥8, *p<0.05) **G-J)** Rat pancreatic section were stained to visualize IAPP (green) and insulin (red) in **G)** lean, untreated **H)** lean, TUS-treated **I)** fatty, untreated **J)** fatty, TUS-treated rats **K)** IAPP staining was quantified and normalized to total islet area showing a significant decrease in IAPP in fatty animals regardless of treatment relative to lean sham-treated control animals (n≥5, *p<0.05)

Chapter 2: Hyperglycemia is required for cytokine-induced transcriptional changes in pancreatic beta cells

Abstract

Chronic hyperglycemia due to a loss of functional beta cell mass is the hallmark characteristic of diabetes. In the development of type two diabetes, multiple factors contribute to the loss of beta cell insulin secretion. Chronic hyperglycemia creates metabolic stress, islet amyloid polypeptide oligomerization leads to protein stress, and cytokine production from infiltrating immune cells promotes proinflammatory stress. The precise mechanism(s) through which these stressors integrate to collectively cause beta cell dysfunction are not fully elucidated. Here, we identify several genes whose expression is altered only when cells are treated with hyperglycemic and proinflammatory conditions concurrently. This includes a downregulation of *IAPP* and upregulation of both *NF-kB* and *IL-1β* in the INS cell line and human pancreatic islets. Immunoprecipitation studies refuted direct binding between TXNIP and NF-kB in this process, suggesting two pro-inflammatory pathways operate in parallel in stressed b-cells.

Introduction

The endocrine pancreas is comprised of clusters of cells, referred to as islets of Langerhans, that are scattered throughout this organ. Within these heterogenous islets, each major cell type has a highly specialized role in the regulation of blood glucose. Alpha cells secrete glucagon in response to hypoglycemia while beta cells release insulin in response to hyperglycemia (Cabrera et al., 2006). Glucagon promotes hepatic glycogenolysis and gluconeogenesis to increase blood glucose (Gromada et al., 1997). In contrast, insulin binding to its receptors on adipose and skeletal muscle tissue promotes the uptake of excess blood glucose. Once brought into these peripheral tissues, this glucose can be used immediately for ATP production or stores as glycogen

for future use (De Meyts, 2000). Other less prevalent cell types include delta cells that act as paracrine regulators through production of somatostatin that further modulates alpha and beta cell secretory functions (Francis et al., 1990).

Diabetes is a heterogenous disease characterized by chronic hyperglycemia due to insufficient insulin secretion. In type one diabetes, autoimmune attack of beta cells eliminates functional beta cell mass resulting in a complete loss of insulin production. Type two diabetes is a multifactorial disease whose development is influenced by genetics, environmental factors, and lifestyle choices. Here, beta cells are unable to produce enough insulin to meet metabolic demands (Goyal et al., 2024a). Beta cells inundated with constant glucose experience cellular stress that leads to their loss of functionality. Constant glucose flux leads to reactive oxygen species formation as beta cells have low expression of antioxidant genes like catalase and glutathione (Lei & Vatamaniuk, 2011b). Left unchecked, these molecules contribute to DNA damage and mitochondrial dysfunction ultimately leading to cell death. To prevent this, beta cells lower their uptake of glucose through downregulation and reduced cycling of the glucose transporter GLUT2 (Thorens et al., 1990).

In addition to metabolic stress, proinflammatory conditions contribute to beta cell failure in type two diabetes. Resident macrophages within the pancreas maintain tissue homeostasis through remodeling and repair of tissue. As disease develops, more proinflammatory M1 macrophages accumulate within islets. Islet cellular stress produces danger-associated molecular patterns like fragmented DNA and islet amyloid polypeptide plaque deposits recruit additional innate immune cells into the tissue (Meshkani & Vakili, 2016). As immune infiltration progresses, interleukin 1-beta (IL-1β) production increases, reducing insulin secretion and inducing endocrine cell apoptosis (Abdulreda & Berggren, 2013). Under chronic hyperglycemic conditions, pancreatic

beta cells themselves also begin producing IL-1β as well as increasing cleavage of this protein. This process is mediated by hyperglycemia-induced O-GlcNAcylation of thioredoxin interacting protein (TXNIP) (Filhoulaud et al., 2019). Across multiple cell types, TXNIP has also been implicated in the formation of the inflammasome (Filhoulaud et al., 2019). This post translational modification promotes TXNIP to interact with NOD-like receptor family pyrin domain containing 3 (NLRP3) required for beta cell inflammasome formation (Filhoulaud et al., 2019; Zhou et al., 2010). NLRP3-TXNIP complex is known to serve as signal integration point between endoplasmic reticulum stress and inflammation that results in IL-1β upregulation and increased apoptosis (Oslowski et al., 2012). Interestingly, TXNIP utilizes other binding partners under different stress conditions. In cardiomyocytes binding between TXNIP and nuclear transcription factor-κB (NF-κB) is required for NF-κB nuclear import (Y. Liu et al., 2014). Additional work has shown the delirious effects of NF-κB activation in pancreatic β cells as shown by NF-κB-mediated upregulation of the proapoptotic Fas ligand by these cells (Maedler et al., 2002); however, little work has been done to confirm or refute TXNIP-NF-kB interactions within pancreatic beta cells.

Here, we assessed the effects of hyperglycemia and proinflammatory cytokines individually and combinatorically. Within the INS cell line model system, we found cytokine-induced downregulation of islet amyloid polypeptide encoded by *IAPP* was glucose independent while cytokine-induced upregulation of *NF-κB* and *IL-1β* only occurred in high glucose conditions. Furthermore, decreased IAPP and increased NLRP3 were observed only in samples co-treated with high glucose and cytokines, supporting a glucose-dependent action of cytokines in pancreatic beta cells. This trend was also found in human pancreatic islets that had reduced *IAPP* and increased *IL-1β* and *NF-κB* when treated with cytokines. Despite this glucose-dependent

effect of cytokines, the high glucose-activated transcription factor TXNIP and the cytokine-activated transcription factor NF-κB do not physically interact in human islets, suggesting an independent pro-inflammatory signaling cascade for TXNIP and inflammasome in these cells.

Methods

Cell Cultures

Rat insulinoma INS 832/13 cells (a generous gift from Christopher Newgard, Duke University) were cultured in RPMI 1640 media (ThermoFisher Scientific catalog number 11875093) supplemented with 1% penicillin/ streptomycin (ATCC catalog number 30-2300), 10mM HEPES (Gibco catalog number 15630-080), 2mM L-glutamate (Sigma Aldrich G8415), 1 mM sodium pyruvate (Sigma Aldrich S8636), 0.05 mM 2-mercaptoethanol (Sigma M3148) , and 10% (v/v) fetal bovine serum (ThermoFisher Scientific catalog number 26140079). Insulinoma cells were stored at 37°C in a humidified incubator with 5% CO_2 and passaged every 3 to 4 days. Prior to treatments, cells were plated on a 96 well plate in 5 mM glucose media and equilibrated for 24 hours.

In addition to INS cell lines, human pancreatic islets from non-diabetic cadavers with >90% viability and purity were obtained through the Integrated Islet Distribution Program (IIDP) for Human Islet Research. These islets are from approved cadaveric organs. Therefore, the tissue is exempt from human studies approval per IIDP guidelines. Privacy and personal identity information of all participants was protected. Studies using human islets were approved by The George Washington University Institutional Review Board (IBC#IBC-20-092). Upon arrival, intact islets were plated on a non-adherent 48 well plate in CMRL media (ThermoFisher Scientific catalog number 11530037) supplemented with 1% (V/V) fetal bovine serum (ThermoFisher Scientific catalog number 26140079) and 1% penicillin/streptomycin (ATCC

catalog number 30-2300). Islets were cultured in a humidified incubator at 37°C with 5% CO_2 and given 24 hours to equilibrate before treatments.

Both cell types were treated with 20 mM glucose in the presence or absence of 5U/mL TNF-α Invitrogen (RMTNFAI), IL-1β (Gibco PHC0814), and IFN-γ (Novus NBP2-76178) overnight, 14 to 18 hours, prior to analysis as previously done in (Sidarala et al., 2020) .

Real Time – Quantitative PCR

After cytokine and high glucose treatments, total RNA was isolated from cells via Qiagen RNeasy mini kit per manufacturer instructions (Qiagen catalog number 74134). RNA concentrations were determined via Nanodrop. From each sample, 400 ng of RNA was converted into cDNA using a multiScribe reverse transcription kit with random primers following manufacture instruction (Applied Biosystems catalog number 4368814). qPCR was then performed with resulting cDNA via iTaq Universal SYBR Green supermix (BioRad catalog number 1725122) and primers listed in Tables 1 and 2. Bio Rad CFX 96 real-time system and C1000 Touch thermal cycler were used for amplification and gene detection. Expression levels of all genes were normalized to β -actin expression. Fold change in expression of these genes was calculated using the 2-delta CT method.

Table 1: Rat qPCR primer sequences

Gene	Forward Primer Sequence	Reverse Primer Sequence
β-actin	5'-GCTACAGCTTCACCACCACA-3'	5'-ATCGTACTCCTGCTTGCTGA-3'
IAPP	5'-AGCTGTTCTCCTCATCCTCT-3'	5'-CTGTGTTGCACTTCCGTTTG-3'
TXNIP	5'-CGAGTCAAAGCCGTCAGGAT-3'	5'-TTCATAGCGCAAGTAGTCCAAGGT-3'
NF-κB	5'-GGCCGGAAGACCTATCCTACT-3'	5'-CTACAGACACAGCGCACACT-3'
IL-1B	5'-CCCTGCAGCTGGAGAGTGTGG	5'-TGTGCTCTGCTTGAGAGGTGCT-3'

Table 2: Human qPCR primer sequences

Gene	Forward Primer Sequence	Reverse Primer Sequence
β-actin	5'-CACATTCTGGAGAGCGAGAAG-3'	5'-CCAGCTTCTCGTATTTCTCCTT-3'
IAPP	5'- GCAAGTATTTCTCATTGTGCTCTC-3'	5'- GATGACAGAATGGCACCAAAGT-3'

TXNIP	5'- ACAGAAAAGGATTCTGTGAAGGTGAT-3'	5'- GCCATTGGCAAGGTAAGTGTG-3'
NF-kB	5'-ACAACCCCTTCCAAGAAGAGC-3'	5'-GCCTGGTCCCGTGAAATACA-3'
IL-1β	5'-AAGCTGATGGCCCTAAACAG-3'	5'-AGGTGCATCGTGCACATAAG-3'

Immunoprecipitation of TXNIP

After high glucose and cytokine treatments, total intracellular protein was collected in NP40 cell lysis buffer (ThermoFisher Scientific 78510). Samples were then precleared with magnetic Dynabeads Protein G (Invitrogen 10004D) at 4°C for 2 hours with rotation. Seven grams of rabbit anti-TXNIP polyclonal antibody (Invitrogen JM60-35) were incubated with fresh Dynabeads at room temperature for 1 hour with rotation. An additional set of beads was prepared using 7 gram of normal rabbit serum as a negative control to ensure TXNIP-specific binding and pull down. The Dynabead-IgG complex was washed three times and cross linked by incubation with 20 mM dimethyl pimelimidate dihydrochloride in 0.2 M triethanolamine, pH 8.2, at room temperature for 30 minutes with rotation. Fixative was removed and washed off during a 15-minute incubation with 50 mM Tris pH 7.5 at room temperature with rotation. Precleared intracellular protein was then incubated with cross linked Dynabeads overnight at 4°C with rotation. Supernatant containing all non-TXNIP interacting proteins was collected. After three washes with PBS, immunoprecipitated materials were dissociated from the cross linked Dynabeads using 5x Laemmli buffer and gentle heating. Samples were then analyzed via western blot.

Western Blot

After cytokine and high glucose treatments, all media was collected from wells and whole cell extracts were collected in RIPA buffer (EMD Millipore, catalog number 20-188) or in NP40 cell lysis buffer (ThermoFisher Scientific 78510) during immunoprecipitation experiments. Extracted protein concentrations were determined using the Pierce BCA Protein Assay Kit (Thermo

Scientific reference number 23227). Four micrograms of protein or an equal volume of collected media were loaded into each well. Proteins were separated by SDS-PAGE on a 4-15% stacking gel (BioRad, catalog number 4561086). Resolved proteins were electrophoretically transferred to nitrocellulose membranes (BioRad catalog number 1704270) using the BioRad Trans-Blot Turbo System. Membranes were blocked with 5% nonfat dry milk. Membranes were probed with primary antibodies for one hour at room temperature with shaking. The following proteins were targeted by primary antibodies: β-actin (Santa Cruz sc-47778 HRP, 1:500), IAPP (Santa Cruz sc-20963 1:300), TXNIP (Invitrogen JM60-35 1:400), NF-κB (Proteintech 10745-1-AP 1:500), and NLRP3 (Proteintech 19771-1-AP 1:500). Then, corresponding horseradish peroxidase-conjugated secondary antibodies were added at 1:2000 and incubated at room temperature for one hour. Resulting blots were developed using pico – (ThermoFisher Scientific no. 34580) or femto – (ThermoFisher Scientific no. 34095) ECL substrate kits and visualized with the ChemiDOC touch gel imaging system (BioRad). Intensity of the resulting bands was quantified using BioRad Image-Lab software where β-actin was used as a loading control.

Confocal Microscopy of INS Cells

INS cells were plated on poly-D-lysine coated 96-well glass bottom black microplates. After high glucose and cytokine treatments, cells were fixed by 1 hour incubation with 4% paraformaldehyde (Sigma Aldrich catalog number 158127) and blocked in PBS supplemented with 1% BSA and 0.1% 100x-Triton. Next, anti-NF-κB antibody (Proteintech 10745-1-AP) incubated with cells at 4°C overnight. Corresponding secondary antibody was then added at 1:400 and incubated at room temperature for 1 hour. Cells were then incubated with DAPI (Cell Signaling catalog number 4083) in PBS for 20 minutes prior to imaging to counterstain nuclei. Two dimensional fluorescent optical sections were acquired across 3 randomly selected fields of

view of each treatment at 63x magnification using a Zeiss LSCM-800 confocal microscope (Carl Zeiss, Thornwood, NY). Quantitative analysis of images began with background subtraction of signal and determining the relative fluorescent intensity (RFUs) at the 488 nm wavelength using Zeiss section ROI analysis tools. Data was derived from three images from two sets of independent experiments.

Statistical Analysis

For all experiments, statistical analysis and graph plotting was performed using GraphPad Prism 10. Datasets were tested for Gaussian distribution and equal variance prior to analysis. If both tests were passed, data was analyzed via one-way ANOVA followed by a Tukey post hoc test with significance established at $p<0.05$. Microscopy analysis was performed using ≥ 3 images from 2 independent experiments. Histograms depict the average of all collected data points +/- SEM.

Results

Cytokine treatment downregulates IAPP production

In order to determine the effect of proinflammatory conditions on glucose-responsive genes, INS cells were cultured under normal (5mM) or high glucose (20 mM) concentrations overnight, in the presence or absence of cytokines, known to promote islet insulitis: TNF-α, IL-1β, and INF- γ. The glucose responsive genes *IAPP* and *TXNIP* were first investigated because they are known to be highly upregulated by hyperglycemia (Shalev et al., 2002). INS cells responded as expected, with increases to both *IAPP* and *TXNIP* expression with 20 mM glucose treatments (Fig. 1 A and B, $p< 0.01$ and $p<0.05$, respectively). TXNIP protein expression mirrored this trend as hyperglycemic conditions increased its expression (Fig. 1C, $p<0.001$). Under 5 mM glucose euglycemic conditions, cytokines treatments had no effect on *TXNIP* gene expression or protein

synthesis (Fig. 1 A and C, p>0.05). In contrast, *IAPP* was downregulated by cytokines treatments in euglycemic conditions (Fig. 1 B, p<0.05); however, IAPP protein levels remained stable (Fig. 1 D, p>0.05). Similarly, cytokine treatment under hyperglycemic conditions did not alter the expression of *TXNIP* at a transcriptional or protein level (Fig. 1 A and C, p>0.05). Additionally, this combination of treatments also downregulated expression of *IAPP;* however, this downregulation was more pronounced and also led to a subsequent decrease in IAPP protein concentrations (Fig. 1 B and D).

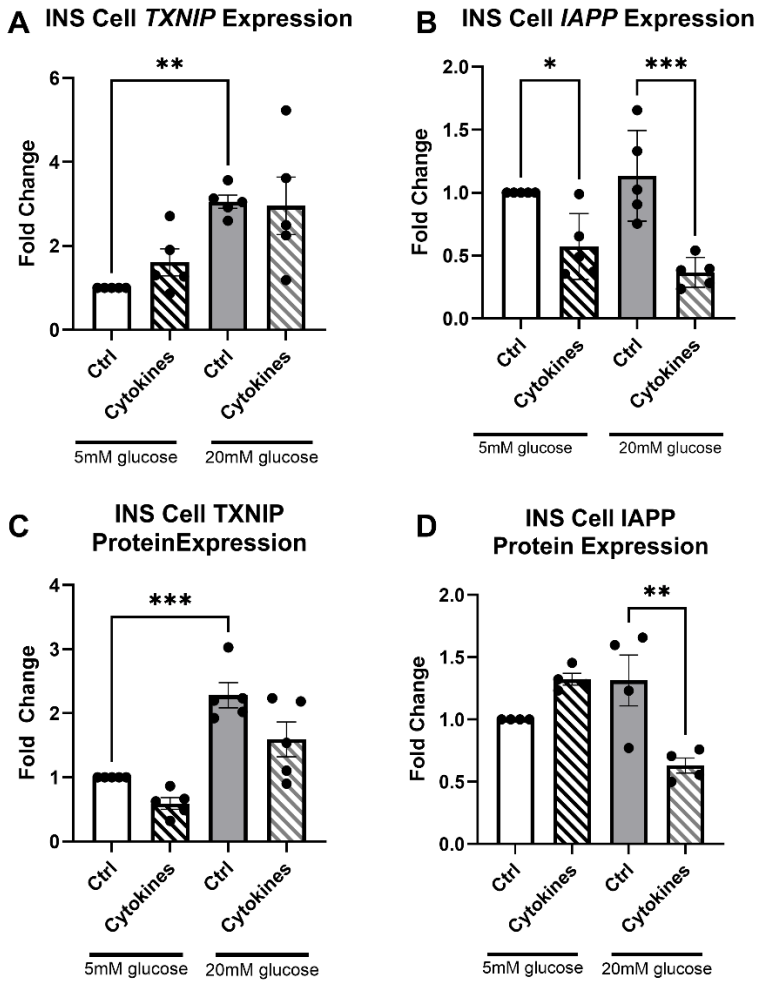

Figure 1: Expression of glucose responsive genes in INS cells INS cells equilibrated in 5 mM glucose were treated with 20 mM glucose and/or 5 U/mL TNF-α, IL-1β, and INF-γ overnight.

qPCR analysis showed **A)** increased expression of *TXNIP* under hyperglycemic conditions with no changes to its expression with cytokine treatments (n=5, **p<0.01) and **B)** decreased expression of *IAPP* with cytokine treatments under both euglycemic and hyperglycemic conditions (n=5, *p<0.05, **p<0.001). Western blot analysis of these samples revealed **C)** increased TXNIP protein in cells treated with 20 mM glucose (n=4, ***p<0.001) and **D)** a decrease in IAPP in cells treated with cytokines under hyperglycemic conditions (n=4, **p<0.01).

Cytokine treatment upregulates proinflammatory markers in a glucose-dependent manner

To determine the effect of high glucose on proinflammatory genes, INS cells were cultured under normal (5 mM) or high glucose (20 mM) concentrations overnight, in the presence or absence of cytokines, known to promote islet insulitis: TNF-α, IL-1β, and INF- γ. Interplay between metabolic (high glucose) and cytokine-mediated pathways on expression of proinflammatory genes including NF-κB and IL-1β were then assessed. Under normal glucose conditions, cytokine treatment did not alter the expression of these genes (Fig. 2 A and B, p>0.05). In contrast, both *NF-κB* and *IL-1β* were upregulated by cytokine treatment under hyperglycemic conditions, suggesting a glucose-dependent mechanism of upregulation (Fig. 2 A and B, p<0.0001 and p<0.01, respectively). Western blot analysis of these samples supported this trend. NF-κB protein levels were increased by a combination of 20 mM glucose and cytokines, but neither of these treatments independently altered its expression (Fig. 2C, P<0.01). Analysis of the inflammasome-related protein, NLRP3, showed a similar trend as its expression was not changed by high glucose or cytokines independently, but was increased when these treatments were combined (Fig. 2 D).

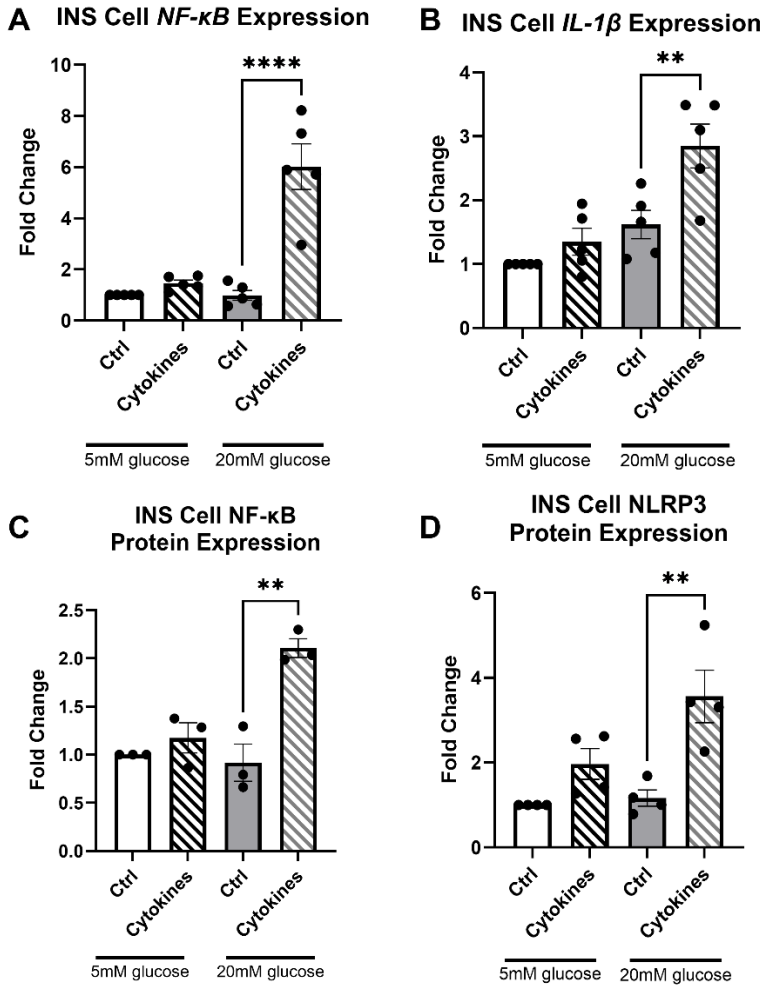

Figure 2: Expression of proinflammatory genes in INS cells INS cells equilibrated in 5 mM glucose were treated with 20 mM glucose and/or 5 U/mL TNF-α, IL-1β, and INF-γ overnight. qPCR analysis showed A) no changes in the expression of NF-κB with hyperglycemia or cytokines independently but a significant increase in its expression when treated with both conditions (n=5, ****<0.0001) and B) no significant changes in expression of IL-1β when cells were treated with 20 mM glucose or cytokines alone but a significant increase in its expression when treated with both (n=5, **p<0.01). Western blot analysis of these samples demonstrated C) increased NF-κB protein content only when cells were treated with both 20 mM glucose and cytokines while these treatments individually had no significant effect (n=3, **p<0.01) and D)

similarly increased NLRP3 content when cells were treated with cytokine in a hyperglycemic condition while these treatments individually had no significant effect (n=4, **p<0.01), ANOVA followed by a Tukey post hoc test.

Microscopy analysis of NF-κB protein levels continued to demonstrate this trend. Both 20 mM glucose and cytokines were required for increased intracellular protein accumulation of NF-κB in INS cells (Fig. 3 A-E, p<0.0001). Combination of high glucose (20mM) and cytokines were also required for nuclear translocation of NFK-b (Fig. 3 B-E). Single cell analysis revealed a ~2-fold increase in nuclear NF-κB b-positive cells treated with combination of high glucose and cytokines for 18 hours as compared to controls, reaching 40% of cellular pool (Fig. 3F, H). However, in ~ 60 % of cells NF-κB largely remains cytosolic (Fig. 3 F, G). This moderate increase in NF-κB nuclear localization was shown to be sufficient to induce inflammasome activation and synthesis of pro-inflammatory -genes like IL-1β and NLRP3 in INS cells Ortis et al, 2008. These data cumulatively illustrate that a higher glucose flux rate is required for cytokine-induced upregulation of proinflammatory genes in pancreatic beta cells.

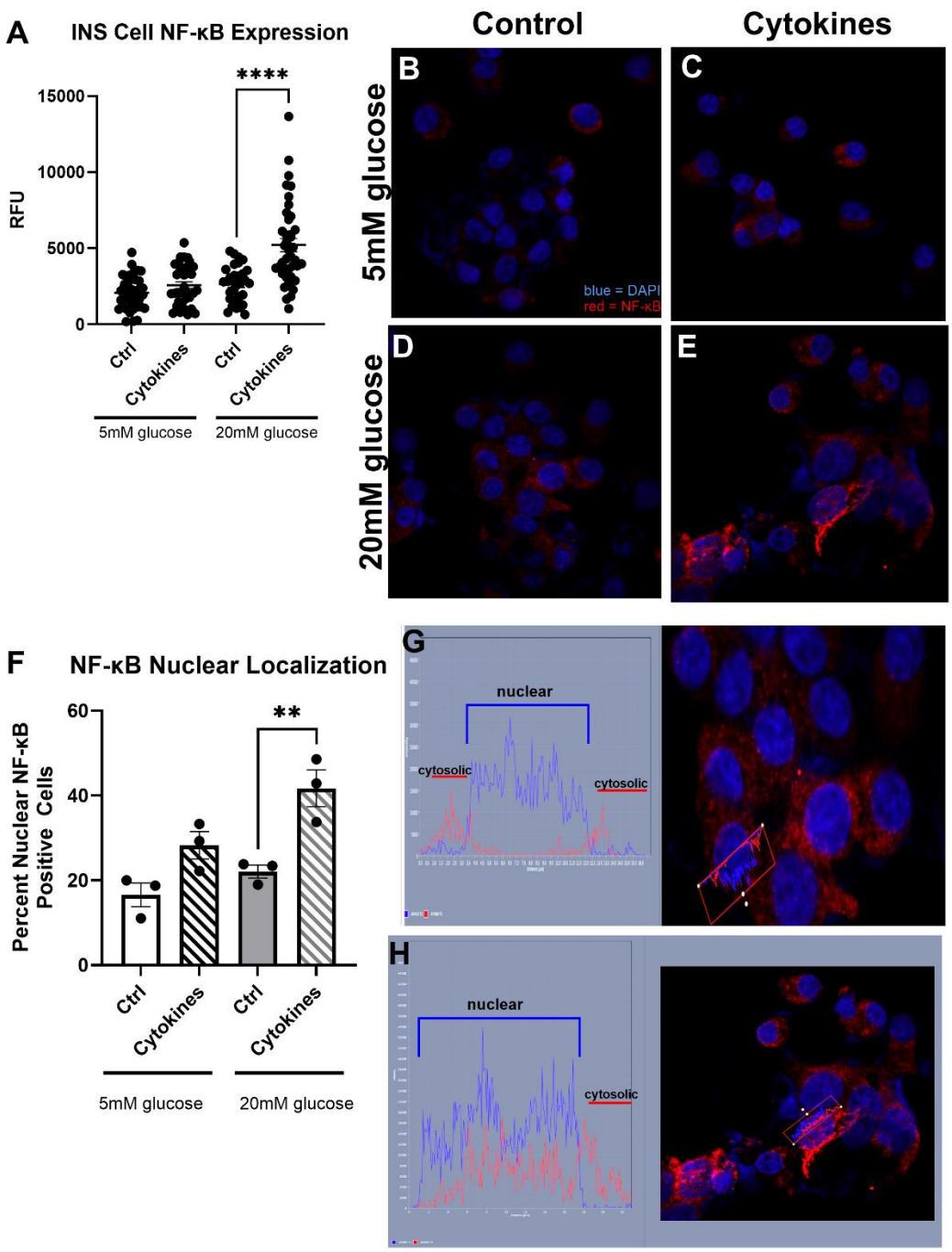

Figure 3: NF-κB expression is increased by cytokine treatments only under hyperglycemic conditions in INS cells. INS cells equilibrated in 5 mM glucose were treated with 20 mM glucose and/or 5 U/mL TNF-α, IL-1β, and INF-γ overnight. **A)** Quantification of NF-κB from 3 independently treated well showed hyperglycemia is required for cytokine-induced upregulation

while hyperglycemia and cytokine treatment independently did not alter its expression. **B-E)** Representative images of cells treated with **B)** 5 mM glucose only, **C)** 5 mM glucose and cytokines, **D)** 20 mM glucose only, and **E)** 20 mM glucose and cytokines where blue show DAPI stained nuclei and red shows NF-κB **F)** Cross sectional analysis shows a significant increase in nuclear NF-kB positive cells only when INS cells are co-treated with high glucose and cytokines ($p<0.001$, n=?, ANOVA followed by >? post hoc test) Representative images and sectional analysis show **G)** little DAPI (blue) and NF-kB (red) co-staining in cells treated with high glucose alone and **F)** increased nuclear accumulation of NF-kB in INS cells treated with both high glucose and cytokines with additional NF-kB remaining in cytosolic areas.

IAPP expression is downregulated by cytokines in human pancreatic islets without TXNIP-NF-κB interactions

Here, we examined the impact and possible cross-talk between canonical (cytokine-induced) and non-canonical (metabolic, high glucose-induced) pro-inflammatory pathways on inflammasome activation by analyzing expression of inflammasome marker and activator, IL-1β and NF-κB, respectively. Similar to INS cells, treatment with 20 mM glucose upregulated *IAPP* as expected, however, treatment with TNF-a, IL-1β, and INF-γ caused a significant downregulation of *IAPP* (Fig. 4 A, $p<0.05$ and $p<0.01$, respectively). As expected, high glucose also upregulated *TXNIP* (Fig. 4B, $p<0.01$) (Shalev et al., 2002). Unlike INS cells, cytokine treatment caused upregulation of *TXNIP* (Fig. 4B, $p<0.05$). Furthermore, cytokine treatment similarly upregulated both *IL-1β* and *NF-κB* expression in human islets (Fig. 4 C and D, $p<0.01$).

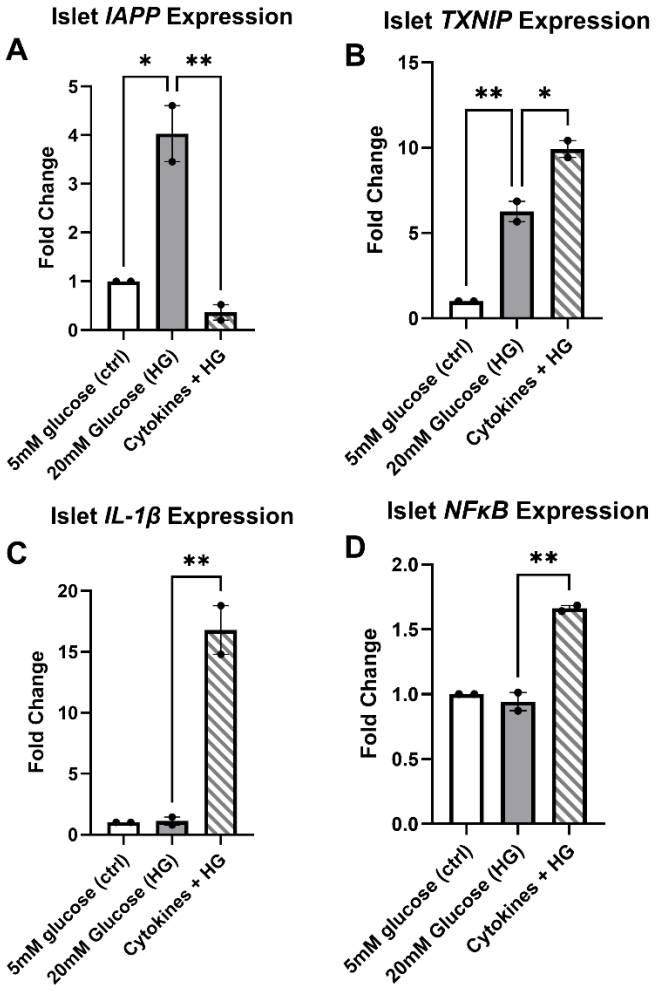

Figure 4: Human pancreatic islet expression of glucose-responsive and proinflammatory genes

Human pancreatic islets were treated with 20 mM glucose in the presence or absence of 5 U/mL TNF-α, IL-1β, and INF-γ overnight. qPCR analysis demonstrated A) Hyperglycemia upregulates *IAPP* while cytokines downregulate its expression (n=2, *p<.0.05, **p<0.01) B) Both hyperglycemia and cytokine treatments significantly upregulate *TXNIP* expression (n=2, *p<0.01 and **p<0.05) C) Cytokine treatment upregulates expression of *IL-1β* (n=2, **p<0.01) D) Treatment with cytokines significantly upregulates *NF-κB* expression (n=2, **p<0.01)

TXNIP mediates multiple signaling pathways in response to elevated glucose concentrations. Similarly, NF-κB coordinates expression of various inflammation-associated genes in response

to stimuli including TNF-a and IL-1β. Because TXNIP can interact with other proinflammatory proteins to promote inflammasome formation, we next assessed potential binding between NF-κB and TXNIP. Through immunoprecipitation of high glucose and cytokine co-treated human islets, we determined that NF-κB and TXNIP do not interact with each other (Fig. 5). A known binding partner of TXNIP, NLRP3, was pulled down with TXNIP demonstrating successful immunoprecipitation. Physical interactions between these TXNIP and NF-κB is not required for them to carry out their functions as transcription factors under hyperglycemic and proinflammatory conditions, respectively.

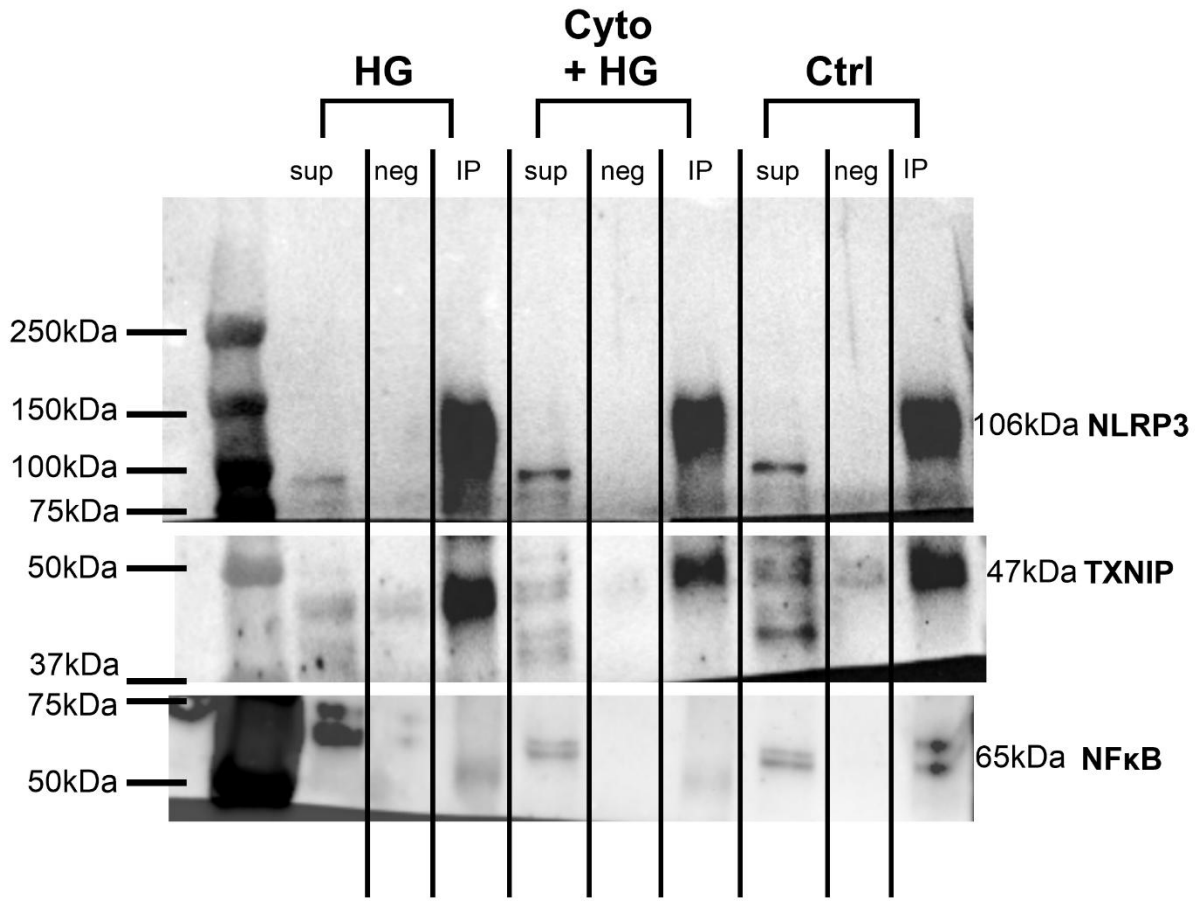

Figure 5: Representative western blots following TXNIP pulldown Human pancreatic islets were treated with 20 mM glucose in the presence or absence of 5 U/mL TNF-α, IL-1β, and INF-γ

overnight. Total intracellular protein was immunoprecipitated through pull down targeting TXNIP (IP) or normal rabbit serum (neg). Supernatant containing non TXNIP-interacting proteins (sup) was also analyzed. Across all treatments, NLRP3 was pulled down with TXNIP while NF-κB was more prominent in supernatant samples (n=2, one set of representative blots shown)

Discussion

Here, we investigated the potential link between metabolic stress and inflammatory stress in pancreatic beta cells. TNF-α, IL-1β, and INF-γ signal through individual pathways that collectively result in beta cell dysfunction allowing treatments with this combination of cytokines to mimic the inflammatory condition of islets in individuals with type two diabetes (Wachlin et al., 2003). When treating the INS model system with the combination of cytokines under normal (5 mM) and high (20 mM) glucose, we observed cytokine-induced downregulation of *IAPP* and a glucose-dependent decrease in IAPP protein. Because TXNIP is known to modulate *IAPP* transcription in response to changes in glucose, our data suggest a TXNIP-independent manner of cytokine-induced *IAPP* downregulation as occurred in both normal and high glucose conditions. Additionally, cytokines had no significant effect on *TXNIP* expression further supporting a TXNIP-independent mechanism of cytokine-induced *IAPP* downregulation. Further analysis of these samples illustrated a hyperglycemia-mediated cytokine-induced upregulation of several proinflammatory markers. Under this combination of conditions, both *NF-κB* and *IL-1B* were upregulated. Similarly, intracellular concentrations of NF-κB and NLRP3 also increased. There was an additional increase in nuclear localization in NF-kB in cells treated with the combination of high glucose and cytokines; however, over half of NF-kB remained

cytosolic. Our results mirror trends previously reported in INS cells where NF-kB nuclear localization occurs in shorter time scales, with peak nuclear accumulation occur within 2 hours of treatment (Ortis et al., 2008). Because the transcriptional changes were of focus within our work, a later time point of approximately 14 hours post treatment was chosen for analysis to allow for transcription and translation to occur. At this later time point, nuclear NF-kB significantly reduces nearly to pre-treatment levels (Ortis et al., 2008). No observed changes occurred in cells treated with only 20 mM glucose or cytokines, demonstrating a necessary link between these conditions required for a proinflammatory phenotype to develop in these cells. Our results support that beta cells can express IL-1β when under inflammatory stress as cytokine treatment resulted in increased IL-1β expression (Maedler et al., 2002; Welsh et al., 2005). While this work focuses on early phases of proinflammatory signaling through potential interactions between TXNIP and NF-kB, future works should address later stages of inflammasome functions including caspase activity, lysosome destabilization, and pyroptosis. However, we identified that this effect is glucose dependent. Our findings also refute the highly debated notion that high glucose alone promotes IL-1β production from beta cells (Maedler et al., 2002; Wang et al., 2010; Welsh et al., 2005). Some reports have shown high glucose alone induces IL-1β production (Maedler et al., 2002). Other conflicting reports demonstrate high glucose alone does not upregulate *IL-1β* transcription as well as its post translation processing in human islets (Welsh et al., 2005). Our results similarly demonstrate that high glucose alone does not induce *IL-1β* upregulation in the INS cell line. Further studies highlight islet resident macrophages as the major source of IL-1β production within islet under conditions that promote type two diabetes development such as metabolic and protein stress (Alfadul et al., 2022; Westwell-Roper et al.,

2014). Our results support a non-beta cell source of IL-1β as we found cytokine treatment was required for IL-1β upregulation.

TXNIP is known to interact with proinflammatory proteins like NLRP3 to induce inflammasome development in multiple tissues including pancreatic islets (Filhoulaud et al., 2019; Zhou et al., 2010). The transcription factor NF-κB is activated by proinflammatory signals like TNF-a and IL-1β and regulates expression of multiple genes involved in inflammation including IL-1β and MCP-1 (T. Liu et al., 2017). Because both hyperglycemia and proinflammatory cytokines are required for these observed transcriptional changes, we assessed potential protein-protein interactions between TXNIP and NF-κB to see if they work in a similar mechanism seen in TXNIP-NLRP3 mediated inflammasome formation Overall, we report cytokine-induced *IAPP* downregulation and glucose-dependent cytokine-induced upregulation of *IL-1β* and *NF-κB* in the INS cell line. We also demonstrated that TXNIP and NF-κB do not physically interact within human pancreatic islets, suggesting independent pro-inflammatory signaling cascade for TXNIP and NF-κB in these cells.

Chapter 3: Proteasome activity is critical for beta cell identity and glucose sensing

Abstract

Type two diabetes is characterized by chronic hyperglycemia due to insufficient insulin secretion and/or peripheral insulin resistance. This disease has multiple contributing factors including oligomerization of the pancreatic peptide hormone islet amyloid polypeptide (IAPP) and protein stress evoked in part by proteasome complex dysfunction. Decreased proteasome activity contributes to the decreased production of this amyloidogenic protein; however, little work has been done to elucidate the global impact of proteasome malfunction and associated protein stress on gene expression and secretory functions of insulin and IAPP producing pancreatic beta cells. Here, we use RNA sequencing and differential gene analysis to assess the effect of both acute, pharmacologically induced proteasome inhibition and type two diabetes induced proteasome inhibition, on global changes in gene expression in human islet cells. Through this transcriptomics analysis, we identified a several trends in gene expression within proteasome inhibitor treated samples including downregulation of beta cell identity marker genes and genes required for glucose sensing and glucose induced insulin secretion such as *SLC2A2*. Through western blot analysis, we observed a decrease in IAPP but not insulin secretion from proteasome inhibited islets. Through multiple glucose utilization assays, we found impaired pyruvate production and decreased mitochondrial membrane potential when proteasome activity was inhibited. Both of these findings suggest that impaired proteasome function and/or associated protein stress reduces beta cell ATP production, resulting in reduced ATP-dependent peptide hormone secretion from these cells. In addition to normal glucose sensing and hormone secretion, transcriptomic analysis revealed that functional proteasome complex is also required for preservation of b-cell identity, which is compromised in T2DM patients.

Introduction

The pancreas is a retroperitoneal organ comprised of heterogeneous exocrine and endocrine tissues. The endocrine pancreas is comprised of islets of Langerhans that function as a major site for blood glucose regulation. These islets are comprised of several endocrine cell types that each have a highly specialized role in blood glucose homeostasis (Travagli & Browning, 2011). Minor pancreatic endocrine cell types like delta cells and gamma cells support and modulate secretory functions of other cells through paracrine signaling (Cabrera et al., 2006). Endocrine alpha and beta cells secrete hormones with antagonist functions to regulate blood glucose. Pancreatic alpha cells produce glucagon that is secreted in response to hypoglycemia. This hormone travels via the circulatory system to the liver where it promotes hepatic glucose mobilization through gluconeogenesis and glycogenolysis in order to raise blood glucose levels (Gromada et al., 1997). In contrast, pancreatic beta cells secrete insulin under hyperglycemic conditions (Wu et al., 1998). Beta cells utilize the glucose transporter GLUT2 to sense raises in blood glucose above euglycemic parameters (Leturque et al., 2005). Upon uptake, this glucose is converted into ATP through glycolysis, the citric acid cycle, and mitochondrial oxidative phosphorylation. The produced ATP then binds to potassium-ATP channel along the plasma membrane to block potassium influx, resulting in membrane depolarization. This depolarization activates voltage-gated calcium channels to allow for calcium influx (Light, 2010). Once inside the cell, calcium is bound by synaptotagmin on insulin granules to promote their exocytosis. After secretion, insulin travels to peripheral tissues like skeletal muscle and adipose where, upon binding to its receptor, promotes these tissues to uptake excess glucose from the blood. Specifically, insulin receptor binding induces SNARE-mediated translocation of glucose transporters to the plasma membrane of cells where they can uptake glucose from blood via facilitated diffusion (Thurmond & Pessin,

2000). Insulin signaling activates various other responses such as protein synthesis and cell growth (De Meyts, 2000).

In addition to insulin, beta cells produce another peptide hormone, islet amyloid polypeptide (IAPP), also referred to as amylin. IAPP is co-synthesized and secreted with insulin as both of these hormones are stored within insulin granules. Transcription of both *insulin* and *IAPP* is regulated by the shared transcription factor PDX1 under hyperglycemic conditions. PDX1 works synergistically with another transcription factor, MafA, to bind to the metabolic responsive elements E1, A1, and A2/C1 to regulate *insulin* transcription (Odagiri et al., 1996; M. Zhao et al., 2005). PDX1 binds to the *insulin* promoter in a calcium-independent manner but requires unidentified calcium response elements to bind to the *IAPP* promoter (Macfarlane et al., 2000a). This difference allows the steady-state levels of *IAPP* mRNA make up to 10-fold less of the steady-state *insulin* mRNA levels (Mulder et al., 1996). Additionally, *insulin* transcription is minimally altered by hyperglycemia while *IAPP* mRNA levels increase by approximately 10-fold (Shalev et al., 2002). Additional regulatory elements modulate *IAPP* expression and allow for different expression patterns from *insulin.* In response to both acute and chronic fatty acid exposure, *IAPP* expression is upregulated in a glucose-independent mechanism (Qi et al., 2010). The redox regulation protein and transcription factor TXNIP impacts *IAPP* but not *insulin* expression. TXNIP downregulates expression of microRNA miR-124a to indirectly upregulate *IAPP.* miR-124a inhibits expression of *FoxA2* which serves as another *IAPP* transcription factor. By releasing *FoxA2* from inhibition by this microRNA, this transcription factor is produced and can bind to its highly conserved proximal binding site within the *IAPP* promoter region (Jing et al., 2014).

Once secreted, IAPP has multiple functions as it acts locally through paracrine signaling while also reaching distal tissues through hormonal signaling. Within islets of Langerhans, IAPP modulates secretory function of neighboring endocrine cells (Akter et al., 2016). Upon binding to its receptors on skeletal muscle, IAPP increases glycogenolysis and decreases glycogen storage. The central nervous system has the highest concentration of IAPP receptors. Here, IAPP binding within the hindbrain area postrema suppresses appetite and reduces food consumption (Bortoletto & Parchem, 2023).

Diabetes is a heterogeneous disease broadly characterized by chronic hyperglycemia as beta cells cannot produce enough insulin to meet metabolic demands. Type two diabetes develops from multiple factors including genetic, environmental, and lifestyle influences (Goyal et al., 2024b). Amyloidosis contributes heavily to beta cell apoptosis as amyloid fibrils are found in the majority of individuals with type two diabetes (Betsholtz et al., 1989). These fibrils are comprised of IAPP oligomers. As IAPP oligomers form, unordered random coil elements are lost as these structures transition into beta-structures, notably beta sheets, within minimal changes to alpha-helices (Rishisree et al., 2024). This self-aggregation occurs within amino acids 20-29. Interesting, proline substitutions occur within this regions in rodent IAPP and prevent self-aggregation (Betsholtz et al., 1989).

The exact cause of IAPP oligomerization is unknown but has been linked to impaired proteasome function. The 26S proteasome, comprised of a 20S proteolytic core and 19S regulatory component, degrades eukaryotic, non-lysosomal polyubiquitinated proteins including IAPP. In other age-related diseases, especially neurodegenerative disorders like Alzheimer's disease, proteasome impairment has been shown to correlate with protein plaque formation and disease progression (Stroo et al., 2017). Age-associated onset of type 2 diabetes only occurs in

species like humans that can form IAPP oligomers, suggesting that both protein aggregation and proteasome impairment may have a role in disease development similar to neurodegenerative disorders (Betsholtz et al., 1989). Decreased proteasome activity has been observed in islets from individuals with type two diabetes, further supporting this notion (Chatterjee Bhowmick & Jeremic, 2018b).

Reduced proteolytic activity allows ubiquitinated proteins to collect within the cell leading to protein stress that activates the unfolded protein response. The unfolded protein response functions primarily through three signaling pathways that are initiated by accumulation of unfolded or misfolded proteins within the endoplasmic reticulum lumen. Through PERK and IRE1 signaling, translation is globally decreased, and RNase activity is increased. These activities limit the amount of new protein production to prevent further protein stress. Through ATF6, both lysosomal and proteasome-mediated proteolysis is increased to expedite removal of misfolded proteins. All three UPR signaling pathways upregulate transcription of chaperon proteins to limit and resolve protein misfolding (Eizirik et al., 2008). Acutely, this response protects beta cells from further damage by reducing protein synthesis and reducing metabolic burden; however, this protection occurs at the expense of the function of these cells. By lowering overall protein synthesis, beta cells reduce their peptide hormone synthesis thereby drastically lowering their insulin output (Pirot et al., 2007). When the UPR becomes chronic, protein stress cannot be handled by beta cells resulting in DNA damage, reactive oxygen species formation, endoplasmic reticulum dysfunction, reduced mitochondrial membrane potential, and decreased proteolytic functions through impaired autophagy and proteasome activity (Eizirik et al., 2008). Here, we have identified multiple genes downregulated by both type two diabetes and pharmacologically induced proteasome inhibition through RNAseq and differentially gene

analysis with verification through qPCR and western blot analysis. We found *HSP* genes and genes related to proteasome function were highly upregulated in islets treated with proteasome inhibitors. In contrast, proteasome-associated genes were only slightly upregulated in islets from individuals with type two diabetes while *HSP* genes were downregulated in these samples. Additional analysis revealed a global loss of essential beta cell genes in islets from individuals with type two diabetes while proteasome inhibitor treatments resulted in only slight global downregulation of these genes; however, expression of select essential genes like *SLC30A8* and *BMP5* are similar decreased among these groups. Furthermore, genes involved in multiple steps of beta cell peptide hormone secretion were downregulated by both disease-induced and pharmacologically induced proteasome inhibition. To identify specific steps affected, functional studies were performed in the INS cell line and revealed compromised mitochondrial activity and glycolytic pathway activity under proteasome inhibition. Althouhg glucose uptake was surprisingly unaffected, pyruvate production and mitochondrial membrane potential were decreased in proteasome inhibitor treated cells.

Methods

Cell Cultures

Rat insulinoma INS 832/13 cells (a generous gift from Christopher Newgard, Duke University) were cultured in RPMI 1640 media (ThermoFisher Scientific catalog number 11875093) supplemented with 1% penicillin/ streptomycin (ATCC catalog number 30-2300), 10mM HEPES (Gibco catalog number 15630-080), 2mM L-glutamate (Sigma Aldrich G8415), 1 mM sodium pyruvate (Sigma Aldrich S8636), 0.05 mM 2-mercaptoethanol (Sigma M3148) , and 10% (v/v) fetal bovine serum (ThermoFisher Scientific catalog number 26140079). Insulinoma cells were stored at 37°C in a humidified incubator with 5% CO_2 and passaged every 3 to 4 days. Prior to

treatments, cells were plated on a 96 well plate in 5 mM glucose media and equilibrated for 24 hours (GET INFO).

In addition to INS cell lines, human pancreatic islets from non-diabetic cadavers with >90% viability and purity were obtained through the Integrated Islet Distribution Program (IIDP) for Human Islet Research. These islets are from approved cadaveric organ. Therefore, the tissue is exempt from human studies approval per IIDP guidelines. Privacy and personal identity information of all participants was protected. Studies using human islets were approved by The George Washington University Institutional Review Board (IBC#IBC-20-092). Upon arrival, intact islets were plated on a non-adherent 48 well plate in CMRL media (ThermoFisher Scientific catalog number 11530037) supplemented with 1% (V/V) fetal bovine serum (ThermoFisher Scientific catalog number 26140079) and 1% penicillin/streptomycin (ATCC catalog number 30-2300). Islets were cultured in a humidified incubator at 37°C with 5% CO_2 and given 24 hours to equilibrate before treatments.

Both cell types were treated supplemented with an additional 15 mM glucose to achieve a final hyperglycemic 20 mM glucose treatment and 200 μM palmitate. Cells were checked daily via bright field microscopy to assess morphological changes indicating stress such as detachment from plates, apoptotic body formation, membrane blebbing, and, for islets only, islet fragmentation. Cells were left to incubate under this metabolic stress until cellular stress was visibly apparent, with a minimum incubation time of 3 days and a maximum of 9 days, in order to more closely mimic the effects of chronic hyperglycemia characteristic of type two diabetes. Once the cells began showing any signs of stress, wells were treated for 8 hours with 2 μM lactacystin (EMD Millipore 426100) or 100 nM Bortezomib (EMD Millipore 5.04314.0001).

Proteasome Activity Assay

Eight hours after proteasome inhibitor treatments, proteasome activity was determined using the 20S Proteasome Assay Kit (Cayman Chemicals #10008041). Following manufacture instructions, total intracellular content was isolated. Activity was assessed by cleavage of the 20S proteasome-specific substrate, *N-succinyl*-LLVY-7-amino-4-methylcoumarin, that produces a highly fluorescent product when cleaved. Increased fluorescence indicates increased 20S proteasome activity. Fluorescence was measured via Molecular Devices Spectra Max M5 using SoftMaxPro5 with excitation/emission spectra set at 360/480 nm. Additional intracellular content was collected and used to perform a bicinchoninic acid to determine total intracellular protein (Thermo Fisher #23228). Proteasome activity data was then normalized to total intracellular protein.

Real Time – Quantitative PCR

Eight hours after proteasome inhibitor treatments, total RNA was isolated from cells via Qiagen RNeasy mini kit per manufacturer instructions (Qiagen catalog number 74134). RNA concentrations were determined via Nanodrop. From each sample, 400 ng of RNA was converted into cDNA using a multiScribe reverse transcription kit with random primers following manufacture instruction (Applied Biosystems catalog number 4368814). qPCR was then performed with resulting cDNA via iTaq Universal SYBR Green supermix (BioRad catalog number 1725122) and primers listed in Tables 1 and 2. Bio Rad CFX 96 real-time system and C1000 Touch thermal cycler were used for amplification and gene detection. Expression levels of all genes were normalized to β -actin expression. Fold change in expression of these genes was calculated using the 2-delta CT method.

Table 1: Rat qPCR primer sequences

Gene	Forward Primer Sequence	Reverse Primer Sequence
β-actin	5’-GCTACAGCTTCACCACCACA-3’	5’-ATCGTACTCCTGCTTGCTGA-3’
IAPP	5’-AGCTGTTCTCCTCATCCTCT-3’	5’-CTGTGTTGCACTTCCGTTTG-3’
TXNIP	5’-CGAGTCAAAGCCGTCAGGAT-3’	5’-TTCATAGCGCAAGTAGTCCAAGGT-3’

FoxA2	5’-CTGAGGTGGGTAGCCAGAAA-3’	5’-CACGGAAGAGTAGCCCTCAG-3’
PDX1	5’-CAAAGCTCACGCGTGGAA-3’	5’-TCCGGTTCTGCTGCGTATG-3’

Table 2: Human qPCR primer sequences

Gene	Forward Primer Sequence	Reverse Primer Sequence
β-actin	5’-CACATTCTGGAGAGCGAGAAG-3’	5’-CCAGCTTCTCGTATTTCTCCTT-3’
IAPP	5’-GCAAGTATTTCTCATTGTGCTCTC-3’	5’-GATGACAGAATGGCACCAAAGT-3’
TXNIP	5’-ACAGAAAAGGATTCTGTGAAGGTGAT-3’	5’-GCCATTGGCAAGGTAAGTGTG-3’
FoxA2	5’-AGATCTACCAGTGGATCATGGA-3’	5’-GGAAACAGTCGTTGAAGGAGAG-3’
PDX1	5’-TGCTAGAGCTGGAGAAGGA-3’	5’-CCAGATCTTGATGTGTCTCTCG-3’

RNA Sequencing

After proteasome inhibitor treatments, total RNA was isolated using the Qiagen RNeasy mini kit per manufacturer instructions (Qiagen catalog number 74134). RNA concentrations were determined via Nanodrop. RNA samples with concentrations greater than 20 ng/μL and A260/290 values above 1.9 were considered for sequencing. To ensure selected samples were responsive to both glucose and proteasome inhibitor treatments, qPCR was performed to determine if *IAPP* and *TXNIP* expression was raised by hyperglycemia and lowered by proteasome inhibition. Samples that passed all checkpoints were then sent for RNA sequencing by Novogene (Sacramento, CA, USA).

In collaboration with the Peng Lab, the sequencing quality of RNA-seq libraries were assessed by FastQC (v0.11.9) (https://www.bioinformatics.babraham.ac.uk/projects/fastqc/). Samtools 20 (v1.7) was used to transfer sam files to bam files and sort bam files (Li et al., 2009). Mapped reads were then processed by htseq-count (v1.99.2) to estimate expression levels of all genes/ to calculate the read count on genes (Anders et al., 2015). The expression level of a gene was expressed as transcripts per million mapped reads (TPM) value. Raw read counts on genes were processed by EdgeR (v3.32.1) to identify differentially expressed genes (DEGs) between a pair of conditions (quasi-likelihood test, foldchange≥1.5 and FDR<0.05, filter By Expr applied with default parameter, adjusted p-value < 0.05) (Robinson et al., 2010). To analyze the overall

expression changes of the DEGs across treatment conditions, we collected the DEGs from pairwise comparison among untreated control, high glucose treated, lactacystin treated, epoxomicin treated, Bortezomib treated, and type two diabetic samples. The expression values of these genes were subject to row-wise z-score transformation. K-means clustering was then applied to group these DEGs into clusters with distinct expression patterns. DEGs related to specific functions were grouped using 'GO:0000502' for proteasome-related genes and 'GO:0051879' for HSP-related genes, from the BiomaRt package in R. Beta cell marker genes were obtained from PanglaoDB (https://panglaodb.se/index.html).

Western Blot

Immediately prior to proteasome inhibitor treatments, total media was collected from cells and replaced with fresh media for peptide secretion analysis. Eight hours after proteasome inhibitor treatments, all media was collected from wells for secretion analysis. Whole cell extracts were collected in RIPA buffer (EMD Millipore, catalog number 20-188). Extracted protein concentrations were determined using the Pierce BCA Protein Assay Kit (Thermo Scientific reference number 23227). Four micrograms of protein or an equal volume of collected media were used for each well. Proteins were separated by SDS-PAGE on a 4-15% stacking gel (BioRad, catalog number 4561086). Resolved proteins were electrophoretically transferred to nitrocellulose membranes (BioRad catalog number 1704270) using the BioRad Trans-Blot Turbo System. Membranes were blocked with 5% nonfat dry milk. Membranes were probed with primary antibodies for one hour at room temperature with shaking. The following proteins were targeted by primary antibodies: β-actin (Santa Cruz sc-47778 HRP, 1:500), hIAPP (Santa Cruz sc-377530 HRP), TXNIP (Invitrogen JM60-35), insulin (Abcam ab181547), PDX1 (Abcam ab47267), and FoxA2 (Abcam ab108422). Then, corresponding horseradish peroxidase-

conjugated secondary antibodies were added at 1:2000 and incubated at room temperature for one hour. Resulting blots were developed using pico – (ThermoFisher Scientific no. 34580) or femto – (ThermoFisher Scientific no. 34095) ECL substrate kits and visualized with the ChemiDOC touch gel imaging system (BioRad). Intensity of the resulting bands was quantified using BioRad Image-Lab software where β-actin was used as a loading control.

Glucose Uptake Assay

Eight hours after proteasome inhibitor treatments, glucose uptake was determined using the Glucose Uptake-Glo Assay kit (Promega J1341). Following manufacture instructions, all cell media was removed and replaced with PBS supplemented with 2-deoxyglucose that was transported into the cell and phosphorylated by glucose-6-phosphate. Upon cell lysis with supplied Stop Buffer, existing NADPH was destroyed, and all 2-deoxyglucose-6-phosphate was released. Oxidation of this molecule was then coupled to NADP+ reduction. Finally, the produced NADPH was coupled to the conversion of proluciferin to luciferin. The light emitted by this reaction was detected via Molecular Devices Spectra Max M5 using SoftMaxPro5 where higher luminescence indicates higher glucose uptake. Resulting luminescence data was normalized to the 5 mM glucose treated control samples, assumed as 1.

Pyruvate Detection Assay

Eight hours after proteasome inhibitor treatments, pyruvate production was determined using the Pyruvate-Glo Assay kit (Promega J4051). Following manufacture instructions, total intracellular contents were isolated. Isolated cellular pyruvate was then oxidized to produce acetyl phosphate and H2O2. An H2O2 substrate was then added and converted to luciferin. The light emitted by this reaction was detected via Molecular Devices Spectra Max M5 using SoftMaxPro5 where

higher luminescence indicates higher pyruvate content. Resulting luminescence data was normalized to the 5 mM glucose treated control samples, assumed as 1.

JC1 Quantification and Imaging

Eight hours after proteasome inhibitor treatments, cells were incubated with 10uM of the mitochondrial membrane potential dye 5,5',6,6'-tetrachloro-1,1',3,3'-tertraethyl-benzimidazolylcarbocyanine iodine (JC-1) (ThermoFisher T3168) at 37°C for 10 minutes. Media was then removed and replaced with PBS. Fluorescence was immediately measured via Molecular Devices Spectra Max M5 using SoftMaxPro5. JC-1 undergoes a fluorescent shift from 525 nm to 590 nm as it exhibits a potential-dependent accumulation within the mitochondria that promotes locally high concentrations and subsequent aggregation. All experiments using JC-1 dye were performed within 30 minutes of dye addition to the analyzed well to minimize the mitochondrial effects of prolonged glucose starvation. Several excitation/emission spectra were used to quantify both the monomer and J-aggregates formed by this dye (Table 3). Collected florescent data was ratioed as J-aggregated only: monomer only to calculate the fraction of dye that formed aggregates. Resulting data was then normalized to the 5 mM glucose treated control samples, assumed as 1.

After this analysis, wells were imaged using a Zeiss LSCM-800 confocal microscope (Carl Zeiss, Thornwood, NY) at 63x magnification.

Table 3: JC-1 Species Detection Spectra

Species Detected	**Excitation (nm)**	**Emission (nm)**
Monomer only	485	530
J-aggregate only	535	590
Monomer and J-aggregate, simultaneously	475	510

Statistical Analysis

Statistical analysis of RNAseq data was performed via EdgeR. For comparisons between two sets of paired data points in boxplots, a two-sided Wilcoxon test was used. For all other experiments, statistical analysis and graph plotting was performed using GraphPad Prism 10. Datasets were tested for Gaussian distribution and equal variance prior to analysis. If both tests were passed, data was analyzed via one-way ANOVA followed by a Tukey post hoc test with significance established at $p<0.05$. Data trending towards significant was established at $p<0.10$. Histograms depict the average of all collected data points +/- SEM.

Results

Islet Proteasome Inhibition Alters Expression of Proteasome and HSP Genes

Primary human islets were cultured in control 5 mM glucose or hyperglycemic 20 mM glucose. When high glucose treated islets were additionally treated with the proteasome inhibitors lactacystin, epoxomicin, and Bortezomib, all had significantly reduced 20S proteasome activity (Fig. 1A). Lactacystin reduced proteasome activity to 53% functionality ($P \leq 0.01$) and Bortezomib reduced function to 27% activity ($p \leq 0.0001$) in comparison to 20 mM glucose treated samples (Fig. 1A). Hyperglycemia alone did not significantly alter proteasome activity with an average activity of 92% (Fig. 1A). Epoxomicin-treated samples provided erratic and inconsistent responses upon further western blot and qPCR analysis. Thus, this treatment has a limited number of samples as unresponsive samples were not used in analysis.

RNA isolated from responsive islets was analyzed via RNA seq. In response to acute proteasome stress through pharmacological proteasome inhibition, *HSP* genes were upregulated relative to untreated samples (Fig. 1B). All three proteasome inhibitor-treated samples clustered together. Despite lower proteasome activity in diabetic islets, islets from individuals with type two diabetes showed similar *HSP* gene expression to untreated islets from non-diabetic individuals

(Fig. 1B). Both diabetic samples clustered together illustrating shared features of this disease while untreated and high glucose treated samples clustered together.

Upon further examination of all proteasome-related genes, type two diabetic islets and proteasome inhibitor-treated islets shared similar expression patterns. Under both proteasome-impaired conditions, there is a general upregulation of proteasome genes in comparison to untreated islets from non-diabetic individuals (Fig. 1C). Similar to *HSP* gene analysis, this upregulation is stronger in islets treated acutely with proteasome inhibitors relative to islets from individuals with type tow diabetes.

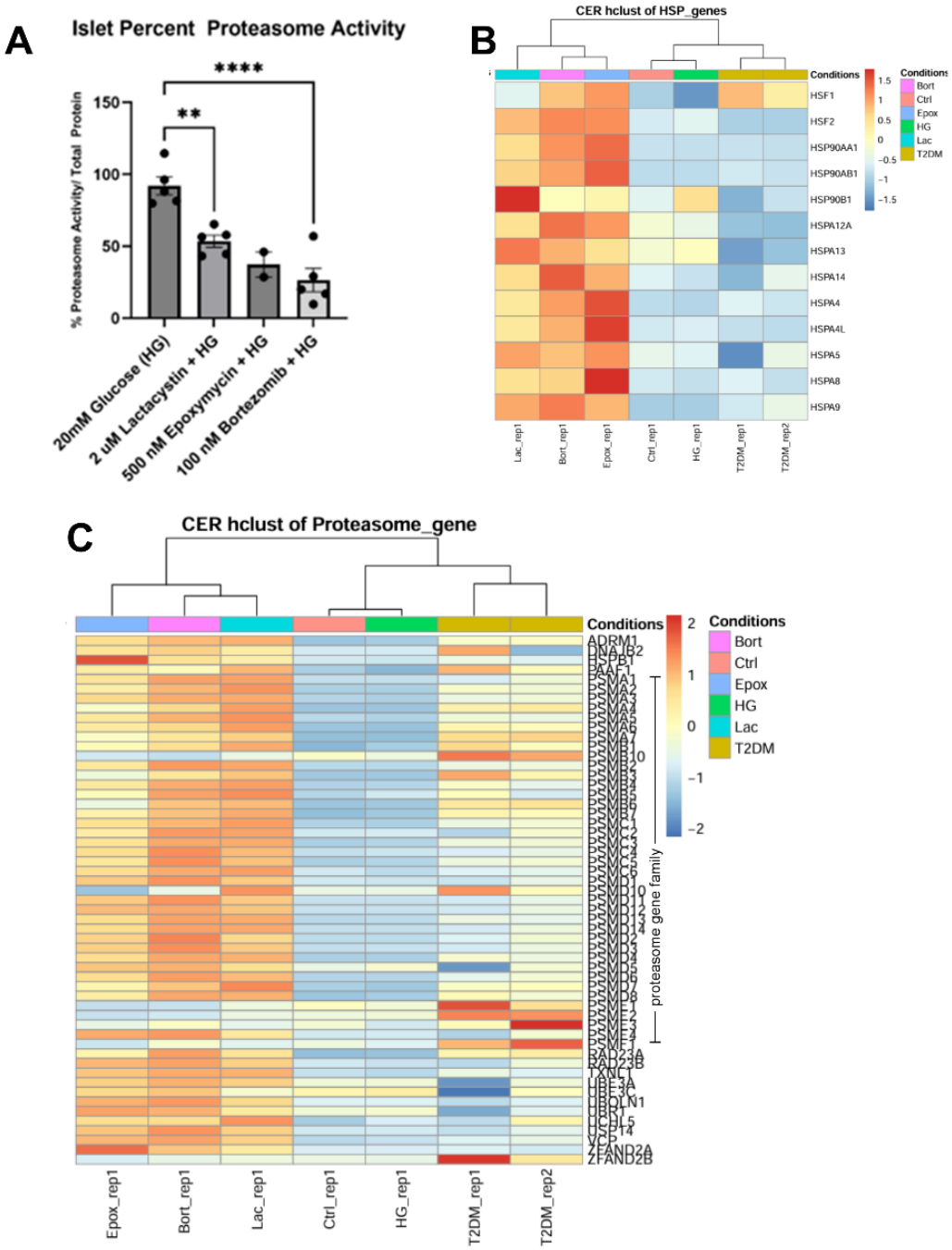

Figure 1: Decreased proteasome activity alters expression of protein-stress response genes Human pancreatic islets from non-diabetic individuals were treated with 5 mM glucose (ctrl) or 20 mM glucose (HG) in combination with 200 µM palmitate (HP), 100 nM Bortezomib (Bort), or 2 µM lactacystin (Lac). Untreated islets from individuals with type two diabetes (T2DM) were additionally analyzed. **A)** Proteasome activity was measured in islets treated with 20 mM glucose, 2 µM lactacystin, 500 nM epoxomicin, and 100 nM Bortezomib and normalized to total intracellular protein. Percent activity was determined relative to untreated controls. Both lactacystin and Bortezomib treatments significantly downregulated proteasome activity (n=5, **p ≤ 0.01, **** p ≤ 0.0001). **B)** Heatmap analysis of differentially expressed *HSP* genes across all treatment groups shows significant upregulation of *HSP* genes under acute proteasome inhibition. **C)** Heatmap analysis showing differential expression of proteasome-related genes across all treatment groups reveals significant upregulation of proteasome-associated genes while islets

from individuals with type two diabetes have slight upregulation of these genes. Genes encoding proteasome subunits are bracketed and referred to as 'proteasome gene family'.

Proteasome Inhibition Downregulates Essential Beta Cell Genes

Under chronic cellular stress typical of type two diabetes, beta cells implement protective adaptations to prevent cell death. These processes often involve a phenotypic shift in which beta cells lose multiple of their physiological functions in order to preserve themselves. Our RNAseq analysis confirms this finding as many beta cell marker genes like *IAPP* are downregulated in islets from individuals with type two diabetes (Fig. 2A). Proteasome-inhibitor treated islet cluster separately from both type two diabetic islets and untreated islets as they show only slight downregulation of some beta cell marker genes (Fig. 2A). This finding highlights the significance of chronic vs acute stress in these cells as multiple years of cellular stress results in much more potent gene downregulation in comparison to several days of proteasome inhibition. Several genes of interest were identified though RNAseq results. Both *TXNIP* and *IAPP* are two of the most inducible genes within beta cells and *IAPP* was significantly upregulated by hyperglycemic treatments, significantly downregulated by type two diabetes, and slightly downregulated by proteasome inhibition. To confirm our RNAseq findings, qPCR of these genes was performed. Both *TXNIP* and *IAPP* were significantly downregulated by lactacystin ($0.1 \geq p \geq 0.05$, respectively) and by Bortezomib ($p \leq 0.05$) (Fig. 2B and C). Further support for RNAseq results was established through western blot analysis. Expression of the essential beta cell transcription factors PDX1 and FoxA2 were assessed as RNAseq analysis showed slight downregulation of PDX1 by proteasome inhibition and FoxA2 shares similar functions. Protein analysis showed no significant decrease in either protein; however, there was a decrease in both proteins under proteasome inhibition that was trending towards significance with all p values less than 0.1 but greater than 0.05 (Fig. 2 D and E).

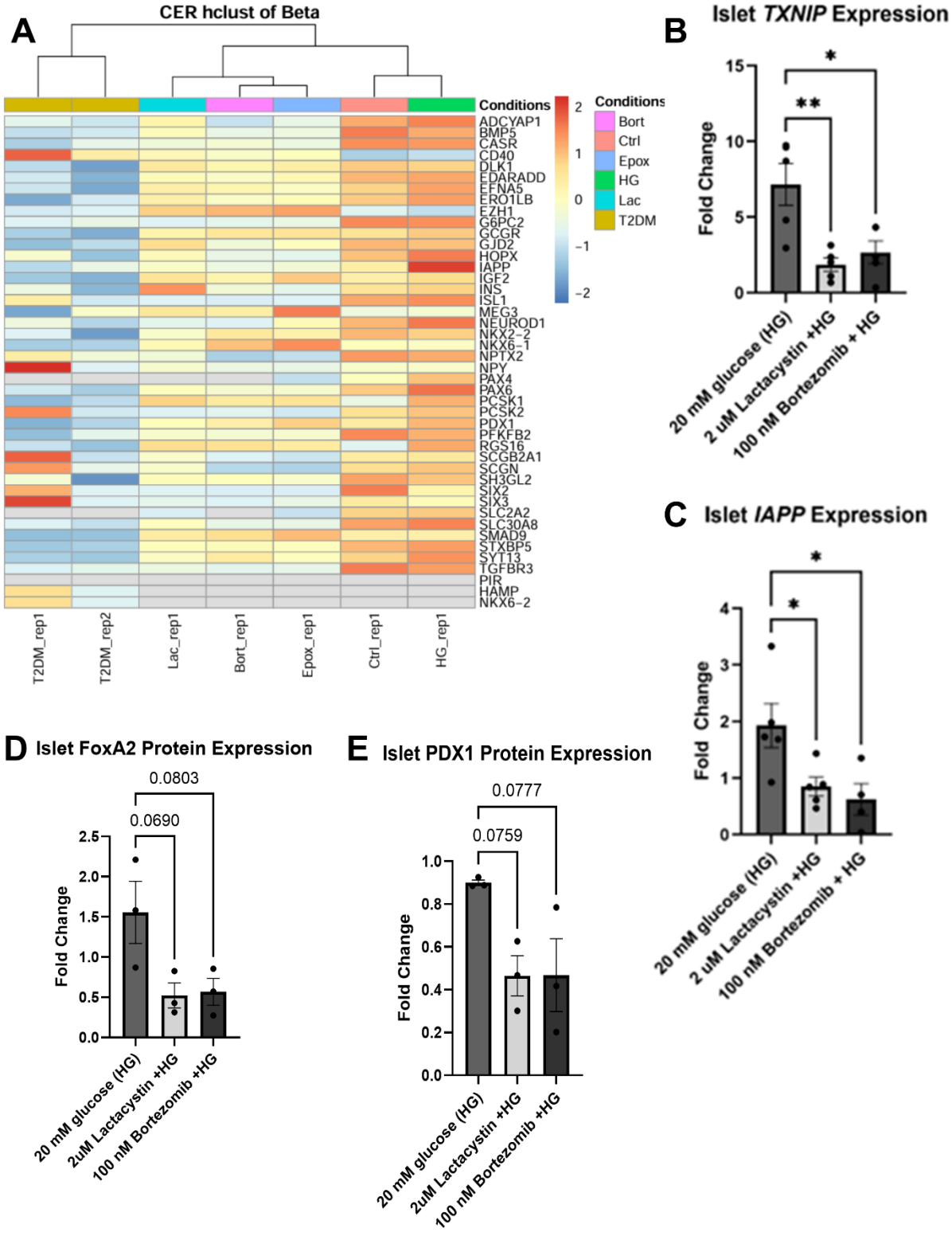
A
CER hclust of Beta
Conditions
ADCYAP1
BMP5
CASR
CD40
DLK1
EDARADD
EFNA5
ERO1LB
EZH1
G6PC2
GCGR
GJD2
HOPX
IAPP
IGF2
INS
ISL1
MEG3
NEUROD1
NKX2-2
NKX6-1
NPTX2
NPY
PAX4
PAX6
PCSK1
PCSK2
PDX1
PFKFB2
RGS16
SCGB2A1
SCGN
SH3GL2
SIX2
SIX3
SLC2A2
SLC30A8
SMAD9
STXBP5
SYT13
TGFBR3
PIR
HAMP
NKX6-2
T2DM_rep1
T2DM_rep2
Lac_rep1
Bort_rep1
Epox_rep1
Ctrl_rep1
HG_rep1
2
1
0
−1
−2
Conditions
Bort
Ctrl
Epox
HG
Lac
T2DM
B
Islet TXNIP Expression
Fold Change
15
10
5
0
*
**
20 mM glucose (HG)
2 uM Lactacystin +HG
100 nM Bortezomib + HG
C
Islet IAPP Expression
Fold Change
4
3
2
1
0
*
*
20 mM glucose (HG)
2 uM Lactacystin +HG
100 nM Bortezomib + HG
D
Islet FoxA2 Protein Expression
0.0803
0.0690
Fold Change
2.5
2.0
1.5
1.0
0.5
0.0
20 mM glucose (HG)
2uM Lactacystin +HG
100 nM Bortezomib +HG
E
Islet PDX1 Protein Expression
0.0777
0.0759
Fold Change
1.0
0.8
0.6
0.4
0.2
0.0
20 mM glucose (HG)
2uM Lactacystin +HG
100 nM Bortezomib +HG

Figure 2: Beta cell marker genes are downregulated by proteasome impairment Human pancreatic islets from non-diabetic individuals were treated with 5 mM glucose (ctrl) or 20 mM glucose (HG) in combination with 200 μM palmitate (HP), 100 nM Bortezomib (Bort), or 2 u μM lactacystin (Lac). Additional untreated islets from individuals with type two diabetes (T2DM) were also analyzed. **A)** Heatmap analysis of differential expression among beta cell marker genes shows general downregulation of this class in islets from individuals with type two diabetes. Proteasome inhibition through treatments with lactacystin, epoxomicin, or Bortezomib result in slight downregulation of some beta cell marker genes relative to islets with functional proteasome complexes, ctrl and HG samples. **B)** qPCR analysis of islets illustrated a decrease in *TXNIP* for both lactacystin and Bortezomib treated samples (n= 4, *$p \leq 0.05$, **$p \leq 0.01$) **C)** Similarly, qPCR analysis of *IAPP* expression showed downregulation of this genes in both proteasome inhibitor treated samples (n= 4, *$p \leq 0.05$) **D)** Western blot analysis of total islet intracellular protein islets demonstrated a reduction in FoxA2 with data trending towards significance in islets treated with lactacystin and Bortezomib (n=3, $0.1 \geq p \geq 0.05$) **E)** Similarly, western blot analysis of islets showed decreased PDX1 in both proteasome inhibitor treated samples (n=3, $0.1 \geq p \geq 0.05$)

Proteasome Inhibition Downregulates Beta Cell Genes Required for Peptide Hormone Secretion

RNAseq analysis of specific genes revealed additional trends during proteasome inhibition. Genes involved in multiple steps of peptide hormone secretion were significantly downregulated under both type two diabetes induced and proteasome inhibitor induced proteasome dysfunction in comparison to 5 mM low glucose treated islets from non-diabetic individuals. Similar to the changes observed in expression of beta cell marker genes, the largest changes in gene expression were generally observed in islets form type two diabetic individuals while smaller changes were seen in islets under acute stress (Fig. 2A). *SLC2A2* encoding the GLUT2 transporter essential to beta cell glucose uptake was significantly downregulated in type two diabetic islets and proteasome inhibitor treated islets (Fig. 3A, p= 7.1e-05 and p=0.0077, respectively). *SLC30A8* encoding a zinc transporter required for insulin granule formation was significantly downregulated in islets from individuals with type two diabetes and was trending towards significant downregulation in proteasome inhibitor treated islets (Fig. 3B, p = 0.0012 and p = 0.10, respectively). Several genes encoding proteins involved in carbohydrate metabolism and glycolysis regulation were additionally downregulated by proteasome inhibition. *G6PC2* encoding a catalytic subunit of glucose-6-phosphatase required for glycogenolysis and gluconeogenesis was significantly downregulated in both type two diabetic islets and proteasome

inhibitor treated islets (Fig. 3C, p = 0.0056 and 0.0017, respectively). *PFKFB2* encoding 6-phosphofructo-2-kinase that modulates glycolysis was trending towards significant downregulation in proteasome inhibitor treated islets while its expression was unaltered in islets from type two diabetic individuals relative to untreated islets from non-diabetic individuals (Fig. 3D, p=0.094 and p=0.39, respectively). Additional genes encoding beta cell transcription factors were similarly downregulated by these conditions. *SIX2* encoding a homeobox protein was trending towards significant downregulation by pharmacological proteasome inhibition, but no changes in transcription were detected in type two diabetic islets (Fig. 3E, p= 0.059 and p=0.4, respectively). As a transcription factor, SIX2 is required for expression of genes governing beta cell insulin processing including *SLC2A2,* therefore, downregulation of this transcription factor may cause downregulation of other genes of interest identified through RNAseq analysis. Additionally, the *CASR* gene encoding a plasma membrane G protein-coupled receptor is downregulated in islets from individuals with type two diabetes and trending towards significant downregulation in proteasome inhibitor treated islets (Fig. 3F, p=0.019 and p=0.067, respectively). Interestingly, metabolic stressors like high glucose and free fatty acids had less effects on gene expression as no genes of interest associated with peptide hormone secretion were significantly affected by 20 mM high glucose treatment. Treatments with the free fatty acid palmitate caused significant downregulation of several analyzed genes including *SLC30A2, G6PC2,* and *CASR* but had no significant effects on other investigated genes (Fig. 3 A-F).

To further examine the effects of proteasome inhibition, western blot analysis was performed to identify changes in IAPP and insulin secretion under these conditions. IAPP secretion was significantly decreased in islets treated with proteasome inhibitors (Fig. 3G, $p \leq 0.05$). In

contrast, insulin secretion was not impaired in proteasome inhibitor treated islets (Fig. 3H, $p \geq 0.05$).

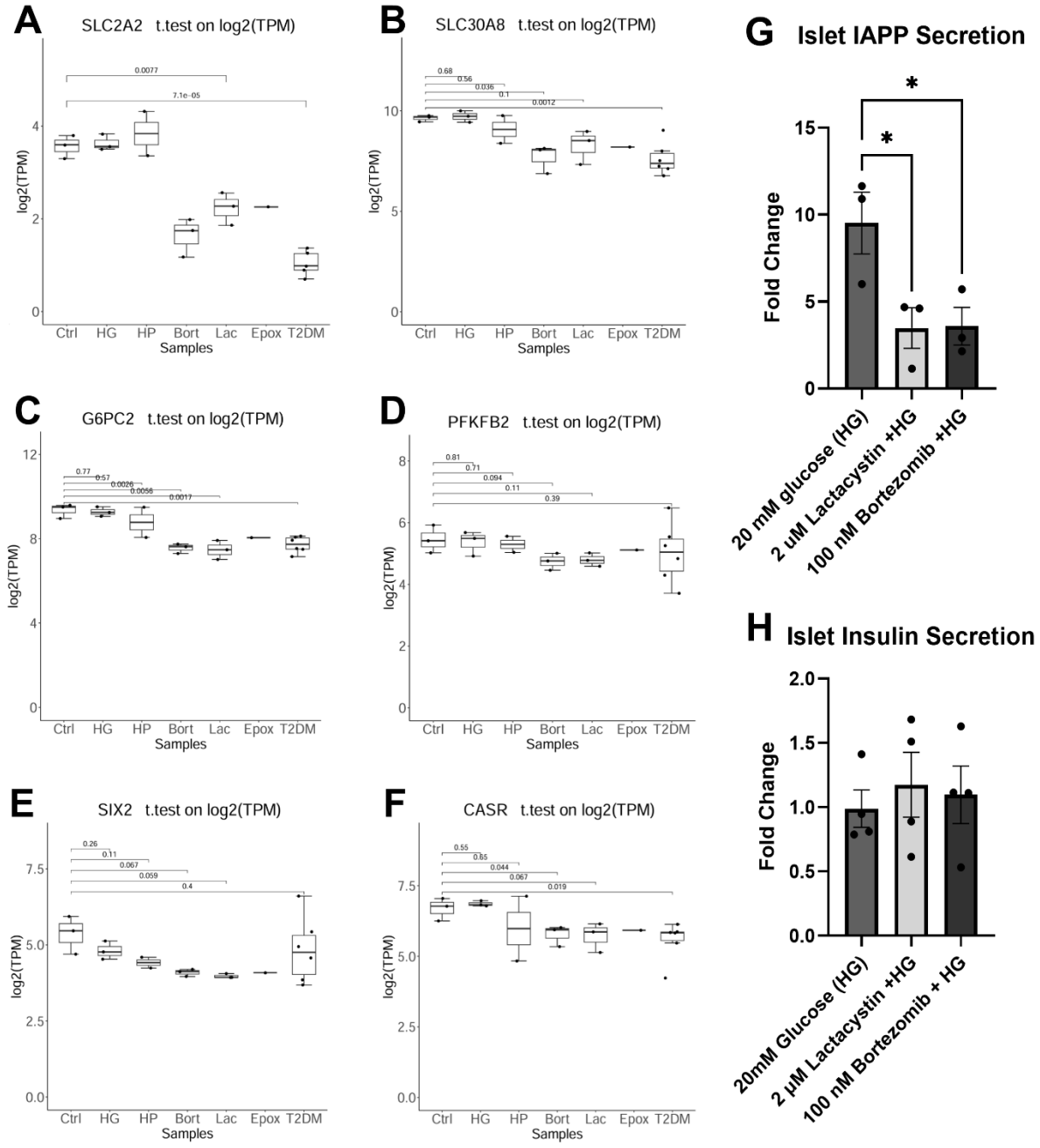

Figure 3: Effects of proteasome inhibition on beta cell peptide hormone secretion Human pancreatic islets from non-diabetic individuals were treated with 5 mM glucose (ctrl) or 20 mM glucose (HG) in combination with 200 μM palmitate (HP), 100 nM Bortezomib (Bort), or 2 μM lactacystin (Lac). Additional untreated islets from individuals with type two diabetes (T2DM) were also analyzed. Analysis of gene expression was performed across genes associated various steps of beta cell peptide hormone secretion including **A)** *SLC2A2* required for glucose uptake **B)** *SLC30A8* essential to insulin granule formation **C** and **D)** *G6PC2* and *PFKFB2* that function as regulators of

glycolysis and gluconeogenesis in beta cells **E)** *SIX2* encoding a transcription factor required beta cell functional maturation and **F)** *CASR* ($n \geq 3$, $p \leq 0.05$). **G)** Western blot analysis of islet media after treatments shows proteasome inhibitors significantly decrease IAPP secretion (n=3, $*p \leq 0.05$) **H)** Western blot analysis of islet media after treatments shows no alteration in insulin secretion relative to 20 mM high glucose samples (n=3, $p \geq 0.05$)

Inhibition of proteasome proteolytic activity impairs mitochondrial function by limiting glucose flux

Multiple steps involved in glucose-induced peptide hormone secretion are affected by gene downregulation associated with proteasome inhibition. To link downregulated genes to a cellular effect, several glucose utilization assays were performed to assess precisely which steps are impacted by proteasome inhibition. INS cells were treated with proteasome inhibitors. Glucose uptake was first assessed and showed no differences were observed among samples (Fig. 4A, $p \geq 0.05$). Because glucose uptake into the cell was not impaired, glucose conversion was next targeted through a pyruvate production assay in which intracellular pyruvate content was measured with a luminescent assay. Both lactacystin and Bortezomib significantly reduced INS cell pyruvate production in comparison to 20 mM glucose treated cells (Fig. 4B, $p \geq 0.001$ and $p \geq 0.01$, respectively). Cells could not compensate for this loss of glycolytic processing as mitochondrial membrane potential was also decreased in proteasome inhibitor treated samples (Fig. 4C). Unstimulated INS cells in 5 mM glucose media showed little aggregation of JC-1 dye, indicative of higher mitochondrial membrane potential, as the cells largely remained green (Fig. 4D). In contrast, 20 mM glucose treated cells appeared red as JC-1 accumulated within the mitochondria due to the higher membrane potential (Fig. 4E). INS cells treated with both 20 mM glucose and lactacystin appeared predominately green with some red aggregates (Fig. 4F).

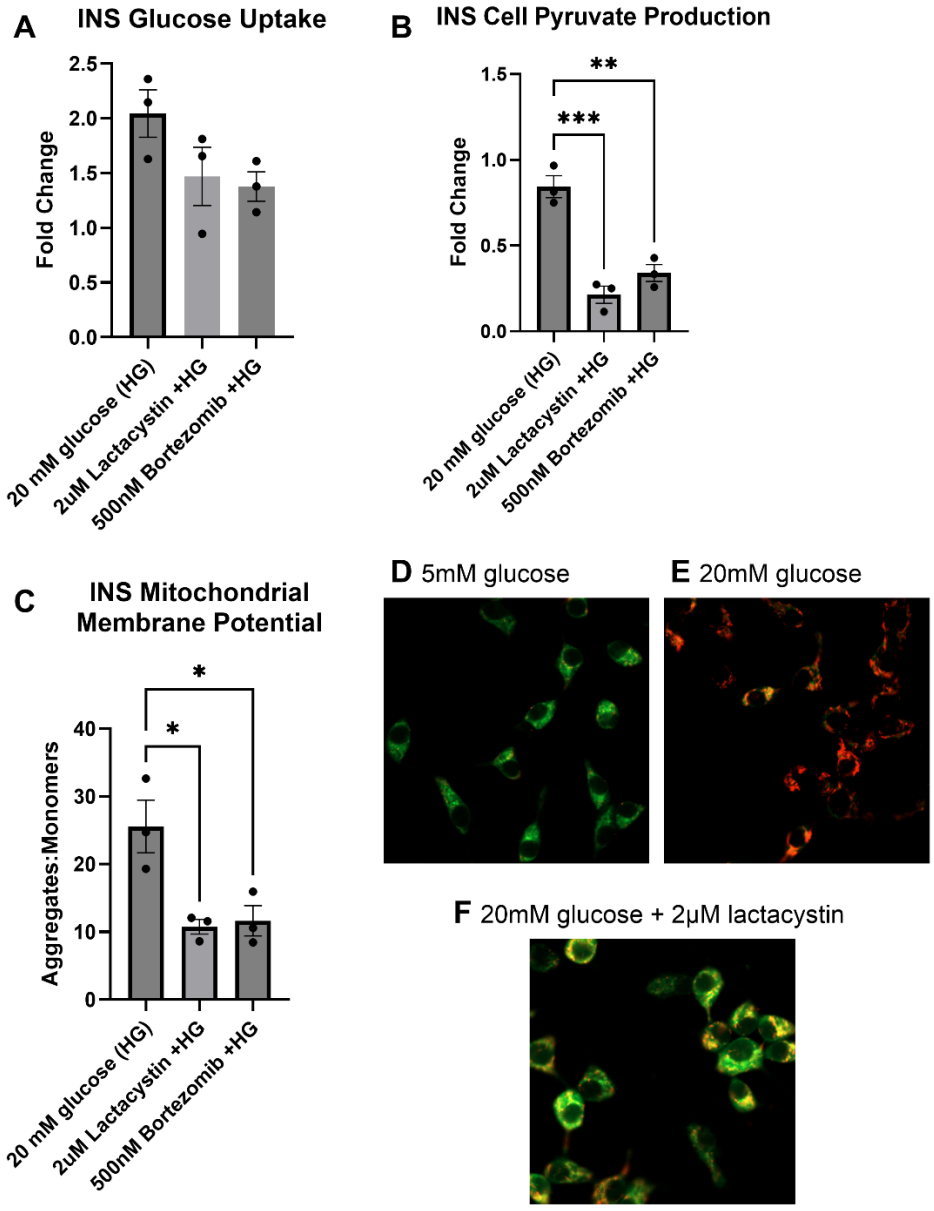

Figure 4: Proteasome inhibition impairs beta cell ATP production INS cells were treated with high glucose in the presence or absence of the proteasome inhibitions lactacystin or Bortezomib. Multiple steps in the conversion of glucose to ATP were assessed **A)** Proteasome inhibition does not alter glucose uptake in INS cells (n=3, $p \geq 0.05$) **B)** Both lactacystin and Bortezomib significantly reduce INS cell pyruvate production (n=3, $^{**}p \geq 0.01$, $^{***}p \geq 0.001$) **C)** Both lactacystin and Bortezomib significantly reduce INS cell mitochondrial membrane potential (n=3, $^{*}p \leq 0.05$), **D-F)** Representative images of JC-1 imaging in INS cells treated with **D)** 5 mM glucose, **E)** 20 mM glucose, and **F)** 20 mM glucose and 2 μM lactacystin

Discussion

Here, we investigated the effects of proteasome inhibition and associated protein stress on pancreatic beta cell gene expression and metabolic functions governing secretion. Both pharmacologically induced and pathophysiological proteasome inhibition observed in islets from individuals with type two diabetes were assessed. Through RNA sequencing and differential gene expression analysis, we observed an increase in both *HSP* genes as well as genes associated with the proteasome in islets treated with proteasome inhibitors. In contrast, we saw a decrease in *HSP* genes and only a minor decrease in proteasome-associated genes in islets from individuals with type two diabetes. These findings highlight the difference in islet responses to acute and chronic stress. Upon metabolic or protein stress, multiple systems are activated in beta cells to prevent cell death (Eizirik et al., 2008). In the case of proteasome inhibition, the primary mechanism activated is the UPR as ubiquitin-tagged proteins marked for degradation accumulate within the cell (Chatterjee Bhowmick & Jeremic, 2018b). The UPR response results in upregulation of chaperon proteins, including HSP, to resolve and prevent further protein misfolding. Additionally, the UPR increases proteolytic activity through both the lysosome and proteasome. To increase proteasome function, additional proteasome subunits can be transcribed and translated to create a larger pool of functional proteasome complexes (Eizirik et al., 2008). In contrast to acute proteasome impairment, chronic stress promotes pancreatic beta cell dysfunction leading to loss of their functionality. This is often characterized by reduced loss of glucose sensitivity and reduced insulin secretion (Patel & Remedi, 2024b). Here, we showed multiple beta cell marker genes including *IAPP* and *NeuroD1* are downregulated in type two diabetic islets. When islets are only acutely treated with stressors like proteasome inhibitors, the global downregulation of beta cell marker genes is minor. However, expression of select genes

including *TXNIP* and *IAPP* that are critical to beta cell identity and functionally are comparable downregulated across proteasome inhibitor treated and type two diabetic samples.

We additionally analyzed the differential expression of several genes required for normal peptide hormone secretion from beta cells. Because ATP production is required for both insulin and IAPP secretion, we identified multiple steps of cellular glucose metabolism where proteasome impairment downregulated essential genes (Light, 2010). The initial transport of glucose into the beta cell is comprised by proteasome inhibition as this condition decreases expression of *SCLC2A2* that encodes the beta cell glucose transporter GLUT2. Once glucose is brought into the cell, it should be converted into ATP via glycolysis, the citric acid cycle, and oxidative phosphorylation; however, proteasome inhibition downregulates several beta cell genes involved in the regulation of glycogenolysis and gluconeogenesis resulting in dysregulation of conflicting pathways for glucose production and glucose catabolism. This ultimately leads to lower ATP production and subsequently less insulin secretion. Furthermore, insulin granule formation is impaired by proteasome inhibition as *SCL30A8* is downregulated. This gene encodes the zinc transporter utilized by peptide hormone vesicle used to internalize the zinc required for proper protein folding needed for insulin granule maturation (Tamaki et al., 2013). Proteasome inhibition also downregulated expression of transcription factors including *SIX2.* Loss of this transcription factor results in reduced calcium flux and mitochondrial functionality which are both required for insulin granule exocytosis (Velazco-Cruz et al., 2020). This phenotype is likely in part due to reduction in GLUT2 as SIX2 regulates the expression of *SCLC2A2.*

Despite the downregulation of *SCL2A2* in human pancreatic islets under proteasome inhibition, INS cells showed no changes in glucose uptake when treated with lactacystin or Bortezomib. It is possible this is due to differences between rodent and human beta cells as other GLUT isoforms

are reported in rodent tissues and/or the compensatory mechanism of other GLUT isoforms that are co-expressed with GLUT-2 (Berger & Zdzieblo, 2020). Despite the unaltered glucose influx, glucose-induced IAPP secretion is still downregulated in proteasome treated islets. We found that this may be due to impaired ATP production despite the presence of glucose within the cell. Specifically, proteasome-inhibitor treated beta cells show lower pyruvate production suggesting a decrease in glycolysis. Furthermore, the NADH produced during the conversion of glucose into pyruvate as well as FADH2 produced during the citric acid cycle may not be well utilized by the mitochondria during proteasome inhibition. We found a decrease in mitochondrial membrane in cells treated with proteasome inhibitors which would disrupt the proton gradient across the inner mitochondrial membrane resulting in lowered ATP production (Zorova et al., 2018). Overall proteasome inhibition results in increased protein stress, decrease in beta cell marker gene expression, lowered IAPP secretion, and reduced ATP production.

References

Abdulreda, M. H., & Berggren, P. -O. (2013). Islet inflammation in plain sight. *Diabetes, Obesity and Metabolism*, *15*(s3), 105–116. https://doi.org/10.1111/dom.12160

Akter, R., Cao, P., Noor, H., Ridgway, Z., Tu, L.-H., Wang, H., Wong, A. G., Zhang, X., Abedini, A., Schmidt, A. M., & Raleigh, D. P. (2016). Islet Amyloid Polypeptide: Structure, Function, and Pathophysiology. *Journal of Diabetes Research*, *2016*, 1–18. https://doi.org/10.1155/2016/2798269

Alberts, B. (2019). *Essential cell biology* (Fifth edition). W.W. Norton & Company.

Alfadul, H., Sabico, S., & Al-Daghri, N. M. (2022). The role of interleukin-1β in type 2 diabetes mellitus: A systematic review and meta-analysis. *Frontiers in Endocrinology*, *13*, 901616. https://doi.org/10.3389/fendo.2022.901616

Alvarez Fallas, M. E., Pedraza-Arevalo, S., Cujba, A.-M., Manea, T., Lambert, C., Morrugares, R., & Sancho, R. (2021). Stem/progenitor cells in normal physiology and disease of the pancreas. *Molecular and Cellular Endocrinology*, *538*, 111459. https://doi.org/10.1016/j.mce.2021.111459

Anders, S., Pyl, P. T., & Huber, W. (2015). HTSeq—A Python framework to work with high-throughput sequencing data. *Bioinformatics*, *31*(2), 166–169. https://doi.org/10.1093/bioinformatics/btu638

Andersson-Rolf, A., Clevers, H., & Dayton, T. L. (2000). Diffuse Hormonal Systems. In K. R. Feingold, B. Anawalt, M. R. Blackman, A. Boyce, G. Chrousos, E. Corpas, W. W. de Herder, K. Dhatariya, K. Dungan, J. Hofland, S. Kalra, G. Kaltsas, N. Kapoor, C. Koch, P. Kopp, M. Korbonits, C. S. Kovacs, W. Kuohung, B. Laferrère, … D. P. Wilson (Eds.), *Endotext*. MDText.com, Inc. http://www.ncbi.nlm.nih.gov/books/NBK279025/

Ashcroft, F. (1996). Mechanisms of the Glycaemic Effects of Sulfonylureas. *Hormone and Metabolic Research*, *28*(09), 456–463. https://doi.org/10.1055/s-2007-979837

Bajetta, E., Ferrari, L., Martinetti, A., Celio, L., Procopio, G., Artale, S., Zilembo, N., Di Bartolomeo, M., Seregni, E., & Bombardieri, E. (1999). Chromogranin A, neuron specific enolase, carcinoembryonic antigen, and hydroxyindole acetic acid evaluation in patients with neuroendocrine tumors. *Cancer*, *86*(5), 858–865. https://doi.org/10.1002/(sici)1097-0142(19990901)86:5<858::aid-cncr23>3.0.co;2-8

Berger, C., & Zdzieblo, D. (2020). Glucose transporters in pancreatic islets. *Pflügers Archiv - European Journal of Physiology*, *472*(9), 1249–1272. https://doi.org/10.1007/s00424-020-02383-4

Berts, A., Gylfe, E., & Hellman, B. (1997). Cytoplasmic Ca2+ in glucagon-producing pancreatic alpha-cells exposed to carbachol and agents affecting Na+ fluxes. *Endocrine*, *6*(1), 79–83. https://doi.org/10.1007/BF02738806

Best, L., Brown, P. D., Sener, A., & Malaisse, W. J. (2010). Electrical activity in pancreatic islet cells: The VRAC hypothesis. *Islets*, *2*(2), 59–64. https://doi.org/10.4161/isl.2.2.11171

Betsholtz, C., Christmansson, L., Engström, U., Rorsman, F., Svensson, V., Johnson, K. H., & Westermark, P. (1989). Sequence divergence in a specific region of islet amyloid polypeptide (IAPP) explains differences in islet amyloid formation between species. *FEBS Letters*, *251*(1–2), 261–264. https://doi.org/10.1016/0014-5793(89)81467-X

Bhaumik, S. R., & Malik, S. (2008). Diverse Regulatory Mechanisms of Eukaryotic Transcriptional Activation by the Proteasome Complex. *Critical Reviews in Biochemistry and Molecular Biology*, *43*(6), 419–433. https://doi.org/10.1080/10409230802605914

Blachier, F., & Malaisse, W. J. (1988). Effect of exogenous ATP upon inositol phosphate production, cationic fluxes and insulin release in pancreatic islet cells. *Biochimica Et Biophysica Acta*, *970*(2), 222–229. https://doi.org/10.1016/0167-4889(88)90182-6

Bortoletto, A., & Parchem, R. (2023). A pancreatic player in dementia: Pathological role for islet amyloid polypeptide accumulation in the brain. *Neural Regeneration Research*, *18*(10), 2141. https://doi.org/10.4103/1673-5374.369095

Bulut Arikan, F. (2020). TRPV2 Polymorphisms Change the Risk of Type 2 Diabetes—Hashimoto Thyroiditis Comorbidity. *Acta Endocrinologica (Bucharest)*, *16*(1), 15–21. https://doi.org/10.4183/aeb.2020.15

Cabrera, O., Berman, D. M., Kenyon, N. S., Ricordi, C., Berggren, P.-O., & Caicedo, A. (2006). The unique cytoarchitecture of human pancreatic islets has implications for islet cell function. *Proceedings of the National Academy of Sciences*, *103*(7), 2334–2339. https://doi.org/10.1073/pnas.0510790103

Castellanos, I., Balteanu, B., Singh, T., & Zderic, V. (2016). Therapeutic Modulation of Calcium Dynamics using Ultrasound and Other Energy-based Techniques. *IEEE Reviews in Biomedical Engineering*, *9*, 177–191. https://doi.org/10.1109/RBME.2016.2555760

Castle, A. L., Kuo, C.-H., Han, D.-H., & Ivy, J. L. (1998). Amylin-mediated inhibition of insulin-stimulated glucose transport in skeletal muscle. *American Journal of Physiology-Endocrinology and Metabolism*, *275*(3), E531–E536. https://doi.org/10.1152/ajpendo.1998.275.3.E531

Center for Disease Control and Prevention. (2024). *Diabetes amoung adults, United States (National) 2022* [Dataset]. Chronic Disease Indicator. https://www.cdc.gov/cdi/overview.html

Cesare, P., Moriondo, A., Vellani, V., & McNaughton, P. A. (1999). Ion channels gated by heat. *Proceedings of the National Academy of Sciences of the United States of America*, *96*(14), 7658–7663. https://doi.org/10.1073/pnas.96.14.7658

Chandra, R., & Liddle, R. A. (2009). Neural and hormonal regulation of pancreatic secretion: *Current Opinion in Gastroenterology*, *25*(5), 441–446. https://doi.org/10.1097/MOG.0b013e32832e9c41

Chatterjee Bhowmick, D., & Jeremic, A. (2018a). Functional proteasome complex is required for turnover of islet amyloid polypeptide in pancreatic β-cells. *Journal of Biological Chemistry*, *293*(37), 14210–14223. https://doi.org/10.1074/jbc.RA118.002414

Chatterjee Bhowmick, D., & Jeremic, A. (2018b). Functional proteasome complex is required for turnover of islet amyloid polypeptide in pancreatic β-cells. *Journal of Biological Chemistry*, *293*(37), 14210–14223. https://doi.org/10.1074/jbc.RA118.002414

Christensen, D. A. (1988). *Ultrasonic bioinstrumentation*. Wiley.

Costello, R. A., Nicolas, S., & Shivkumar, A. (2024). Sulfonylureas. In *StatPearls*. StatPearls Publishing. http://www.ncbi.nlm.nih.gov/books/NBK513225/

Dasgupta, I., & McCollum, D. (2019). Control of cellular responses to mechanical cues through YAP/TAZ regulation. *Journal of Biological Chemistry*, *294*(46), 17693–17706. https://doi.org/10.1074/jbc.REV119.007963

De Meyts, P. (2000). The Insulin Receptor and Its Signal Transduction Network. In K. R. Feingold, B. Anawalt, M. R. Blackman, A. Boyce, G. Chrousos, E. Corpas, W. W. de Herder, K. Dhatariya, K. Dungan, J. Hofland, S. Kalra, G. Kaltsas, N. Kapoor, C. Koch, P. Kopp, M. Korbonits, C. S. Kovacs, W. Kuohung, B. Laferrère, … D. P. Wilson (Eds.), *Endotext*. MDText.com, Inc. http://www.ncbi.nlm.nih.gov/books/NBK378978/

Deivasikamani, V., Dhayalan, S., Abudushalamu, Y., Mughal, R., Visnagri, A., Cuthbertson, K., Scragg, J. L., Munsey, T. S., Viswambharan, H., Muraki, K., Foster, R., Sivaprasadarao, A., Kearney, M. T., Beech, D. J., & Sukumar, P. (2019a). Piezo1 channel activation mimics high glucose as a stimulator of insulin release. *Scientific Reports*, *9*(1), 16876. https://doi.org/10.1038/s41598-019-51518-w

Deivasikamani, V., Dhayalan, S., Abudushalamu, Y., Mughal, R., Visnagri, A., Cuthbertson, K., Scragg, J. L., Munsey, T. S., Viswambharan, H., Muraki, K., Foster, R., Sivaprasadarao, A., Kearney, M. T., Beech, D. J., & Sukumar, P. (2019b). Piezo1 channel activation mimics high glucose as a stimulator of insulin release. *Scientific Reports*, *9*(1), 16876. https://doi.org/10.1038/s41598-019-51518-w

Del Prato, S., & Marchetti, P. (2004). Beta- and Alpha-Cell Dysfunction in Type 2 Diabetes. *Hormone and Metabolic Research*, *36*(11/12), 775–781. https://doi.org/10.1055/s-2004-826163

Eizirik, D. L., Cardozo, A. K., & Cnop, M. (2008). The Role for Endoplasmic Reticulum Stress in Diabetes Mellitus. *Endocrine Reviews*, *29*(1), 42–61. https://doi.org/10.1210/er.2007-0015

Filhoulaud, G., Benhamed, F., Pagesy, P., Bonner, C., Fardini, Y., Ilias, A., Movassat, J., Burnol, A.-F., Guilmeau, S., Kerr-Conte, J., Pattou, F., Issad, T., & Postic, C. (2019). O-GlcNacylation Links TxNIP to Inflammasome Activation in Pancreatic β Cells. *Frontiers in Endocrinology*, *10*, 291. https://doi.org/10.3389/fendo.2019.00291

Francis, B. H., Baskin, D. G., Saunders, D. R., & Ensinck, J. W. (1990). Distribution of somatostatin-14 and somatostatin-28 gastrointestinal-pancreatic cells of rats and humans. *Gastroenterology*, *99*(5), 1283–1291. https://doi.org/10.1016/0016-5085(90)91151-u

Freeman, A. M., Acevedo, L. A., & Pennings, N. (2024). Insulin Resistance. In *StatPearls*. StatPearls Publishing. http://www.ncbi.nlm.nih.gov/books/NBK507839/

Fu, Z., Gilbert, E. R., & Liu, D. (2013). Regulation of insulin synthesis and secretion and pancreatic Beta-cell dysfunction in diabetes. *Current Diabetes Reviews*, *9*(1), 25–53.

Galaviz, K. I., Narayan, K. M. V., Lobelo, F., & Weber, M. B. (2018). Lifestyle and the Prevention of Type 2 Diabetes: A Status Report. *American Journal of Lifestyle Medicine*, *12*(1), 4–20. https://doi.org/10.1177/1559827615619159

Giuntini, F., Foglietta, F., Marucco, A. M., Troia, A., Dezhkunov, N. V., Pozzoli, A., Durando, G., Fenoglio, I., Serpe, L., & Canaparo, R. (2018). Insight into ultrasound-mediated reactive oxygen species generation by various metal-porphyrin complexes. *Free Radical Biology and Medicine*, *121*, 190–201. https://doi.org/10.1016/j.freeradbiomed.2018.05.002

Goyal, R., Singhal, M., & Jialal, I. (2024a). Type 2 Diabetes. In *StatPearls*. StatPearls Publishing. http://www.ncbi.nlm.nih.gov/books/NBK513253/

Goyal, R., Singhal, M., & Jialal, I. (2024b). Type 2 Diabetes. In *StatPearls*. StatPearls Publishing. http://www.ncbi.nlm.nih.gov/books/NBK513253/

Gromada, J., Bokvist, K., Ding, W. G., Barg, S., Buschard, K., Renström, E., & Rorsman, P. (1997). Adrenaline stimulates glucagon secretion in pancreatic A-cells by increasing the Ca2+ current and the number of granules close to the L-type Ca2+ channels. *The Journal of General Physiology*, *110*(3), 217–228. https://doi.org/10.1085/jgp.110.3.217

Henderson, J. R., & Moss, M. C. (1985). A MORPHOMETRIC STUDY OF THE ENDOCRINE AND EXOCRINE CAPILLARIES OF THE PANCREAS. *Quarterly Journal of Experimental Physiology*, *70*(3), 347–356. https://doi.org/10.1113/expphysiol.1985.sp002920

Hu, G., Oboukhova, E. A., Kumar, S., Sturek, M., & Obukhov, A. G. (2009). Canonical Transient Receptor Potential Channels Expression Is Elevated in a Porcine Model of Metabolic Syndrome. *Molecular Endocrinology*, *23*(5), 689–699. https://doi.org/10.1210/me.2008-0350

Janssen, S. W. J., Hoenderop, J. G. J., Hermus, A. R. M. M., Sweep, F. C. G. J., Martens, G. J. M., & Bindels, R. J. M. (2002). Expression of the Novel Epithelial Ca $^{2+}$ Channel ECaC1 in Rat Pancreatic Islets. *Journal of Histochemistry & Cytochemistry*, *50*(6), 789–798. https://doi.org/10.1177/002215540205000605

Jia, C., Xu, L., Han, T., Cai, P., Yu, A. C. H., & Qin, P. (2018). Generation of Reactive Oxygen Species in Heterogeneously Sonoporated Cells by Microbubbles with Single-Pulse Ultrasound. *Ultrasound in Medicine & Biology*, *44*(5), 1074–1085. https://doi.org/10.1016/j.ultrasmedbio.2018.01.006

Jing, G., Westwell-Roper, C., Chen, J., Xu, G., Verchere, C. B., & Shalev, A. (2014). Thioredoxin-interacting Protein Promotes Islet Amyloid Polypeptide Expression through miR-124a and FoxA2. *Journal of Biological Chemistry*, *289*(17), 11807–11815. https://doi.org/10.1074/jbc.M113.525022

Kalwat, M. A., & Thurmond, D. C. (2013). Signaling mechanisms of glucose-induced F-actin remodeling in pancreatic islet β cells. *Experimental & Molecular Medicine*, *45*(8), e37–e37. https://doi.org/10.1038/emm.2013.73

Kaneto, H., Katakami, N., Matsuhisa, M., & Matsuoka, T. (2010). Role of Reactive Oxygen Species in the Progression of Type 2 Diabetes and Atherosclerosis. *Mediators of Inflammation*, *2010*, 1–11. https://doi.org/10.1155/2010/453892

Kiriyama, Y., & Nochi, H. (2018). Role and Cytotoxicity of Amylin and Protection of Pancreatic Islet β-Cells from Amylin Cytotoxicity. *Cells*, *7*(8), 95. https://doi.org/10.3390/cells7080095

Le Dain, A. C., Saint, N., Kloda, A., Ghazi, A., & Martinac, B. (1998). Mechanosensitive Ion Channels of the Archaeon Haloferax volcanii. *Journal of Biological Chemistry*, *273*(20), 12116–12119. https://doi.org/10.1074/jbc.273.20.12116

Lei, X. G., & Vatamaniuk, M. Z. (2011a). Two Tales of Antioxidant Enzymes on *β* Cells and Diabetes. *Antioxidants & Redox Signaling*, *14*(3), 489–503. https://doi.org/10.1089/ars.2010.3416

Lei, X. G., & Vatamaniuk, M. Z. (2011b). Two Tales of Antioxidant Enzymes on *β* Cells and Diabetes. *Antioxidants & Redox Signaling*, *14*(3), 489–503. https://doi.org/10.1089/ars.2010.3416

Leloup, C., Tourrel-Cuzin, C., Magnan, C., Karaca, M., Castel, J., Carneiro, L., Colombani, A.-L., Ktorza, A., Casteilla, L., & Pénicaud, L. (2009a). Mitochondrial reactive oxygen species are obligatory signals for glucose-induced insulin secretion. *Diabetes*, *58*(3), 673–681. https://doi.org/10.2337/db07-1056

Leloup, C., Tourrel-Cuzin, C., Magnan, C., Karaca, M., Castel, J., Carneiro, L., Colombani, A.-L., Ktorza, A., Casteilla, L., & Pénicaud, L. (2009b). Mitochondrial reactive oxygen species are obligatory signals for glucose-induced insulin secretion. *Diabetes*, *58*(3), 673–681. https://doi.org/10.2337/db07-1056

Lembrechts, R., Brouns, I., Schnorbusch, K., Pintelon, I., Timmermans, J.-P., & Adriaensen, D. (2012). Neuroepithelial Bodies as Mechanotransducers in the Intrapulmonary Airway

Epithelium: Involvement of TRPC5. *American Journal of Respiratory Cell and Molecular Biology*, *47*(3), 315–323. https://doi.org/10.1165/rcmb.2012-0068OC

Leturque, A., Brot-Laroche, E., Le Gall, M., Stolarczyk, E., & Tobin, V. (2005). The role of GLUT2 in dietary sugar handling. *Journal of Physiology and Biochemistry*, *61*(4), 529–537. https://doi.org/10.1007/BF03168378

Li, H., Handsaker, B., Wysoker, A., Fennell, T., Ruan, J., Homer, N., Marth, G., Abecasis, G., Durbin, R., & 1000 Genome Project Data Processing Subgroup. (2009). The Sequence Alignment/Map format and SAMtools. *Bioinformatics*, *25*(16), 2078–2079. https://doi.org/10.1093/bioinformatics/btp352

Light, P. (2010). The molecular mechanisms and pharmacotherapy of ATP-sensitive potassium channel gene mutations underlying neonatal diabetes. *Pharmacogenomics and Personalized Medicine*, 145. https://doi.org/10.2147/PGPM.S6969

Liu, T., Zhang, L., Joo, D., & Sun, S.-C. (2017). NF-κB signaling in inflammation. *Signal Transduction and Targeted Therapy*, *2*(1), 17023. https://doi.org/10.1038/sigtrans.2017.23

Liu, Y., Lian, K., Zhang, L., Wang, R., Yi, F., Gao, C., Xin, C., Zhu, D., Li, Y., Yan, W., Xiong, L., Gao, E., Wang, H., & Tao, L. (2014). TXNIP mediates NLRP3 inflammasome activation in cardiac microvascular endothelial cells as a novel mechanism in myocardial ischemia/reperfusion injury. *Basic Research in Cardiology*, *109*(5), 415. https://doi.org/10.1007/s00395-014-0415-z

Macfarlane, W. M., Campbell, S. C., Elrick, L. J., Oates, V., Bermano, G., Lindley, K. J., Aynsley-Green, A., Dunne, M. J., James, R. F., & Docherty, K. (2000a). Glucose regulates islet amyloid polypeptide gene transcription in a PDX1- and calcium-dependent

manner. *The Journal of Biological Chemistry*, *275*(20), 15330–15335. https://doi.org/10.1074/jbc.M908045199

Macfarlane, W. M., Campbell, S. C., Elrick, L. J., Oates, V., Bermano, G., Lindley, K. J., Aynsley-Green, A., Dunne, M. J., James, R. F. L., & Docherty, K. (2000b). Glucose Regulates Islet Amyloid Polypeptide Gene Transcription in a PDX1- and Calcium-dependent Manner. *Journal of Biological Chemistry*, *275*(20), 15330–15335. https://doi.org/10.1074/jbc.M908045199

Maedler, K., Sergeev, P., Ris, F., Oberholzer, J., Joller-Jemelka, H. I., Spinas, G. A., Kaiser, N., Halban, P. A., & Donath, M. Y. (2002). Glucose-induced β cell production of IL-1β contributes to glucotoxicity in human pancreatic islets. *Journal of Clinical Investigation*, *110*(6), 851–860. https://doi.org/10.1172/JCI200215318

Marín-Peñalver, J. J., Martín-Timón, I., Sevillano-Collantes, C., & Cañizo-Gómez, F. J. D. (2016). Update on the treatment of type 2 diabetes mellitus. *World Journal of Diabetes*, *7*(17), 354. https://doi.org/10.4239/wjd.v7.i17.354

Masaba, B. B., & Mmusi-Phetoe, R. M. (2021). Determinants of Non-Adherence to Treatment Among Patients with Type 2 Diabetes in Kenya: A Systematic Review. *Journal of Multidisciplinary Healthcare*, *Volume 13*, 2069–2076. https://doi.org/10.2147/JMDH.S270137

Matos, G. M., Andersson, B., & Islam, Md. S. (2022). Expression of Transient Receptor Potential Channel Genes and Their Isoforms in Alpha-Cells and Beta-Cells of Human Islets of Langerhans. *Journal of Diabetes Research*, *2022*, 1–10. https://doi.org/10.1155/2022/3975147

Matthews, M. J., & Stretanski, M. F. (2024). Ultrasound Therapy. In *StatPearls*. StatPearls Publishing. http://www.ncbi.nlm.nih.gov/books/NBK547717/

Meli, A., Perrella, G., Curcio, F., Saverio, F., & Impiombato, A. (1998). Response to hypogravity of normal in vitro cultured follicular cells from thyroid. *Acta Astronautica*, *42*(1–8), 465–472. https://doi.org/10.1016/S0094-5765(98)00139-8

Meshkani, R., & Vakili, S. (2016). Tissue resident macrophages: Key players in the pathogenesis of type 2 diabetes and its complications. *Clinica Chimica Acta*, *462*, 77–89. https://doi.org/10.1016/j.cca.2016.08.015

Mietlicki-Baase, E. G., & Hayes, M. R. (2014). Amylin activates distributed CNS nuclei to control energy balance. *Physiology & Behavior*, *136*, 39–46. https://doi.org/10.1016/j.physbeh.2014.01.013

Miley, H. E., Sheader, E. A., Brown, P. D., & Best, L. (1997). Glucose-induced swelling in rat pancreatic β-cells. *The Journal of Physiology*, *504*(1), 191–198. https://doi.org/10.1111/j.1469-7793.1997.00191.x

Mulder, H., Ahren, B., & Sundler, F. (1996). Islet amyloid polypeptide and insulin gene expression are regulated in parallel by glucose in vivo in rats. *American Journal of Physiology-Endocrinology and Metabolism*, *271*(6), E1008–E1014. https://doi.org/10.1152/ajpendo.1996.271.6.E1008

Nakatsuma, A., Kiriyama, Y., Kino, K., & Ninomiya, M. (2016). Diabetes drugs that protect pancreatic β cells. *Integrative Molecular Medicine*, *3*(1). https://doi.org/10.15761/IMM.1000189

Odagiri, H., Wang, J., & German, M. S. (1996). Function of the Human Insulin Promoter in Primary Cultured Islet Cells. *Journal of Biological Chemistry*, *271*(4), 1909–1915. https://doi.org/10.1074/jbc.271.4.1909

Ohtsubo, K., Chen, M. Z., Olefsky, J. M., & Marth, J. D. (2011). Pathway to diabetes through attenuation of pancreatic beta cell glycosylation and glucose transport. *Nature Medicine*, *17*(9), 1067–1075. https://doi.org/10.1038/nm.2414

Omar-Hmeadi, M., & Idevall-Hagren, O. (2021). Insulin granule biogenesis and exocytosis. *Cellular and Molecular Life Sciences*, *78*(5), 1957–1970. https://doi.org/10.1007/s00018-020-03688-4

Ortis, F., Pirot, P., Naamane, N., Kreins, A. Y., Rasschaert, J., Moore, F., Théâtre, E., Verhaeghe, C., Magnusson, N. E., Chariot, A., Ørntoft, T. F., & Eizirik, D. L. (2008). Induction of nuclear factor-κB and its downstream genes by TNF-α and IL-1β has a pro-apoptotic role in pancreatic beta cells. *Diabetologia*, *51*(7), 1213–1225. https://doi.org/10.1007/s00125-008-0999-7

Oslowski, C. M., Hara, T., O'Sullivan-Murphy, B., Kanekura, K., Lu, S., Hara, M., Ishigaki, S., Zhu, L. J., Hayashi, E., Hui, S. T., Greiner, D., Kaufman, R. J., Bortell, R., & Urano, F. (2012). Thioredoxin-Interacting Protein Mediates ER Stress-Induced β Cell Death through Initiation of the Inflammasome. *Cell Metabolism*, *16*(2), 265–273. https://doi.org/10.1016/j.cmet.2012.07.005

Pandol, S. (2010). Introduction. In *The Exocrine Pancreas*. Morgan & Claypool Life Sciences. https://www.ncbi.nlm.nih.gov/books/NBK54131/

Patel, S., & Remedi, M. S. (2024a). Loss of β-cell identity and dedifferentiation, not an irreversible process? *Frontiers in Endocrinology*, *15*, 1414447. https://doi.org/10.3389/fendo.2024.1414447

Patel, S., & Remedi, M. S. (2024b). Loss of β-cell identity and dedifferentiation, not an irreversible process? *Frontiers in Endocrinology*, *15*, 1414447. https://doi.org/10.3389/fendo.2024.1414447

Petersen, M. C., & Shulman, G. I. (2018). Mechanisms of Insulin Action and Insulin Resistance. *Physiological Reviews*, *98*(4), 2133–2223. https://doi.org/10.1152/physrev.00063.2017

Philippaert, K., & Vennekens, R. (2017). The Role of TRP Channels in the Pancreatic Beta-Cell. In T. L. R. Emir (Ed.), *Neurobiology of TRP Channels*. CRC Press/Taylor & Francis. http://www.ncbi.nlm.nih.gov/books/NBK476117/

Pirot, P., Naamane, N., Libert, F., Magnusson, N. E., Ørntoft, T. F., Cardozo, A. K., & Eizirik, D. L. (2007). Global profiling of genes modified by endoplasmic reticulum stress in pancreatic beta cells reveals the early degradation of insulin mRNAs. *Diabetologia*, *50*(5), 1006–1014. https://doi.org/10.1007/s00125-007-0609-0

Prentki, M. (2006). Islet cell failure in type 2 diabetes. *Journal of Clinical Investigation*, *116*(7), 1802–1812. https://doi.org/10.1172/JCI29103

Qi, D., Cai, K., Wang, O., Li, Z., Chen, J., Deng, B., Qian, L., & Le, Y. (2010). Fatty acids induce amylin expression and secretion by pancreatic β-cells. *American Journal of Physiology-Endocrinology and Metabolism*, *298*(1), E99–E107. https://doi.org/10.1152/ajpendo.00242.2009

Rishisree, A., Mallory, B., Elena, K., Teodora, J., Gordana, Z., Katarina, Š., & Aleksandar, J. (2024). Pomegranate peel, chokeberry leaves and Ironwort extract as novel natural

inhibitors of amylin aggregation and cellular toxicity in pancreatic β cells. *Biophysical Chemistry*, *304*, 107130. https://doi.org/10.1016/j.bpc.2023.107130

Robinson, M. D., McCarthy, D. J., & Smyth, G. K. (2010). edgeR: A Bioconductor package for differential expression analysis of digital gene expression data. *Bioinformatics*, *26*(1), 139–140. https://doi.org/10.1093/bioinformatics/btp616

Röder, P. V., Wu, B., Liu, Y., & Han, W. (2016). Pancreatic regulation of glucose homeostasis. *Experimental & Molecular Medicine*, *48*(3), e219–e219. https://doi.org/10.1038/emm.2016.6

Rorsman, P., & Huising, M. O. (2018). The somatostatin-secreting pancreatic δ-cell in health and disease. *Nature Reviews. Endocrinology*, *14*(7), 404–414. https://doi.org/10.1038/s41574-018-0020-6

Sawatani, T., Kaneko, Y. K., Doutsu, I., Ogawa, A., & Ishikawa, T. (2019a). TRPV2 channels mediate insulin secretion induced by cell swelling in mouse pancreatic β-cells. *American Journal of Physiology-Cell Physiology*, *316*(3), C434–C443. https://doi.org/10.1152/ajpcell.00210.2017

Sawatani, T., Kaneko, Y. K., Doutsu, I., Ogawa, A., & Ishikawa, T. (2019b). TRPV2 channels mediate insulin secretion induced by cell swelling in mouse pancreatic β-cells. *American Journal of Physiology-Cell Physiology*, *316*(3), C434–C443. https://doi.org/10.1152/ajpcell.00210.2017

Shalev, A., Pise-Masison, C. A., Radonovich, M., Hoffmann, S. C., Hirshberg, B., Brady, J. N., & Harlan, D. M. (2002). Oligonucleotide microarray analysis of intact human pancreatic islets: Identification of glucose-responsive genes and a highly regulated TGFbeta

signaling pathway. *Endocrinology*, *143*(9), 3695–3698. https://doi.org/10.1210/en.2002-220564

Sidarala, V., Pearson, G. L., Parekh, V. S., Thompson, B., Christen, L., Gingerich, M. A., Zhu, J., Stromer, T., Ren, J., Reck, E. C., Chai, B., Corbett, J. A., Mandrup-Poulsen, T., Satin, L. S., & Soleimanpour, S. A. (2020). Mitophagy protects β cells from inflammatory damage in diabetes. *JCI Insight*, *5*(24), e141138. https://doi.org/10.1172/jci.insight.141138

Singh, T., Suarez Castellanos, I., Bhowmick, D. C., Cohen, J., Jeremic, A., & Zderic, V. (2020a). Therapeutic Ultrasound-Induced Insulin Release in Vivo. *Ultrasound in Medicine & Biology*, *46*(3), 639–648. https://doi.org/10.1016/j.ultrasmedbio.2019.10.022

Singh, T., Suarez Castellanos, I., Bhowmick, D. C., Cohen, J., Jeremic, A., & Zderic, V. (2020b). Therapeutic Ultrasound-Induced Insulin Release in Vivo. *Ultrasound in Medicine & Biology*, *46*(3), 639–648. https://doi.org/10.1016/j.ultrasmedbio.2019.10.022

Skrzypski, M., Kakkassery, M., Mergler, S., Grötzinger, C., Khajavi, N., Sassek, M., Szczepankiewicz, D., Wiedenmann, B., Nowak, K. W., & Strowski, M. Z. (2013). Activation of TRPV4 channel in pancreatic INS-1E beta cells enhances glucose-stimulated insulin secretion via calcium-dependent mechanisms. *FEBS Letters*, *587*(19), 3281–3287. https://doi.org/10.1016/j.febslet.2013.08.025

Stroo, E., Koopman, M., Nollen, E. A. A., & Mata-Cabana, A. (2017). Cellular Regulation of Amyloid Formation in Aging and Disease. *Frontiers in Neuroscience*, *11*. https://doi.org/10.3389/fnins.2017.00064

Suarez Castellanos, I., Jeremic, A., Cohen, J., & Zderic, V. (2017a). Ultrasound Stimulation of Insulin Release from Pancreatic Beta Cells as a Potential Novel Treatment for Type 2

Diabetes. *Ultrasound in Medicine & Biology*, *43*(6), 1210–1222. https://doi.org/10.1016/j.ultrasmedbio.2017.01.007

Suarez Castellanos, I., Jeremic, A., Cohen, J., & Zderic, V. (2017b). Ultrasound Stimulation of Insulin Release from Pancreatic Beta Cells as a Potential Novel Treatment for Type 2 Diabetes. *Ultrasound in Medicine & Biology*, *43*(6), 1210–1222. https://doi.org/10.1016/j.ultrasmedbio.2017.01.007

Suarez Castellanos, I. M., Balteanu, B., Singh, T., & Zderic, V. (2016). Therapeutic Modulation of Calcium Dynamics Using Ultrasound and Other Energy-Based Techniques. *IEEE Reviews in Biomedical Engineering*, *9*, 177–191. https://doi.org/10.1109/RBME.2016.2555760

Suarez Castellanos, I., Singh, T., Balteanu, B., Bhowmick, D. C., Jeremic, A., & Zderic, V. (2017a). Calcium-dependent ultrasound stimulation of secretory events from pancreatic beta cells. *Journal of Therapeutic Ultrasound*, *5*(1), 30. https://doi.org/10.1186/s40349-017-0108-9

Suarez Castellanos, I., Singh, T., Balteanu, B., Bhowmick, D. C., Jeremic, A., & Zderic, V. (2017b). Calcium-dependent ultrasound stimulation of secretory events from pancreatic beta cells. *Journal of Therapeutic Ultrasound*, *5*, 30. https://doi.org/10.1186/s40349-017-0108-9

Suarez-Castellanos, I., Singh, T., Chatterjee Bhowmick, D., Cohen, J., Jeremic, A., & Zderic, V. (2021). Effect of Therapeutic Ultrasound on the Release of Insulin, Glucagon, and Alpha-Amylase from Ex Vivo Pancreatic Models. *Journal of Ultrasound in Medicine*, *40*(12), 2709–2719. https://doi.org/10.1002/jum.15661

Tamaki, M., Fujitani, Y., Hara, A., Uchida, T., Tamura, Y., Takeno, K., Kawaguchi, M., Watanabe, T., Ogihara, T., Fukunaka, A., Shimizu, T., Mita, T., Kanazawa, A., Imaizumi, M. O., Abe, T., Kiyonari, H., Hojyo, S., Fukada, T., Kawauchi, T., … Watada, H. (2013). The diabetes-susceptible gene SLC30A8/ZnT8 regulates hepatic insulin clearance. *Journal of Clinical Investigation*, *123*(10), 4513–4524. https://doi.org/10.1172/JCI68807

Teitelman, G. (2019). Heterogeneous Expression of Proinsulin Processing Enzymes in Beta Cells of Non-diabetic and Type 2 Diabetic Humans. *Journal of Histochemistry & Cytochemistry*, *67*(6), 385–400. https://doi.org/10.1369/0022155419831641

Thorens, B., Weir, G. C., Leahy, J. L., Lodish, H. F., & Bonner-Weir, S. (1990). Reduced expression of the liver/beta-cell glucose transporter isoform in glucose-insensitive pancreatic beta cells of diabetic rats. *Proceedings of the National Academy of Sciences*, *87*(17), 6492–6496. https://doi.org/10.1073/pnas.87.17.6492

Thurmond, D. C., & Pessin, J. E. (2000). Discrimination of GLUT4 vesicle trafficking from fusion using a temperature-sensitive Munc18c mutant. *The EMBO Journal*, *19*(14), 3565–3575. https://doi.org/10.1093/emboj/19.14.3565

Travagli, R. A., & Browning, K. N. (2011). Central Autonomic Control of the Pancreas. In I. J. Llewellyn-Smith & A. J. M. Verberne (Eds.), *Central Regulation of Autonomic Functions* (pp. 274–291). Oxford University Press. https://doi.org/10.1093/acprof:oso/9780195306637.003.0015

Tsuchiya, Y., Saito, M., & Kohno, K. (2016). Pathogenic Mechanism of Diabetes Development Due to Dysfunction of Unfolded Protein Response. *YAKUGAKU ZASSHI*, *136*(6), 817–825. https://doi.org/10.1248/yakushi.15-00292-4

Velazco-Cruz, L., Goedegebuure, M. M., Maxwell, K. G., Augsornworawat, P., Hogrebe, N. J., & Millman, J. R. (2020). SIX2 Regulates Human β Cell Differentiation from Stem Cells and Functional Maturation In Vitro. *Cell Reports*, *31*(8), 107687. https://doi.org/10.1016/j.celrep.2020.107687

Wachlin, G., Augstein, P., Schröder, D., Kuttler, B., Klöting, I., Heinke, P., & Schmidt, S. (2003). IL-1β, IFN-γ and TNF-α increase vulnerability of pancreatic beta cells to autoimmune destruction. *Journal of Autoimmunity*, *20*(4), 303–312. https://doi.org/10.1016/S0896-8411(03)00039-8

Wagner, A. P., Chinnathambi, S., Titze, I. R., & Sander, E. A. (2016). Vibratory stimulation enhances thyroid epithelial cell function. *Biochemistry and Biophysics Reports*, *8*, 376–381. https://doi.org/10.1016/j.bbrep.2016.10.008

Wang, C., Guan, Y., & Yang, J. (2010). Cytokines in the Progression of Pancreatic β -Cell Dysfunction. *International Journal of Endocrinology*, *2010*, 1–10. https://doi.org/10.1155/2010/515136

Welsh, N., Cnop, M., Kharroubi, I., Bugliani, M., Lupi, R., Marchetti, P., & Eizirik, D. L. (2005). Is There a Role for Locally Produced Interleukin-1 in the Deleterious Effects of High Glucose or the Type 2 Diabetes Milieu to Human Pancreatic Islets? *Diabetes*, *54*(11), 3238–3244. https://doi.org/10.2337/diabetes.54.11.3238

Westermark, P., Andersson, A., & Westermark, G. T. (2011). Islet Amyloid Polypeptide, Islet Amyloid, and Diabetes Mellitus. *Physiological Reviews*, *91*(3), 795–826. https://doi.org/10.1152/physrev.00042.2009

Westermark, P., Li, Z.-C., Westermark, G. T., Leckström, A., & Steiner, D. F. (1996). Effects of beta cell granule components on human islet amyloid polypeptide fibril formation. *FEBS Letters*, *379*(3), 203–206. https://doi.org/10.1016/0014-5793(95)01512-4

Westwell-Roper, C. Y., Ehses, J. A., & Verchere, C. B. (2014). Resident Macrophages Mediate Islet Amyloid Polypeptide–Induced Islet IL-1β Production and β-Cell Dysfunction. *Diabetes*, *63*(5), 1698–1711. https://doi.org/10.2337/db13-0863

Wiederhold, K., & Fasshauer, D. (2009). Is Assembly of the SNARE Complex Enough to Fuel Membrane Fusion? *Journal of Biological Chemistry*, *284*(19), 13143–13152. https://doi.org/10.1074/jbc.M900703200

Wu, L., Fritz, J. D., & Powers, A. C. (1998). Different Functional Domains of GLUT2 Glucose Transporter Are Required for Glucose Affinity and Substrate Specificity[1]. *Endocrinology*, *139*(10), 4205–4212. https://doi.org/10.1210/endo.139.10.6245

Xin, Y., Dominguez Gutierrez, G., Okamoto, H., Kim, J., Lee, A.-H., Adler, C., Ni, M., Yancopoulos, G. D., Murphy, A. J., & Gromada, J. (2018). Pseudotime Ordering of Single Human β-Cells Reveals States of Insulin Production and Unfolded Protein Response. *Diabetes*, *67*(9), 1783–1794. https://doi.org/10.2337/db18-0365

Ye, Y., Barghouth, M., Dou, H., Luan, C., Wang, Y., Karagiannopoulos, A., Jiang, X., Krus, U., Fex, M., Zhang, Q., Eliasson, L., Rorsman, P., Zhang, E., & Renström, E. (2022). A critical role of the mechanosensor PIEZO1 in glucose-induced insulin secretion in pancreatic β-cells. *Nature Communications*, *13*(1), 4237. https://doi.org/10.1038/s41467-022-31103-y

Yoon, C. W., Lee, N. S., Koo, K. M., Moon, S., Goo, K., Jung, H., Yoon, C., Lim, H. G., & Shung, K. K. (2020). Investigation of Ultrasound-Mediated Intracellular Ca2+

Oscillations in HIT-T15 Pancreatic β-Cell Line. *Cells*, *9*(5), 1129. https://doi.org/10.3390/cells9051129

Zhao, M., Amiel, S. A., Christie, M. R., Rela, M., Heaton, N., & Huang, G. C. (2005). Insulin-producing cells derived from human pancreatic non-endocrine cell cultures reverse streptozotocin-induced hyperglycaemia in mice. *Diabetologia*, *48*(10), 2051–2061. https://doi.org/10.1007/s00125-005-1888-y

Zhao, Y., Liu, Y., Tao, T., Zhang, J., Guo, W., Deng, H., Han, M., Mo, H., Tong, X., Lin, S., Yang, J., Zhai, H., Wang, Q., Hu, Z., Zhang, W., Chen, H., & Xu, G. (2024). Gastric mechanosensitive channel Piezo1 regulates ghrelin production and food intake. *Nature Metabolism*, *6*(3), 458–472. https://doi.org/10.1038/s42255-024-00995-z

Zhong, F., & Jiang, Y. (2019). Endogenous Pancreatic β Cell Regeneration: A Potential Strategy for the Recovery of β Cell Deficiency in Diabetes. *Frontiers in Endocrinology*, *10*, 101. https://doi.org/10.3389/fendo.2019.00101

Zhou, R., Tardivel, A., Thorens, B., Choi, I., & Tschopp, J. (2010). Thioredoxin-interacting protein links oxidative stress to inflammasome activation. *Nature Immunology*, *11*(2), 136–140. https://doi.org/10.1038/ni.1831

Zorova, L. D., Popkov, V. A., Plotnikov, E. Y., Silachev, D. N., Pevzner, I. B., Jankauskas, S. S., Babenko, V. A., Zorov, S. D., Balakireva, A. V., Juhaszova, M., Sollott, S. J., & Zorov, D. B. (2018). Mitochondrial membrane potential. *Analytical Biochemistry*, *552*, 50–59. https://doi.org/10.1016/j.ab.2017.07.009